Large igneous provinces of the Amazonian Craton and their metallogenic potential in Proterozoic times

Nelson Joaquim Reis[1]*, W. Teixeira[2], M. S. D'Agrella-Filho[3], J. S. Bettencourt[2], R. E. Ernst[4,5] and L. E. A. Goulart[6]

[1]Geological Survey of Brazil/Manaus, Manaus, Brazil

[2]Institute of Geosciences, University of São Paulo, São Paulo, Brazil

[3]Institute of Astronomy, Geophysics and Atmospheric Science, University of São Paulo, São Paulo, Brazil

[4]Department of Earth Sciences, Carleton University, Ottawa, Canada

[5]Faculty of Geology and Geography, Tomsk State University, Tomsk, Russia

[6]Geological Survey of Brazil/Belo Horizonte, Brazil

NJR, 0000-0003-3409-5354; JSB, 0000-0002-2120-7495; REE, 0000-0001-9474-0314
*Correspondence: nelson.reis@cprm.gov.br

Abstract: This paper overviews the Proterozoic large igneous provinces (LIPs) of the Amazonian Craton, characterized by large volumes of extrusive and intrusive magmatic rocks. We reassess the geologic, geochronological and geochemical information to stablish three intracontinental felsic volcanic–plutonic igneous belts (i.e. SLIPs), namely: Orocaima (1.98–1.96 Ga), Uatumã (1.88–1.87 Ga) and Alta Floresta (1.80–1.79 Ga). The Avanavero LIP (1.79–1.78 Ga), as well as the Rincón del Tigre-Huanchaca LIP (1.11 Ga) are also revisited. The relationships of these events to intraplate settings through time and space are apparent. We examine the main characteristics of each magmatic event in light of the U–Pb zircon and baddeleyite ages and coupled isotopic–geochemical constraints, the geodynamic significance and metallogenetic potential. The Uatumã and Alta Floresta SLIPs host the most important mineral resources within the Amazonian Craton. Global barcode matches of the Proterozoic SLIP/LIP events of Amazonia are also addressed, as well as their possible links with geological timescale periods: the Orosirian, Statherian and Stenian boundaries. We also evaluate the available palaeomagnetic data to address issues related to the barcode match of such SLIP/LIP events in the context of supercontinent cycles.

Large igneous provinces (LIPs) and silicic LIPs (SLIPs) have become some of the most important themes in the evolution of the Earth, on issues that include the nature of plumbing systems, mantle dynamics and supercontinent cycles, metallogeny and environmental changes through time, (e.g. Bryan and Ernst 2008; Ernst 2014; Ernst and Jowitt 2013; Ernst and Youbi 2017). LIPs are a powerful tool for palaeogeographic reconstructions by comparison of the LIP 'barcode' between different blocks to identify neighbouring blocks and by matching the foci of radiating dyke swarms between blocks (Bleeker and Ernst 2006; Ernst and Bleeker 2010; Peng *et al.* 2011). In addition, LIP events, owing to their short duration or pulsed character in an intracontinental setting are prominent time-markers for break-up attempts of the Earth's lithosphere in addition to coeval intraplate episodes such as anorogenic magmatism and tectonic basins. These events occur at a variable rate that averages approximately one event every 20–30 myr (Ernst 2014). LIP-type components are extensive flood basalts, mafic dyke swarms and sills, silicic volcanic–plutonic associations and mafic–ultramafic layered intrusions. Some SLIPs display linear distribution as a belt that suggests a primary association with hydrothermal fluid dynamics from earlier subduction zones inducing pervasive melt of the lithospheric mantle (e.g. Bryan and Ferrari 2013; Ernst 2014).

From an economic perspective, LIP and SLIP pulses have usually been associated with metallogenetic systems, such as native Cu, hydrothermal volcanogenic massive sulfide and iron-oxide–copper–gold (IOCG) deposits, orthomagmatic Ni–Cu–platinum group element (PGE) sulfides, Sn–W, Nb–Ta–rare earth element (REE) and diamond–gold among others (Ernst and Jowitt 2013). Orogenic gold deposits may also have an indirect link with LIPs and a marked break-up (or attempted break-up) event that may correlate in time with compression and transpression episodes on distal convergent plate margins (e.g. Ernst and Jowitt 2013). However, intraplate settings have also been

From: Srivastava, R. K., Ernst, R. E., Buchan, K. L. and de Kock, M. (eds) 2022. *Large Igneous Provinces and their Plumbing Systems*. Geological Society, London, Special Publications, **518**, 493–529.
First published online October 13, 2021, https://doi.org/10.1144/SP518-2021-7

envisaged, for instance in the southwestern portion of the Amazonian Craton (e.g. Oliveira and Almeida 2019; Rizzotto *et al.* 2019). Particularly in humid tropical climatic zones, the surface records of ore deposits are incomplete or absent, sometimes having leached and reprecipitated. These processes eventually result in thick weathering profiles (Butt and Zeegers 1989) with enriched Al, Ni–Co, Mn, Fe and Cr within laterites, developed from primary mineralized mafic–ultramafic rocks (e.g. Mudd 2010, 2012), as well as Nb–Ta–REE phosphate, iron ore, Cu, Zr, Th, U, fluorine/fluorite and vermiculite resources from carbonatite laterites (Ernst and Jowitt 2013).

When it comes to the Amazonian Craton, several Proterozoic LIP/SLIP-scale events have been recognized in the last decade by means of precise U–Pb dating and coupled isotopic and geochemical characterization. The growing knowledge of LIP events has allowed insights into their nature and tectonic significance related to their polycyclic evolution, as well as for palaeogeographic constraints on the positioning of Amazonia in the Columbia and Rodinia supercontinents (Klein *et al.* 2012; Reis *et al.* 2013*a*; Teixeira *et al.* 2015, 2019; D'Agrella-Filho *et al.* 2016*a*; Rizzotto *et al.* 2019; Antonio *et al.* 2021). However, the linkage between LIPs and/or SLIPs and the processes and potential for concentrating metal deposits throughout the Amazonian Craton are still poorly explored.

This review reassesses the role of Paleo- and Mesoproterozoic LIP/SLIP events of the Amazonian Craton (Guiana and Brazil Central shields) and the potential links with metallogeny in space and time. We emphasize the importance of five events of LIP scale, although additional potentially important intraplate igneous activities are apparent through time and space (e.g. CPRM 2010; Klein *et al.* 2012; Reis *et al.* 2013*a*; Teixeira *et al.* 2015, 2019). For this purpose, we distinguish two intraplate LIP events and three SLIPs that are characterized physically as silicic igneous belts (silicic LIPs) composed of voluminous volcanic–plutonic associations with post-orogenic to anorogenic characteristics. Important sedimentary basins and mafic magmatism follow the associations. The SLIP events in the Amazonian Craton, from the older to younger, are: Orocaima (1.98–1.96 Ga), Uatumã (1.88–1.87 Ga) and Alta Floresta (1.80–1.79 Ga). The Alta Floresta SLIP is coeval with the Avanavero LIP (1.79–1.78 Ga) that occurs throughout those oldest igneous provinces, mostly in the Guiana Shield. The Rincón del Tigre–Huanchaca (1.11 Ga) LIP that extends in the southeastern portion of the Amazonian Craton and the Bolivian Precambrian Shield represents the youngest Proterozoic voluminous mafic to mafic–ultramafic magmatism.

We also provide palaeogeographic implications for Proterozoic Amazonia in the context of supercontinent cycles.

Silicic and mafic intraplate events (including SLIPs and LIPs) and associated intracratonic basins

Overview

The country rocks of the Amazonian Craton crop out over two regions overlain by the Solimões and Amazonas basins: the Guiana Shield in the north and Central Brazil Shield in the south (Fig. 1). The tectonic evolution of the Amazonian Craton remains under discussion (Tassinari and Macambira 2004; Santos *et al.* 2006; Cordani and Teixeira 2007; Fraga *et al.* 2008). When it comes to the SLIPs, three large volcanic–plutonic belts are apparent, in general associated with voluminous sedimentary rocks (Fraga *et al.* 2017*b*, 2020; Reis *et al.* 2013*a*, 2021). In this work, we follow the concept of Fraga *et al.* (2008) that distinguishes at least two large igneous belts (i.e. SLIPs adjacent to the *c.* 2.0 Ga Cauarane–Coeroeni supracrustal belt and the granite–greenstone terrane at 2.21–2.07 Ga), the main tectonic features recognized in the Guiana Shield.

This section outlines the distribution of LIP/SLIP scale magmatism and their respective nodes throughout the Amazonian Craton. The two oldest SLIPs – Orocaima (1.98–1.96 Ga) and Uatumã (1.88–1.87 Ga) – form roughly sinuous igneous belts and are related to an intracontinental setting. Both SLIPs extend discontinuously for more than 1000 km, have a width of around 200 km and thus contain a huge volume of magmatic material within their main time interval of 20–10 Ma. They show rocks normally with $SiO_2 > 65\%$ and do not includes expanded suites, which are more common in orogenic environments, in addition to minor mafic enclaves, notably of quartz diorite. Large sedimentary basins underlie these SLIPs and are exemplified by isolated tablelands suggesting some previous extension across the continental crust. They were interpreted as rifted basins formed in an intraplate environment (Reis *et al.* 2017*a*) and accommodate large mafic sills and dykes such as the 1.79–1.78 Ga Avanavero LIP (Fig. 1).

The Avanavero LIP matches the Alta Floresta SLIP (1.80–1.79 Ga) in the Central Brazil Shield which, in turn, displays a peculiar sinuous geometry that contrasts with the other SLIPs. This one is distributed as a narrow string of volcanic–plutonic rocks, extending from the southern flank of the Alto Tapajós Horst, to the SE where it borders a nucleus of older rocks *c.* 2.03–1.87 Ga old (Fig. 1), and exhibiting a larger exposure towards the NE,

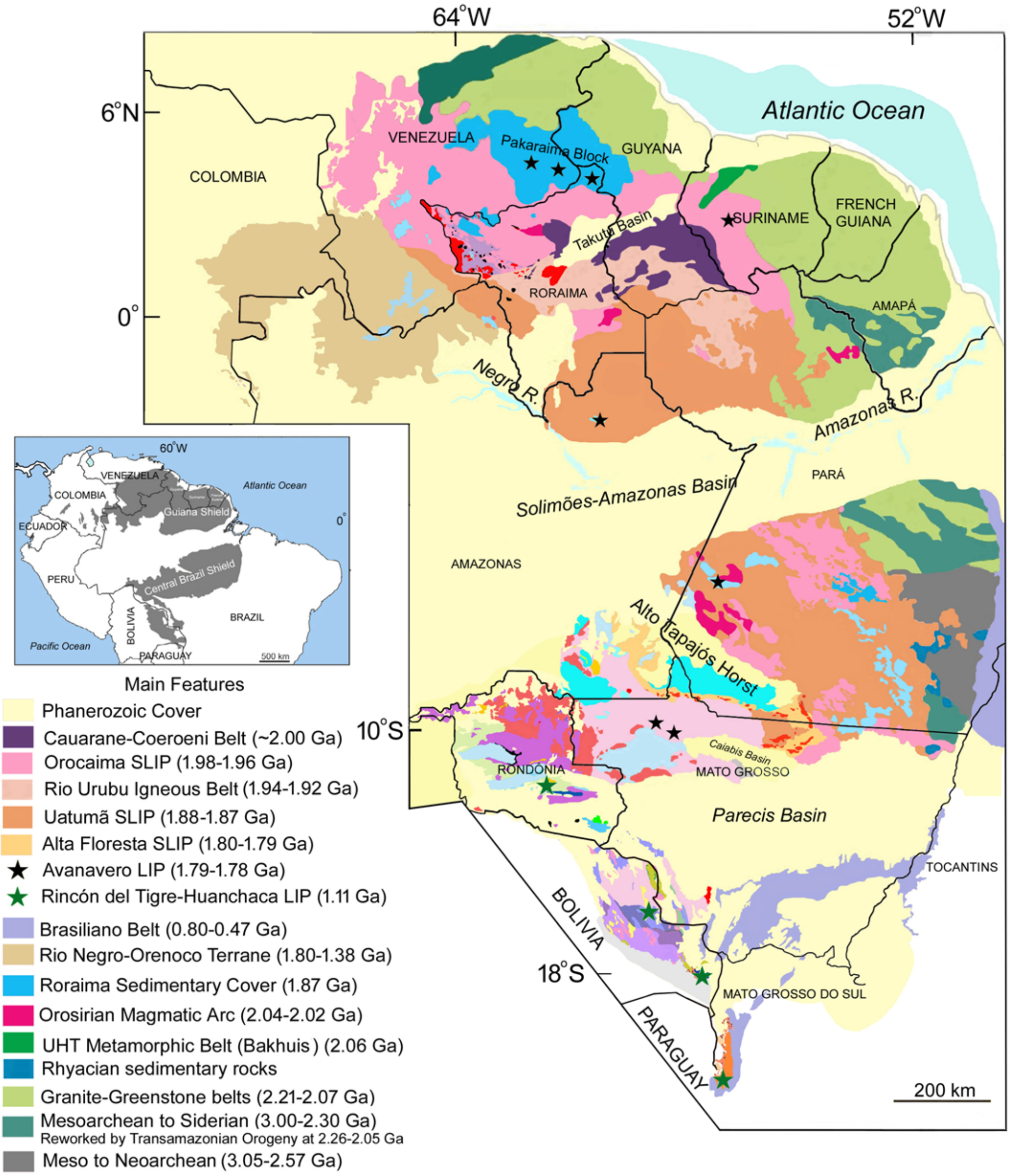

Fig. 1. Simplified geological map of the Amazonian Craton (modified from Fraga *et al.* 2017*c*; Reis *et al.* 2021).

overlain by Phanerozoic cover rocks. The structural framework of the youngest LIP – Rincón del Tigre-Huanchaca (1.11 Ga) – roughly follows the NW–SE trend in the southwestern Amazonian Craton.

Below we summarize the geological–tectonic aspects of those LIP/SLIP episodes in a chronological order and also discuss their related mineral potential. We note a linkage between mineral deposits and multi-age intracratonic volcanics, granitoids and mafic–ultramafics rocks through time and space.

The Orocaima SLIP (1.98–1.96 Ga)

Distribution. The Orocaima SLIP – OSL (Reis *et al.* 2014) – occurs in the Guiana Shield as a continuous volcanic–plutonic domain throughout the Venezuela, Brazil (Roraima and Pará States), Guyana and Suriname, where the magmatic units are known by different names.

According to Fraga *et al.* (2017*b*) and based on previous petrographic and chemical studies (Fraga *et al.* 1997; CPRM 2010; Reis and Ramos 2017), the OSL consists mainly of 1.98–1.96 Ga high-K calc-alkaline, A-type and shoshonitic magmatic rocks, interpreted in this paper as having formed in an intracontinental setting. However, the tectonic significance of the belt remains under debate as the previous interpretations of Santos (2003) and Fraga *et al.* (1997) suggested in collisional and post-collisional settings, respectively.

The OSL contrasts in age with the surrounding Rhyacian country rocks at the easternmost portion of Suriname and the northernmost portion of Guyana where a granite–greenstone terrane dominates (Fig. 2). The same relationship can be seen in the vicinity of the greenstone belts of Venezuela.

The Orosirian framework of the Guiana Shield shows a complex relation between the Cauarane–Coeroeni supracrustal Belt, the Rio Urubu Igneous Belt and the OSL. According to Fraga *et al.* (2017*a*), the Cauarane–Coeroeni Belt represents multiphase supracrustal rocks outcropping from NW Roraima to SW Suriname. On both sides of the belt, to the north and south, the 1.98–1.96 Ga OSL and the 1.94–1.92 Ga Rio Urubu Belt emerge, respectively (Fig. 1). U–Pb SHRIMP detrital zircons for paragneisses of the Cauarane–Coeroeni Belt show Archean, Siderian and Rhyacian sources, as well as major provenance from Rhyacian to Orosirian sources. The belt can be interpreted as a back-arc-type basin associated with the development of the 2.04–2.03 Ga magmatic arc, with suturing and high-grade metamorphism around 2.02 Ga (Fraga *et al.* 2017*a*). The Rio Urubu Belt (Fraga *et al.* 2017*a*) includes foliated granitoids, charnockites and gneisses formed in a transpressional post-collisional setting. It hosts two intraplate anorthosite–mangerite–rapakivi granite complexes dated at 1.53–1.52 Ga (Heinonen *et al.* 2012) and 1.43–1.42 Ga (Lira and Lopes 2020).

Terrigenous formations with pyroclastic to volcaniclastic contributions, metamorphosed to greenschist facies, have been distinguished from the dominantly volcanic rocks and the Roraima sedimentary cover as described by Briceño *et al.* (1989) in SW Venezuela and by Santos *et al.* (2003*a*) in the westernmost portion of Roraima State. Both formations have been considered the best targets for gold investigations everywhere.

The Pakaraima Block represented by the Roraima Supergroup (Fig. 1) is the most important Orosirian sedimentary basin, covering 73 000 km^2 in parts of Venezuela, Brazi, and Guyana (Reis and Yánez 2001; Reis *et al.* 2017*a*). The U–Pb age of tuffs in the middle section at 1.87 Ga defines the minimum age of deposition whereas the mafic sills of the Avanavero Dolerite (LIP) intrudes into the strata levels at 1.79–1.78 Ga (Santos *et al.* 2003*b*; Reis *et al.* 2013*a*). Both magmatisms register the tectonic stability of the Amazonian Craton at that period of time. Some sedimentary outliers, also cut by Avanavero sills, show significant levels of dark shales (Reis and de Carvalho 1996) and reveal good targets for timescale and palaeoenvironmental studies.

Towards the south portion of the Amazonian Craton, the Central Brazil Shield encompasses to the east, a large granite-greenstone terrane as well as supracrustal and granitoid rocks at 3.05–2.30 Ga (Carajás), sometimes reworked by Transamazonian Orogeny at 2.26–2.05 Ga (Vasquez *et al.* 2019). To the west of these oldest rocks, Orosirian volcanic–plutonic rocks (*c.* 1.98 Ga) have been described by Lamarão *et al.* (2005, 2008) and can be chronologically related to the OSL (Fig. 1). They crop out amidst dominantly younger sedimentary, plutonic and volcanic rocks *c.* 1.88–1.78 Ga. In this area, the basement rocks, gneisses, metavolcanic–sedimentary successions and granitoids are genetically related to subduction settings with ages of *c.* 2.03–2.01 Ga (Santos *et al.* 2000, 2004; Vasquez *et al.* 2008).

Mineral resources. The Amazonian Craton is recognized for hosting world-class deposits. However, the few direct dates on the ores and coupled isotopic constraints of the metallogenic systems limit the development of regional models, especially for the subsequent period of the Transamazonian Orogeny (e.g. Tedeschi *et al.* 2020). We discuss below the mineral resources potentially linked to the period 1.98–1.96 Ga referred to as the OSL. See the summary in Table 1.

In some cases, the mineralizing processes are directly associated with the development of the SLIP. However, in most cases, the mineralization is approximately coeval with, but indirectly linked to, the SLIP.

The OSL has low metallogenic potential based on the published information (see Table 1 for details). The Aricheng deposit in Guyana (Alexandre 2010; Renaud 2014) represents a uranium occurrence hosted in the high-K calc-alkaline batholith at *c.* 2.10–2.07 Ga (Alexandre 2010). The mineralization is of the albitite-hosted uranium type, with zirconium ore (Cinelu and Cuney 2006), and occurs in an associated breccia fault controlled by east–west shear zones crossing the batholith. Typical IOCG mineral alteration assemblages were identified in drill cores of the batholith domains (Renaud 2014). U–Pb dating of hydrothermal zircons from the mineralized zone yielded an intercept age of 1.99 Ga, interpreted as the minimum age of mineralization, allowing a tentative age match with the OSL. The Eagle Mountain deposit, some 230 km SE of Georgetown (Guyana), is of the porphyry gold type (Voicu *et al.* 2001) and the mineralization is related to granitoids at 1.98 Ga (Nadeau *et al.* 2013), in turn hosted by

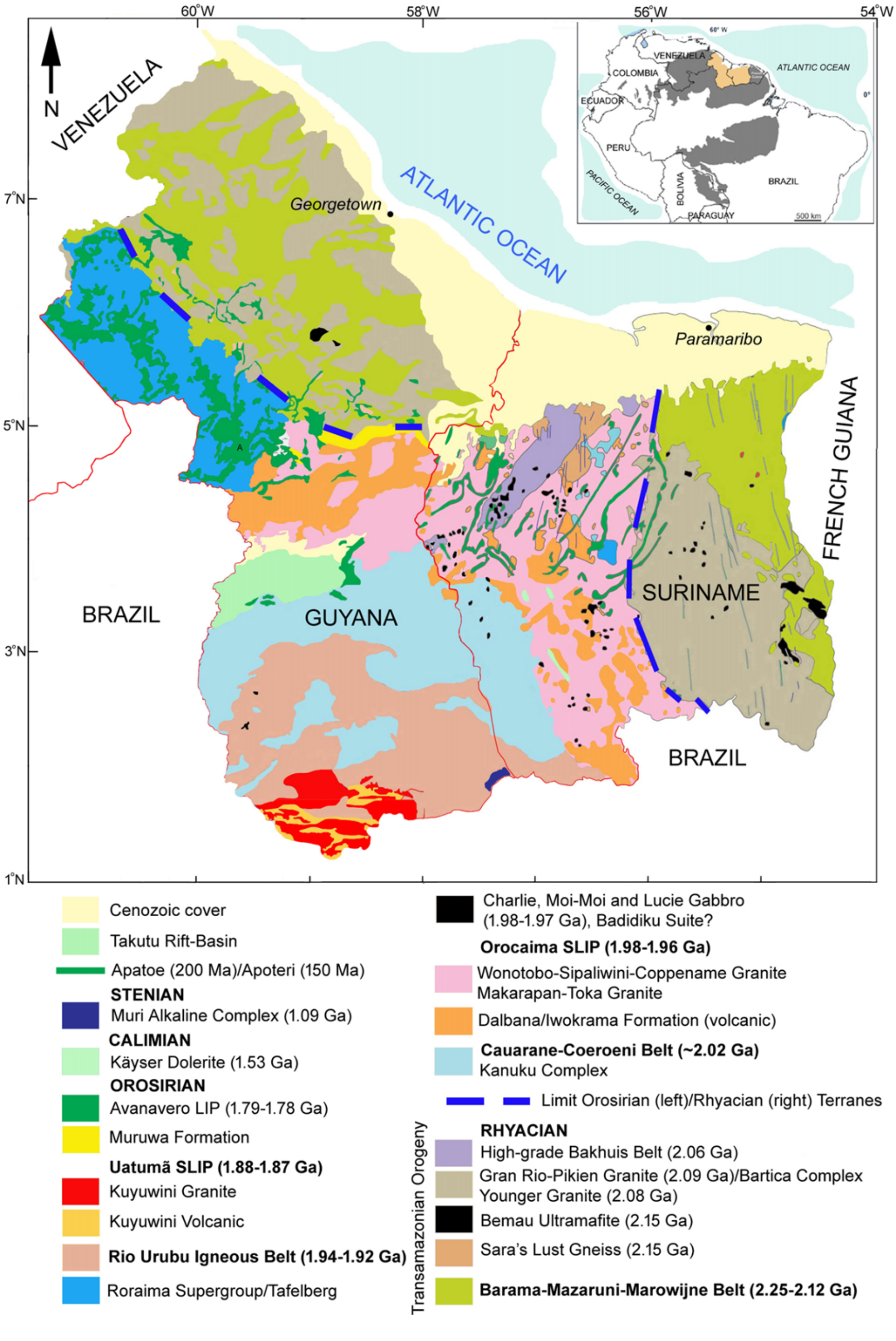

Fig. 2. An overview of the Orocaima silicic large igneous province (SLIP) across Suriname and Guyana, and the limit between Orosirian (left) and Rhyacian (right) terranes (blue dashed line). Adapted from Nadeau and Heesterman (2010) and Kroonenberg *et al.* (2016).

Table 1. *Important mineral resources associated directly or indirectly with the Orocaima silicic large igneous provinces (SLIPs) of the Amazonian Craton*

Slip	Local name	Polymetallic association	Host unit/age	Mineralization age	Reference
Orocaima	Aricheng (GU)	Albitite-hosted uranium (+zircon)	Kurupung Batholith [(ZrnTtn) 2.07–2.10 Ga]	(ZrnTtn) 1995 Ma	Alexandre (2010)
	Mountain Eagle (GU)	Au + Mo porphyry or orogenic	Iwokrama Granite [(ZrnLA)1980 Ma]	(ZrnLA) 1980 Ma	Nadeau *et al.* (2013)
	Morro do Bezerro (RR)	Mo-bearing granite	Saracura Suite [(ZrnS) ~1970 Ma]	(ZrnS) ~1970 Ma	CPRM (1999); Fraga *et al.* (2017*b*)
	Tocantinzinho (PA)	Au–PO	Tocantinzinho Granite [(ZrnTtn, ZrnS) 1989–1982 Ma]	(ZrnTtn; ZrnS) 1989–1982 Ma; (AmpAA) 1967	Borgo *et al.* (2017)
	Coringa (PA)	Au + Ag- (base metal) low-sulfidation EPI	Vila Riozinho Group (2002–1966 Ma) Serra Granite (1999–1989 Ma)	~1989 Ma	Lamarão *et al.* (2002) Guimarães and Klein (2020)

Abbreviations: Method – S, U–Pb SHRIMP; LA, U–Pb laser ablation; AA, Ar–Ar. Minerals (according to Whitney and Evans 2010) – Amp, amphibole; Ttn, titanite; Zrn, zircon. Deposits – EPI, epithermal; PO, porphyry. Country/state – GU, Guyana; PA, Pará; RR, Roraima.

metavolcanic rocks of the Barama–Mazaruni greenstone belt (Kroonenberg and de Roever 2010). The ore is widespread in the saprolitic rock or as stockworks, where it forms a bimetallic association with Mo and Cu.

In Venezuela, Mo-rich granitoids occurs in the contact with volcanic rocks (Sidder and Mendoza 1991). Similarly, in the northeastern portion of the Roraima State, Brazil, molybdenite-bearing granite was described in spatial association with volcanic–plutonic rocks attributed to the OSL. The granite has been affected by east–west shear zones related to the K'Mudku tectonothermal event about 1.20 Ga (CPRM 1999).

Towards the Central Brazil Shield, important gold deposits are associated with the Tapajós Mineral Province (TMP). They give a wide range of ages, from 2.03 to 1.80 Ga, attributed to the rocks of the province (Lamarão *et al.* 2002; Borgo *et al.* 2017; Guimarães and Klein 2020 and references therein). Tentatively, some of these deposits may be associated with the OSL, as detailed below:

Two of the largest mineral deposits are recognized in the TMP: Coringa and Tocantinzinho. The first one is an Au–Ag (Cu–Pb–Zn) polymetallic deposit hosted in a volcanic–plutonic association dated at 1.99–1.96 Ga old (Guimarães and Klein 2020 and references therein). The mineralization occurs in veins or in shear zones where gold is associated with quartz, silver, sphalerite, pyrite, and subordinately, galena, chalcopyrite and hematite. Gold also occurs disseminated in alteration zones of host rock as well as in pyrite, sphalerite and silver telluride inclusions. The deposit is interpreted as a low-sulfidation epithermal type (Tokashiki *et al.* 2013; Corrêa-Lima and Klein 2020 and references therein).

The Tocantinzinho gold deposit is associated with high-K calc-alkaline plutonic rocks dated at 1.98–1.97 Ga, constrained by NW–SE strike-slip faults and with an elongated geometry (Borgo *et al.* 2017). Subvolcanic types, believed to have formed in an intraplate setting are coeval or slightly younger than the granitoid rocks and may be linked to feeder dykes in depth (Santiago *et al.* 2013; Biondi 2020 and references therein). The mineralization occurs associated with mild to moderate hydrothermalized rock varieties (e.g. Santiago *et al.* 2013 and references therein). Gold is associated with sericitization zones also containing pyrite, chalcopyrite, sphalerite and galena in veinlets and breccias or disseminated in pyrite, feldspar and quartz. In the breccias, high gold concentrations are associated with chlorite ± carbonate ± quartz ± rutile ± pyrite ± galena. The deposit has varied characteristics with similarities to intrusion-related gold deposits and mesozonal intrusion-hosted gold deposits as well as Au-rich porphyry deposits hosted in oxidized granites (Biondi *et al.* 2018 and references therein) or (magmatic-hydrothermal) oxidized calc-alkaline granite-related gold deposits (Lopes and Moura 2019 and references therein).

Matches with 1.98–1.96 Ga magmatism on other crustal blocks. The 1.98–1.96 Ga mafic and silicic magmatism of Amazonia matches in age the Pechenga–Onega LIP event of the Kola and Karelia cratons in the Baltic Shield (Lubnina *et al.* 2016; Davey 2019). Additional age matches include the 1.97 Ga Khajuraho (Jhansi) dolerite dyke swarm of the Bundelkhand craton (Samal *et al.* 2019) and the 1.97 Ga dolerite Xiwangshan swarm of the North China craton (Peng 2015).

The Uatumã SLIP (1.88–1.87 Ga)

Distribution. Another very large event covering more than 1 600 000 km^2 is the 1.88–1.87 Ga Orosirian felsic volcanic–plutonic rocks, which occur in both shields of the Amazonian Craton. This event was first described as a being related to a large igneous province by Fernandes *et al.* (2011), later designated as the Uatumã SLIP – USL – by Klein *et al.* (2012) – Figure 1.

In the Guiana Shield, the USL occurs in the southern portion of Roraima State (Almeida 2006; Reis *et al.* 2021), in the NE of Amazonas State (Valério *et al.* 2009; Ferron *et al.* 2010; Klein *et al.* 2012), in the NW of Pará State (Barreto *et al.* 2014; Leal *et al.* 2018) and south of Guyana (Gibbs and Barron 1993).

The northwestern portion of the Central Brazil Shield is the largest area of the USL, but recently a U–Pb investigation was done in rocks of the southmost sector of the shield, as an inlier into the Parecis Basin, providing results of *c.* 1.88 Ga that match those of the USL (Lima *et al.* 2021; Figure 1). Some anorogenic granites cross-cut Archean domains (Carajás) and also probably belong to the SLIP, as well as the adjoining 1.88 Ga mafic dyke swarm (Teixeira *et al.* 2019; Antonio *et al.* 2021).

As the OSL, the USL is exceptionally well preserved, with no influence of the Transamazonian Orogeny or its late stages. Where itcrops out, the USL encompasses high-K calc-alkaline and A-type volcanics and granites (Fernandes *et al.* 2008; Juliani and Fernandes 2010; Fraga *et al.* 2017*c*). The timing between both rock types suggests that the high-K calc-alkaline magmatism preceded the alkaline magmatism. Nevertheless, recurrences of magmatic pulses and coexistence of these magmas have been suggested by the geochemistry of the layers (acid to intermediate) and geochronological data (Vasquez and Dreher 2011). In addition, a charnockitic magmatism (1.87 Ga) has been described in the SE of the Roraima State (Almeida *et al.* 2008), matching in age the USL. From a tectonic point of view, this SLIP magmatism has been tectonically assigned to either an extensional environment related to underplating mechanisms or post-dating a soft collision process related to the Orosirian orogenic evolution that eventuallly formed the Tapajós crust (Santos *et al.* 2000, 2001, 2004; Fernandes *et al.* 2011; Antonio *et al.* 2017; Teixeira *et al.* 2019; Vasquez *et al.* 2019; Guimarães and Klein 2020).

Mineral resources. In the Central Brazil Shield, the TMP, where USL rocks are widespread, hosts a large gold panning production area where the country rocks are as old as 2.03–2.01 Ga (Santos *et al.* 2000, 2004; Vasquez *et al.* 2008; Figure 3). There has been unofficial historical production of greater than 600 tons of gold extracted from alluvial sources from more than 2200 'garimpos' sites since the 1980s (Borgo *et al.* 2017; Corrêa-Lima and Klein 2020). In this millennium, dozens of previous studies (Santos *et al.* 2004; Santiago *et al.* 2013; Villas *et al.* 2013; Assunção and Klein 2014; Juliani *et al.* 2014; Klein *et al.* 2016 and references therein) were mainly focused on hydrothermal alteration and mineralization, as well as the geological history of the province in terms of geotectonic evolution and structural controls.

Detailed studies of some of the main deposits, with a focus on proposing genetic models, have consisted of the characterization of host rocks, hydrothermal and metasomatic processes and the nature and evolution of ore fluids (Juliani *et al.* 2005, 2013; Borges *et al.* 2009; Tokashiki *et al.* 2013; Assunção and Klein 2014; Silva and Klein 2016; Borgo *et al.* 2017; Biondi *et al.* 2018; Queiroz and Klein 2018; Lopes and Moura 2019; Oliveira *et al.* 2019; Biondi 2020; Corrêa-Lima and Klein 2020; Guimarães and Klein 2020 and references therein). Primary gold from the TMP generally occurs in quartz veins hosted in felsic volcanic and volcaniclastic rocks and also in granitoids. Hydrothermal breccias have also been recognized and often follow the mineralized veins (Dreher *et al.* 1999). Generally, the individual deposits of the TMP have been described as orogenic, intrusion-related/magmatic-hydrothermal, porphyry, epithermal and palaeoplacer (Guimarães *et al.* 2021).

Epithermal gold mineralization and high to low-sulfidation occurrences are mostly associated with volcanic and volcaniclastic rocks, which have been strongly altered by hydrothermal processes and associated with caldera complexes (Juliani *et al.* 2005). The high-sulfidation gold mineralization can be attributed to hydrothermal breccia pipes and related alteration processes forming very fine grains of native Au, Ag and Cu. These deposits are related to the final stages of the post-collapse phase of the volcanic calderas (e.g. Au–Cu–Ag and Cu–Zn–Mo, see Table 2 to Botica Velha deposit). Ar–Ar alunite dating of the high-sulfidation epithermal mineralization shows ages of *c.* 1.87 Ga and volcanic quiescence at 1.84 Ga (Juliani *et al.* 2005).

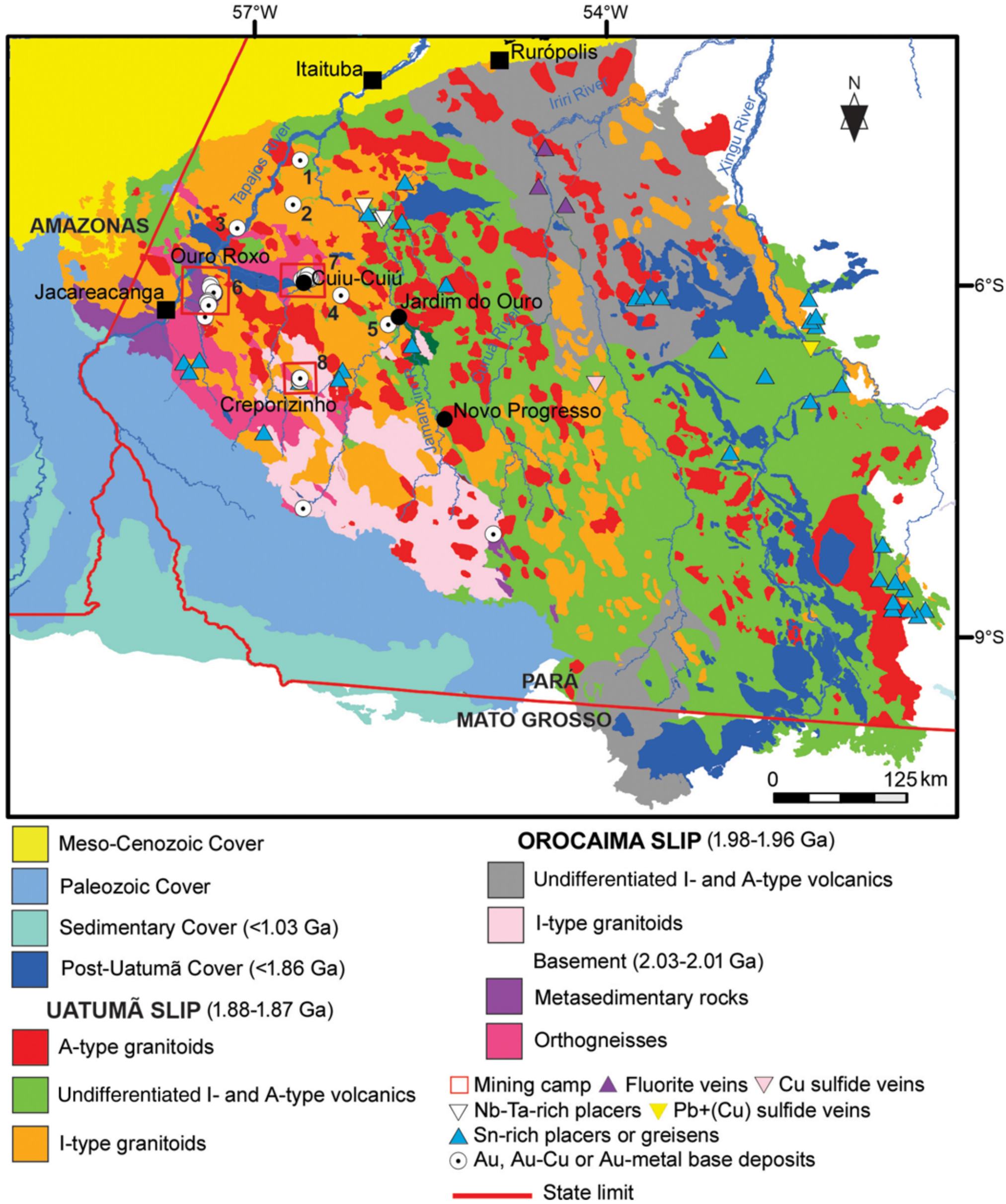

Fig. 3. Simplified geological map of the Tapajós Mineral Province, Central Brasil Shield. Main deposits: 1, Chapéu do Sol; 2, Botica; 3, Batalha; 4, Tocantinzinho; 5, Palito; 6, Cantagalo–Ouro Roxo mining camp (includes São José, Ouro Roxo and Porto Rico deposits, see Table 2); 7, Cuiu-Cuiú mining camp (includes Guarim, Moreira Gomes, Central, Jerimum de Cima, Jerimum de Baixo, Pau da Merenda and Babi deposits, see Table 2); 8, Creporizinho mining camp.

The low-sulfidation gold mineralization is located at the border of a caldera complex and shows an overprint of porphyry style Cu–Mo–(Au) mineralization associated with several porphyry dykes. Porphyry-type gold mineralization mainly consists of Au–(Cu) (see Table 2 for Palito and Chapéu do Sol deposits; Echeverri-Misas 2010, 2015; Aguja-Bocanegra 2013) formed during the syn-post-collapse phase of the volcanic caldera and emplacement of high-K calc-alkaline granites at 1.88 Ga.

Specialized, 1.88 Ga A-type granites host Sn, W, Bi, Nb, Ta, Be and Li (Lamarão *et al.* 2002; Pinho

Table 2. *Important mineral resources associated directly or indirectly with the Uatumã SLIP of the Amazonian Craton*

Slip	Local name	Polymetallic association	Host unit/age	Mineralization age	Reference
Uatumã	(RR)	VTM anorthosite and gabbro	Uraricaá Suite [(ZrnS) 1882 Ma]	(ZrnS) 1882 Ma	Reis and Ramos (2017)
	(PA)	TM anortosite and gabbro	Jutaí Anorthosite [(TtnS) 1878 Ma]	(TtnS) 1878 Ma	Santos *et al.* (2001)
	Sossego-Curral (PA)	IOCG	Granophyric granite [(ZrnLA) 2740 Ma]	(MnzLA) 1879–1904 Ma	Moreto *et al.* (2015)
	Alvo 118 (PA)	IOCG	Grão Pará Group [(ZrnS) >2680 Ma]	(XtmS) 1868–1869 Ma; (BtAA) 1885 Ma	Pollard *et al.* (2018); Trendall *et al.* (1998); Tallarico (2003)
			Metavolcanic [(ZrnS) 2645 Ma]		Tallarico *et al.* (2004)
			Tonalite [(ZrnS) 2743 Ma]		Tallarico *et al.* (2004)
					Tallarico *et al.* (2004)
	Breves (PA)	Cu + Au–(Mo–W–Bi–Sn)	A-type granitoid [(ZrnS) 1878–1880 Ma]	(Xtm + MnzS) 1872 Ma; (BtAA) 1885 Ma	Pollard *et al.* (2018); Tallarico *et al.* (2004)
			Metasedimentary hydrothermalized rock/Águas Claras Formation [(ZrnT) 2778–3048 Ma]		Macambira *et al.* (2001)
	Estrela (PA)	Cu + Au–(Li–Be–Sn–W–Mo)	A-type granitoid [(ZrnT) 1880–1875 Ma]	(BtAA) 1896 Ma	Pollard *et al.* (2018); Lindenmayer *et al.* (2005)
			Grão Pará Group [(ZrnS) >2680 Ma]		Trendall *et al.* (1998)
	Gameleira (PA)	Cu + Au–(Co–F–U–Mo–REE)	Pojuca Granite [(ZrnT) 1874 Ma]	(BtAA) 1907 Ma	Machado *et al.* (1991); Pinheiro (2019)
			Metavolcanosedimentary [(ZrnT) ~2760 Ma]		Machado *et al.* (1991)
	Águas Claras (PA)	Cu + Au + W	Águas Claras Formation [(ZrnT) 2778–3020 Ma]	(E)1880 Ma	Grainger *et al.* (2008)
			Águas Claras Formation [(ZrnT) 2871–3048 Ma]		Macambira *et al.* (2001)
	Pojuca (PA)	VMS Cu + Zn	Igarapé Pojuca Group (>2700 Ma)	(E) 1874* Ma	Machado *et al.* (1991); Schwarz and Frantz (2013)
	Tarzan (PA)	Cu + Co	Igarapé Cigarra Formation [(E) ~2750 Ma]	(ZrnT) 1880 Ma	Machado *et al.* (1991); Pinheiro (2019)
	Serra Pelada (PA)	Au + Pd + Pt	Águas Claras Formation [(ZrnT) 2778–3048 Ma]	(BtAA) 1882 Ma	Macambira *et al.* (2001); Grainger *et al.* (2008)
	Antonio Vicente (PA)	Sn + W + Nb + Ta and related greisens	Velho Guilherme Suite [(ZrnPE) 1867 Ma]	~1867 Ma	Teixeira *et al.* (2002)
	Mocambo (PA)	Sn + W + Nb + Ta and related greisens	Velho Guilherme Suite [(ZrnPE) 1862 Ma]	~1862 Ma	Teixeira *et al.* (2002)
	Pedra Preta (PA)	Sn + W + Nb + Ta and related greisens	Velho Guilherme Suite [(ZrnPE) ~1870 Ma]	~1870 Ma	Teixeira *et al.* (2002)
	Maloquinha (PA)	Sn, W, Bi, Nb, Ta, Be and Li	Maloquinha Suite [(ZrnPE) 1880 Ma]	~1880 Ma	Lamarão *et al.* (2002)
	Batalha (PA)	Deeper PO gold	Parauari Suite [(ZrnT) 1879–1883 Ma]	~1879 Ma	Santos *et al.* (2000)
	Palito (PA)	PO Au + Cu	Parauari Suite [(ZrnPE) 1883 Ma]	~1883 Ma	Echeverri-Misas (2015)
	Chapéu do Sol (PA)	Cu–Mo–(Au) low-sulfidation	Subvolcanic porphyry [(ZrnS) 1880–1861 Ma]	~1861 Ma	Aguja-Bocanegra (2013)
	Botica Velho (PA)	Au–Cu–Ag–(Cu–Zn–Mo) high sulfidation	Volcanosedimentary (1877–1888 Ma)	(AluAA) 1869–1876 Ma	Santos *et al.* (2001); Lamarão *et al.* (2002)
	Ouro Roxo (PA)	Au–Cu–Bi mesothermal	Tropas Suite [(Zrn + tT) 1983–1987 Ma; 1900–1880 Ma]	(PyPP isochron age) 1858 Ma	Santos *et al.* (2004); Veloso and Santos (2013); Klein and Carvalho (2008)
	Porto Rico (PA)	Au–Cu–Bi mesothermal	Tropas Suite [(Zrn + tT) 1983–1987 Ma; 1900–1880 Ma]	(E) 1858 Ma	Klein and Carvalho (2008)
	São José (PA)	Au–Cu–Bi mesothermal	Tropas Suite [(Zrn + tT) 1983–1987 Ma; 1900–1880 Ma]	(E) 1858 Ma	Klein and Carvalho (2008)
	Moreira Gomes (PA)	Orogenic gold	CreporiZrnão Suite [(ZrnPE) 1997 Ma]	(PyPP model age) 1816–1858 Ma	Silva *et al.* (2015)
	Central (PA)	Orogenic gold	Parauari Suite [(ZrnPE) 1885 Ma]	(PyPP model age) 1908–1888 Ma	Silva *et al.* (2015)
	Guarim (PA)	Orogenic gold	Cuiu-Cuiú Complex (2033–2005 Ma)	>1871 Ma (E)	Santos *et al.* (2004)
	Pau da Merenda (PA)	Orogenic gold	Cuiu-Cuiú Complex (2033–2005 Ma)	(PyPP model age) 1885–1871 Ma	Santos *et al.* (2004); Silva *et al.* (2015)
	Jerimum de Cima (PA)	Orogenic gold	Cuiu-Cuiú Complex (2033–2005 Ma)	>1871 Ma (E)	Santos *et al.* (2004)
	Jerimum de Baixo (PA)	Orogenic gold	CreporiZrnão Suite [(ZrnPE) 1997 Ma]	>1858 Ma (E)	Silva *et al.* (2015)
	Babi (PA)	Orogenic gold	Cuiu-Cuiú Complex (2033–2005 Ma)	>1871 Ma (E)	Santos *et al.* (2004)

Abbreviations: Method – S, U–Pb SHRIMP; LA, U–Pb laser ablation; AA, Ar–Ar; PE, single zircon Pb-evaporation; PP, Pb-Pb step-leaching; T, ID-TIMS; E, estimated. Minerals (according to Whitney and Evans 2010) – Alu, alunite; Bt, biotite; Mnz, monazite; Py, pyrite; Ttn, titanite; Xtm, xenotime; Zrn, zircon. Deposits – VTM, vanadiferous–titanomagnetite-bearing; TM, titanomagnetite-bearing; VMS, volcanic-exhalative massive sulfide; IOCG, iron oxide–copper–gold; PO, porphyry. Country/state – PA, Pará; RR, Roraima.

et al. 2006). In contrast, the calk-alkaline, I-type granites with U–Pb–thermal ionization mass spectrometry zircon ages of *c.* 1.88–1.87 Ga (Santos *et al.* 2000; Silva *et al.* 2015 and references therein) show more significant contributions to the concentration of gold and base metals, both correlated to magmatic–hydrothermal fluids in plutonic rocks. Such mineral resources can be grouped into two types: (1) deep porphyry, intrusion-related and orogenic deposits; and (2) volcanic–plutonic, porphyry–epithermal systems. Batalha is a deep porphyry-style gold deposit, whereas Cuiu-Cuiú, Crepori, Ouro Roxo, São José and Porto Rico are intrusion-related deposits (Assunção and Klein 2014; Silva *et al.* 2015; Silva and Klein 2016; Oliveira *et al.* 2019; see Table 2 for details).

The Cuiu-Cuiú gold district includes several occurrences and deposits associated with shear zones developed in granitoids and the gold mineralization can be related to 1.88 Ga rocks (see Table 2 for details). Gold occurs in free form or as inclusions in the paragenesis of sulfides in quartz veins, where an intense sericitization occurs in some deposits (see Table 2 to Moreira Gomes, Central, Pau da Merenda deposits, among others). Pb–Pb isochron ages at 1.85 Ga provide an estimate of the mineralization timing of the deposits (Veloso and Santos 2013; Silva *et al.* 2015).

The Carajás Mineral Province (Fig. 4), in the southeastern Amazonian Craton, is one of the largest metalliferous provinces in the world, with giant iron ore deposits in addition to Cu–Au, Cu–Zn, Mn, Ni, REE and PGE. A recent tectonic evolution model for the province (e.g. Tavares *et al.* 2018) discusses the presence of superimposed orogenic and extensional cycles from the Archean to the Neoproterozoic–Cambrian times. The province documents three major Archean–Paleoproterozoic orogenic

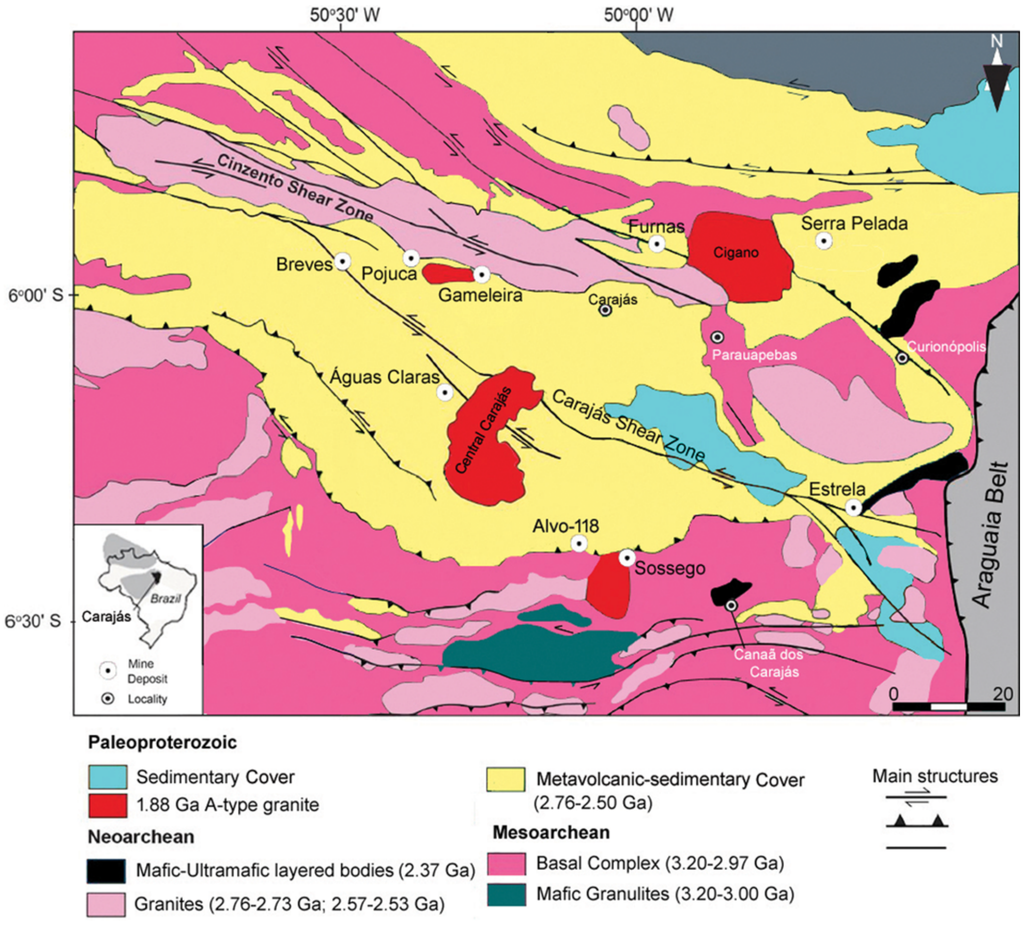

Fig. 4. Simplified geological map of the Carajás Mineral Province with location of some deposits and mines. Modified from Trunfull *et al.* (2020). See Table 2 for details.

events with the latest followed by late to post-orogenic sedimentation, swarms of felsic and mafic dykes and 1.88 Ga anorogenic alkaline to subalkaline A-type magmatism (Giovanardi *et al.* 2019; Trunfull *et al.* 2020; Antonio *et al.* 2021).

It is widely accepted that the USL granitic plutons (e.g. Central Carajás, Young Salobo, Cigano, Pojuca and Breves plutons, among others) were probably the main cause of the thermal disturbance that affected the older rocks forming a complex hydrothermal system in pre-existing regional shear zones (e.g. Bettencourt *et al.* 2016 and references therein). This hydrothermal system was responsible for the genesis of IOCG and Cu-rich polymetallic deposits. A younger epigenetic phase related to Cu–Zn and Cu–Co deposits can be related to the remobilization of pre-existing mineralizations during the 1.88 Ga magmatism. The percolation of fluids during the younger emplacement is also believed to have been caused by the latter phase of hydrothermal alteration linked to the IOCG-type deposits (see Table 2 for all details), where multiphase mineralization pulses with ages of *c.* 2.71–2.57 Ga and 2.0–1.88 Ga are recognized.

A younger phase of A-type magmatism at 1.87 Ga hosts Sn, W and Nb–Ta mineralization (Trunfull *et al.* 2020). Post-magmatic alteration and Sn–W mineralization are reported in granitic plutons and greisenized zones and to a lesser extent are associated with Nb and Ta.

In the Guiana Shield, there are few records of mineral occurrences related to the 1.88–1.87 Ga USL event. According to Teixeira *et al.* (2019), several mafic bodies are contemporaneous with the Uatumã magmatism based on tight age matches and a similar intraplate setting. In Roraima State, near the border with Guyana, an occurrence of anorthosite with vanadiferous titanomagnetite was reported by Goulart *et al.* (2019); this mineralization occurs in a gabbro-anorthositic layered intrusion. Other mafic–ultramafic bodies in the Roraima State have been grouped with the Uraricaá Suite, for which a U–Pb age of 1.88 Ga is reported (see Table 2).

Matches with 1.88–1.87 Ga magmatism on other crustal blocks. In a broader perspective this 1.88–1.87 Ga volcanic–plutonic episode matches the early Svecoffenian magmatism in Baltica (Nironen *et al.* 2000), the circum-Superior LIP in the Superior Craton (Jowitt and Ernst 2013) and also the intraplate magmatism in the Slave, southern Siberian, Indian and Kalahari cratons (Ernst *et al.* 2013, 2021; Ernst 2014 and references therein).

The Alta Floresta SLIP (1.80–1.79 Ga)

Distribution. The term 'Alta Floresta SLIP' – AFSL – is proposed in this study to comprise calc-alkaline volcanic and granitic rocks emplaced over a short-lived period of 10 myr, between 1.80 and 1.79 Ga, that covered parts of Mato Grosso and Amazonas State, Central Brazil Shield (Fig. 1). This SLIP surrounds the southern and western flanks of the Alto Tapajós Horst along the boundary between Amazonas, Pará and Mato Grosso State (Fig. 5). Some alkaline granites with the above age may be also attributed to the AFSL, but there is still no strong evidence for associated alkaline volcanic rocks. The tectonic setting of the volcano-plutonism remains debated, as to whether it is a post-collisional (Cordani and Teixeira 2007; Assis 2015; Scandolara *et al.* 2017) or an intracontinental setting (Rizzotto *et al.* 2019).

The AFSL includes volcanic and subvolcanic rocks associated with the pyroclastic and sometimes epiclastic rocks that were previously grouped into the Colíder Group (Rizzotto *et al.* 2004). In the western sector of the horst, in Amazonas State, they show dominant calc-alkaline affinity and are medium to high-K. Noteworthy, the Alto Tapajós Horst that bounds the AFSL contains a lower volcanic–sedimentary succession *c.* 1.76–1.74 Ga cut by the Mata-Matá Gabbro at 1.57 Ga (Betiollo *et al.* 2009) and an upper, significantly younger sedimentary one (<1.03 Ga; Reis *et al.* 2013*b*, 2017*b*). They are related to the development of a large intracratonic rift system, following multiple stages of magmatism.

The granitoid rocks of the AFSL are grouped into the Paranaíta Suite (P.S.E. Ribeiro and Duarte 2010), represented by oxidized, high-potassium calc-alkaline I-types, which are meta- to peraluminous and strongly magnetic. An important feature in the field is the presence of a large concentration of volcanic enclaves, as well as interdigitated and lobed contacts between the plutonic and volcanic rocks, suggesting the contemporaneous nature of these lithologies. Further south, the AFSL surrounds a calc-alkaline suite dated in the 1.78–1.76 Ga interval (Fig. 5) and which was previously considered to be part of the province (Rizzotto *et al.* 2019). Importantly, these rocks are not considered here to be part of the AFSL, whose minimum age does not exceed 1.79 Ga. These authors coined the name 'Western Amazonia Igneous Belt' for the plutonic suites that occur in the area of the AFSL, where the more evolved granitic intrusions have A-type characteristics and an intraplate character. According to our conception, ages of about 1.77–1.75 Ga documented for the volcanic rocks in the same area can be attributed to the younger volcano-sedimentary succession at the base of the Alto Tapajós Horst. Our interpretation also diverges from the sedimentary stratigraphic propositions by Simões *et al.* (2020) for the Alta Floresta Province, given that they did not consider the most recent regional mapping

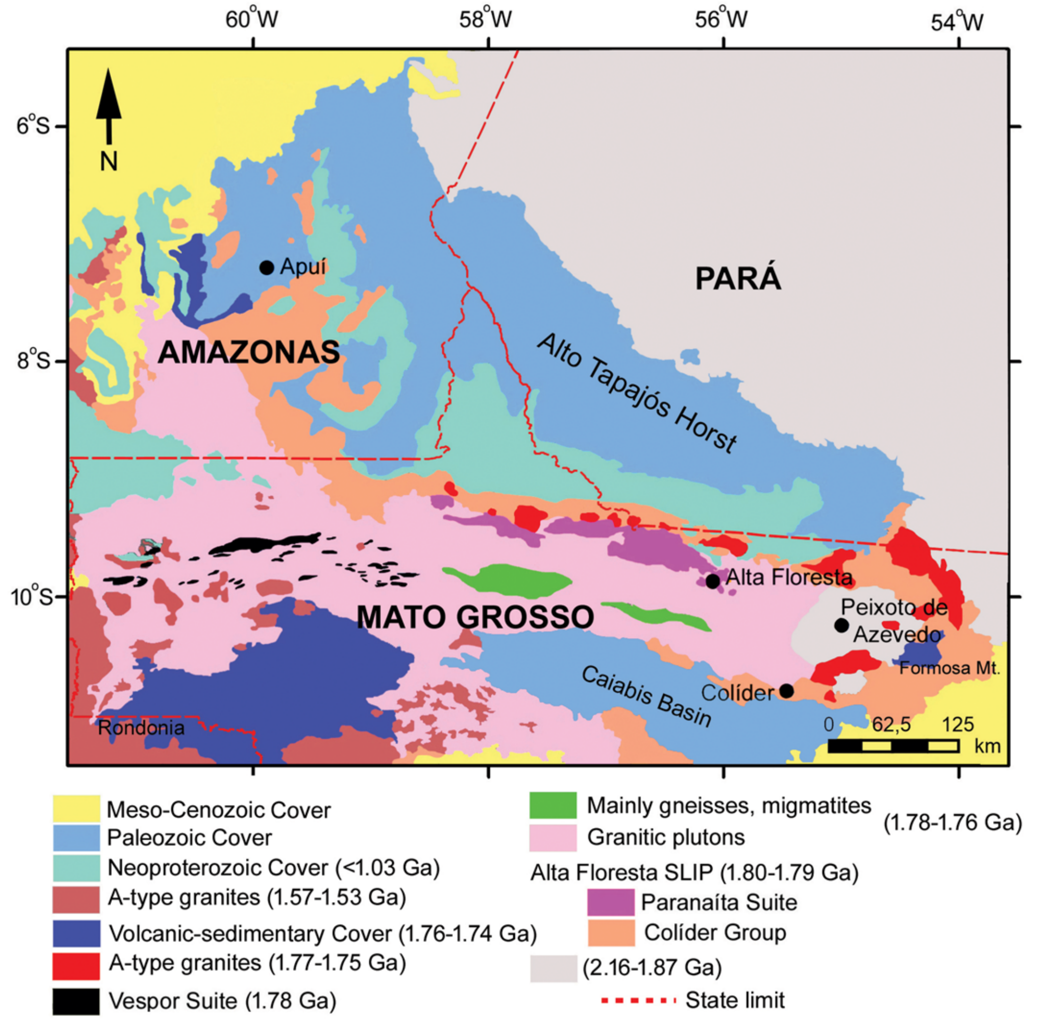

Fig. 5. Simplified geological map of the Alta Floresta SLIP (after Ribeiro and Duarte 2010).

results available for the whole area (Almeida 2016; Reis *et al.* 2017*b*).

Mineral resources. The Alta Floresta Mineral Province (Fig. 6), to which the AFSL are genetically and spatially related, hosts numerous occurrences of gold and gold + base metals closely associated with the volcanic and volcanoclastic rocks, and also granitoids (Alves *et al.* 2019; Rios *et al.* 2019 and references therein). For instance, the calc-alkaline rocks of the Paranaíta Suite are associated with the main gold deposits of the Alta Floresta Mineral Province. Some deposits are better known, with well-defined ages and with a proposed model for the ore concentration (for details and references see Table 3 and Fig. 6). Geochronological data suggest that the deposits of the Alta Floresta Mineral Province may have been controlled by a complex hydrothermal system, with the development of deposits formed in the epizone and mesozone, directly related to a volcano-plutonic activity in an intraplate environment (Silva and Abram 2008; Miguel 2011; Assis 2015 and references therein). The volcanic–plutonic magmatism (i.e. AFSL) was the source of the fluid and heat, controlling the hydrothermal system during the development of the gold and polymetallic deposits in the province.

Analytical results indicate the link between some mineralized deposits and the volcanic or volcanic–plutonic magmatic phases (Silva and Abram 2008; Assis 2015; Rios *et al.* 2019 and references therein). U–Pb SHRIMP zircon dating performed by Serrato

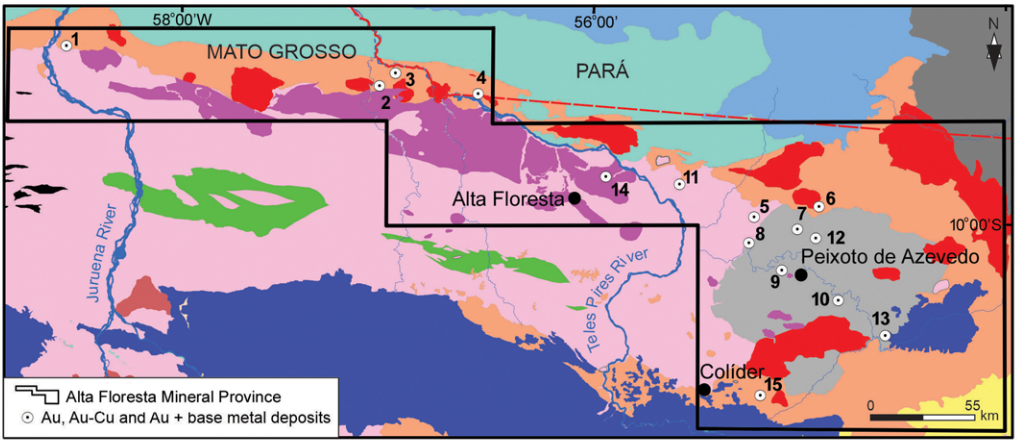

Fig. 6. Simplified geological map of the Alta Floresta Mineral Province (after Ribeiro and Duarte 2010). Deposits: 1, Juruena; 2, Papagaio; 3, Pé de Anta; 4, Cajueiro; 5, Luizão; 6, Guarantã Ridge Target; 7, Serrinha de Guarantã; 8, Aragão; 9, Paraíba; 10, Pé Quente; 11, Trairão; 12, X1; 13, Francisco; 14, Pé de Fora; 15, Edu. See Table 1 for details. Legend as in Figure 5.

(2014) supports the temporal relation of the AFSL at 1.80–1.79 Ga to the evolution of the mineral systems. The author reported ore dating in the mineralized zone yielding an Re–Os model age in molybdenite of 1.80 Ga. The Ar–Ar, U–Pb and Re–Os results available for other deposits of the province (see Table 3 for details) indicate a consistent period of mineralization between 1.80 and 1.78 Ga. Re–Os analyses in pyrite from mineralized zones of the Pé-Quente and Luizão deposits yielded model ages of *c.* 1.80–1.79 Ga, while the Re–Os data in molybdenite (X1 deposit) provided an age of 1.78 Ga (Serrato 2014; Assis *et al.* 2017). These robust Re–Os ages in the 1.79–1.78 Ga interval link the AFSL development to an important metallogenic time in the Amazonian Craton. Recent U–Th–Pb SHRIMP dating in hydrothermal monazites from Trairão and Chumbo Grosso gold deposits (Rocha *et al.* 2020) yielded upper intercept ages of 1.80 and 1.79 Ga (see Table 3).

Towards the Guiana Shield, in the Pitinga Mineral Province, the Nb-, Ta-, U-, REE-, Zr- and F-rich Água Boa and Madeira granitic plutons belong to the Madeira Suite dated at 1.82–1.81 Ga (Bastos Neto *et al.* 2014 and references therein). The plutons are tin-mineralized and exploited (Fig. 7, Table 3).

The Água Boa pluton is composed of four facies where the earlier corresponds to a coarse-grained rapakivi facies, followed by a fine-grained porphyritic biotite syenogranite, a coarse- to medium-grained biotite alkali feldspar granite and topaz-bearing porphyritic granite. The topaz-bearing porphyritic granite is the younger facies dated at 1.80 Ga (Lenharo 1998), similar in age to the AFSL. Cassiterite-rich greisens and episyenites are associated with the hydrothermalized facies of the Água Boa pluton (Borges *et al.* 2003; Feio *et al.* 2007 and references therein). An Ar–Ar plateau age in mica of 1.78 Ga from greisens defines the closing temperature of the hydrothermal activity (Lenharo *et al.* 2003).

The Madeira pluton (Fig. 7) exhibits four facies (Lenharo *et al.* 2003; Costi *et al.* 2009 and references therein). The oldest facies comprises a fine- to medium-grained porphyritic rapakivi granite (amphibole–biotite syenogranite). This facies is intruded by the medium- to fine-grained equigranular biotite alkali feldspar granite, in turn cut by an alkali feldspar hypersolvus porphyritic granite, and finally by an albite-enriched granite as the third facies. The latter facies hosts uncommon cryolite mineralization, along with columbite–tantalite, pyrochlore and to a lesser extent, rare earth minerals, cryolite, torite, uraninite, ilmenite and magnetite (Borges *et al.* 2009; Bastos Neto *et al.* 2012 and references therein). Pb–Pb and U–Pb zircon ages at 1.82–1.79 Ga are known for the Madeira pluton facies (Lenharo 1998; Costi *et al.* 2000; Bastos Neto *et al.* 2014). The albite granite facies mineralization is dated with a U–Pb SHRIMP zircon age of 1.79 Ga and with an Ar–Ar mica age of 1.78 Ga (Lenharo 1998).

Matches with 1.80–1.79 Ga magmatism on other crustal blocks. AFSL roughly matches the 1.81–1.76 Ga Transscandinavian Igneous Belt (Åhäll and Larson 2000; Johansson 2009) that similarly comprises granitoids and felsic volcanic rocks with subordinate mafic components that crop out from southern Sweden to northern Norway (Baltica).

Table 3. *Important mineral resources associated directly or indirectly with the Alta Floresta SLIP of the Amazonian Craton*

Slip	Local name	Polymetallic association	Host unit/age	Mineralization age	Reference
Alta Floresta	Água Boa (AM)	Sn–greisen/Sn–episyenite (topaz–Be–F–Zr–Zn–Ti–Pb–Cu)	Madeira Suite [(ZrnLA) 1824–1816 Ma; (ZrnS) 1815 Ma; (ZrnLA) 1798 Ma]	(MsAA) 1783 Ma	Bastos Neto *et al.* (2014)
	Madeira (AM)	Ta + Nb + U + Th + ETR + Sn cryolite-bearing albite-enriched granite	Madeira Suite [(ZrnPE)1824 Ma–1818 Ma; (ZrnS) 1810 Ma; (ZrnS) 1794 Ma; (ZrnLA) 1822 Ma]	(MsAA) 1782 Ma	Costi *et al.* (2000); Bastos Neto *et al.* (2014)
	(PA)	Nb–Ta–Sn-bearing granite	Porquinho Suite [(ZrnS) 1786 Ma]	~1786 Ma	Santos *et al.* (2004)
	Trairão (MT)	PO or intrusion-related gold	Matupá Suite [(ZrnLA) 1889 Ma; (ZrnS) 1854–1878 Ma]	(MnzS) 1798 Ma; (MolAA) 1785 Ma	Rocha *et al.* (2020); Silva and Abram (2008)
	Chumbo Grosso (MT)	PO or intrusion-related gold	Matupá Suite [(ZrnS) 1878–1854 Ma]	(MnzS) 1805 Ma	Rocha *et al.* (2020)
	Pé Quente (MT)	EPI or intrusion-related gold	Pé Quente Tonalite [(ZrnS) 1901 Ma]	(PyRO) 1784–1792 Ma; (MolAA) 1830–1853 Ma	Assis *et al.* (2017); Assis (2015)
	Francisco (MT)	Au + (Zn–Pb–Cu) intermediate sulfidation	Porphyry União (1775 Ma)	(MsAA) 1777–1779 Ma	Assis (2015); Miguel (2011)
	Luizão (MT)	EPI or intrusion-related gold	Novo Mundo Granite [(ZrnS) 1970–1956 Ma]	(PyRO) 1782–1805 Ma	Assis *et al.* (2017)
	Juruena (MT)	Porphyry gold	Paranaíta Suite [(ZrnS) ~1792–1790 Ma]	(MolRO) 1805 Ma	Serrato (2014)
	Serrinha de Guarantã (MT)	EPI or intrusion-related gold	Metatonalite*, metaultramafic, intermediate to acid subvolcanic intrusion [*(ZrnLA) 1977 Ma]	Maximum age: 1977 Ma.	Rios (2019)
	Papagaio (MT)	EPI or intrusion-related gold	Colíder Group [(ZrnS) 1796–1780 Ma]	>1780 Ma (E)	Galé (2018)
	Paraíba (MT)	EPI or intrusion-related gold	Matupá Suite/Flor da Serra Suite (1872 Ma–1879 Ma)	(MsAA) 1511 Ma	Silva and Abram (2008)
	Pé de Fora (MT)	Intrusion-related gold	Paranaíta Suite [(ZrnS) ~1792–1790 Ma]	1803–1793 Ma	Silva and Abram (2008)
	Pé de Anta (MT)	EPI or intrusion-related gold	Colíder Group [(ZrnS) 1796–1780 Ma]	~1790 Ma (E)	Silva and Abram (2008); Alves *et al.* 2010; Duarte and Lopes (2015); Pinho *et al.* (2003)
	Cajueiro (MT)	EPI or intrusion-related gold	Teles Pires Suite [(ZrnT; ZrnLA) 1780–1793 Ma]	1780–1793 Ma (E)	Silva and Abram (2008); Alves *et al.* (2019)
			Colíder Group [(ZrnS) 1796–1780 Ma]		Silva and Abram (2008); Alves *et al.* 2010; Duarte and Lopes (2015); Pinho *et al.* (2003)
	Guarantã (MT)	Au + (Zn–Pb–Cu) intermediate sulfidation	Colíder Group [(ZrnS) 1796–1780 Ma]	~1790 Ma (E)	Silva and Abram (2008); Alves *et al.* 2010; Duarte and Lopes (2015); Pinho *et al.* (2003)
	Aragão (MT)	PO or intrusion-related gold	Aragão Granite [(ZrnLA) 1931 Ma]		Miguel (2011)
	Edu (MT)	EPI or intrusion-related gold	Nhandú Suite [(ZrnS) 1968–1963 Ma; (ZrnLA) 1889–1879 Ma]		Dezula *et al.* (2018); Silva and Abram (2008)
	X1 (MT)	PO or intrusion-related gold	Granitoid pluton; porphyry subvolcanic intrusion [(ZrnPE) 1872 Ma]	(MolRO) 1785–1787; (ZrnS) 1773 Ma; (MsAA) 1751–1733 Ma	Assis *et al.* (2017); Assis (2015)

Abbreviations: Method – S, U–Pb SHRIMP; LA, U–Pb laser ablation; AA, Ar–Ar; RO, Re–Os model age; PE, single zircon Pb-evaporation; T, ID-TIMS; E, estimated. Mineral (according to Whitney and Evans 2010) – Mnz, monazite; Mol, molybdenite; Ms, muscovite; Py, pyrite; Zrn, zircon; *, secondary mineralization/mobilized ore. Deposits – EPI, epithermal; PO, porphyry. Country/state – PA, Pará; AM, Amazonas; MT, Mato Grosso.

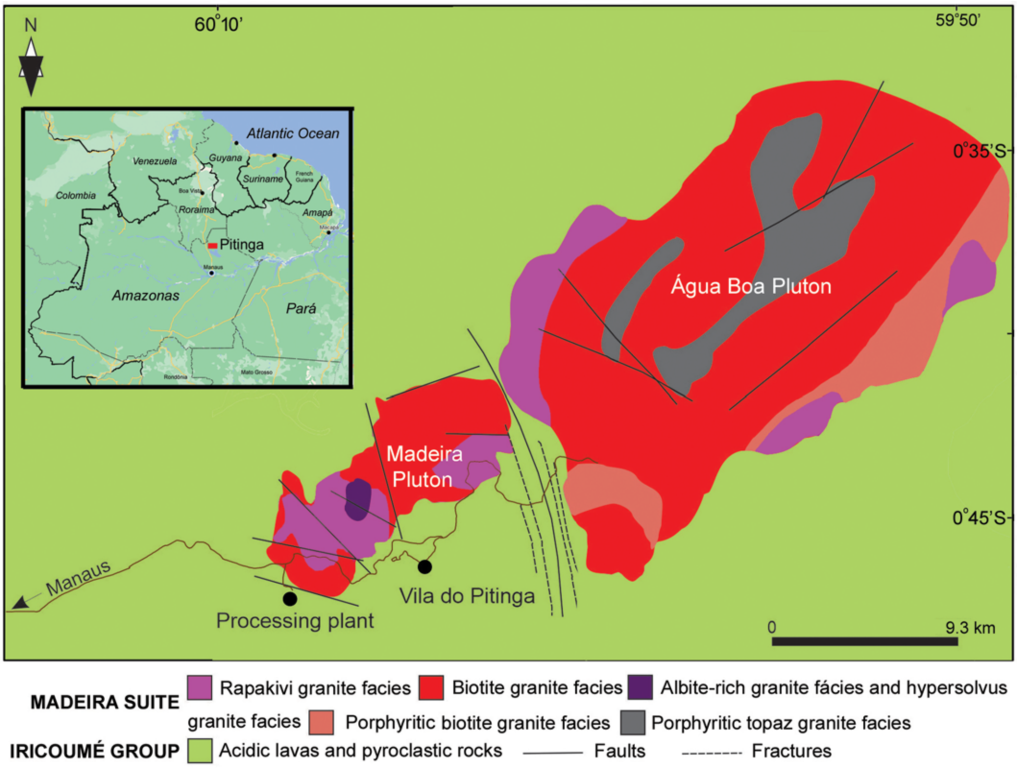

Fig. 7. Main mineralized plutonic bodies of the Pitinga Province (adapted from Borges *et al.* 2003).

Also, it matches several 1.80–1.78 Ga mafic units from Baltica, such as the Ropruchey sills (Fedotova *et al.* 1999), Hoting Gabbro (Elming *et al.* 2009) and Småland intrusion (Pisarevsky and Bylund 2010), as well as ultramafic–mafic dykes, coeval tholeiitic and jutonitic dykes and anorthosite–mangerite–charnockite–granite (rapakivi) complexes described in the Ukranian shield (Shumlyanskyy *et al.* 2016*a*, *b*; 2017).

The Avanavero LIP (1.79–1.78 Ga)

Distribution. The Avanavero LIP has been considered the most widespread and important mafic magmatism in the Amazonian Craton. It extends along the Orocaima, Uatumã and AFSLs. The maximum life span for the Avanavero LIP is *c.* 10 myr constrained by ages between 1.79 and 1.78 Ga (Santos *et al.* 2003*b*; Reis *et al.* 2013*a*; Fig. 1), such as the large mafic sills within the Roraima Supergroup (Reis *et al.* 2013*a*, 2017*a*). Although they occur mainly within the Roraima sedimentary rocks, its type-area in Suriname exposes swarms of dykes with a NE–SW trend intruding both basement and cover.

Additional U–Pb SHRIMP baddeleyite ages at 1.78 Ga were obtained by Santos *et al.* (2002) for the Crepori sill in southwestern Pará State and for the Quarenta Ilhas sill in northeastern Amazonas State (Fig. 1), allowing a correlation with the Avanavero LIP.

We note that the U–Pb age of 1.78 Ga documented for a gabbro of the Vespor Suite (Rizzotto *et al.* 2019) has a tight match with the Avanavero LIP. In this way, we associate the Vespor magmatism with the Avanavero LIP rather than as an evolved product of the Western Amazonia Belt as postulated by the mentioned author.

Mineral resources. At present, the Avanavero LIP has no economic interest, despite its large exposure across the Amazonian Craton. Tropical weathering on mafic rocks establishes good targets for prospecting in lateritic crusts or regoliths, such as the Amazon rainforest; therefore, potential economic targets may exist.

The most important metallogenetic epoch to the TMP has been established on the base of Re–Os, Ar–Ar and U–Th–Pb ages at 1.80 and 1.78 Ga (Serrato 2014; Assis *et al.* 2017; Rocha *et al.* 2020), which correlates with the *c.* 1.79–1.78 Ga Avanavero LIP event.

Matches with 1.79–1.78 Ga magmatism on other crustal blocks. On a global scale, the Avanavero LIP is correlative with the Svecoffenian magmatism in Baltica. This block among others was a close neighbour to Amazonia at that time, as supported by the palaeomagnetic evidence (see Section 4). The U–Pb age of 1.79 Ga for the Libiri dyke swarm of Niger (Baratoux *et al.* 2019) represents one LIP barcode line for the West African craton and can also be matched with Avanavero LIP of the Amazonian Craton. The Avanavero LIP is probably equivalent to the dolerite dykes at 1.79 Ga which form a large-scale Prutivka–Novogol LIP event in the Ukrainian Shield (Shumlyanskyy *et al.* 2016*a*, *b*, *c*). The age match of the Avanavero LIP with the AFSL suggests a genetic link, possibly to a common mantle plume.

The Rincón del Tigre–Huanchaca LIP (1.11 Ga)

Distribution. This 1.11 Ga LIP has widespread occurrence across the southwestern portion of the Amazonian Craton and includes two younger major tectonic elements that have an important bearing for the scope of this paper: the Sunsás and Aguapeí belts. The 1.11–1.00 Ga Sunsás Belt marks the final consolidation of the Amazonian Craton (Teixeira *et al.* 2010). It hosts the 1.11 Ga Rincón del Tigre–Huanchaca LIP that matches in age the mafic dykes of the Rio Perdido mafic swarm in the southernmost portion of the Amazonian Craton (Teixeira *et al.* 2020). The Aguapeí Belt is a structurally confined zone of folded supracrustal rocks with little or no metamorphism which is roughly coeval with the Sunsás Belt (Geraldes *et al.* 2001; Teixeira *et al.* 2010).

Components of the Huanchaca–Rincón del Tigre LIP are scattered in the Bolivian and the adjoining Brazilian Precambrian shield, respectively, and can be distinguished by four nodes. The 720 km^2 Rincón del Tigre mafic–ultramafic layer complex and the Huanchaca sills at 1.11 Ga are located *c.* 500 km apart in the eastern portion of Bolivian shield. A larger volume for the Rincón del Tigre Complex is envisaged from the nearby small exposures of mafic–ultramafic bodies that exhibit roughly similar NW-trending strikes (e.g. Mitchell 1979; Landivar *et al.* 1996). It is noteworthy that the structural framework matches the NW–SE trend of the Sunsás shear zones and the overprinting deformation and low-grade metamorphism in the country rocks (e.g. Litherland *et al.* 1986; Teixeira *et al.* 2015). The Rincón del Tigre Complex comprises a 4.5 km thick sill deformed during the *c.* 1.1–1.0 Ga Sunsás Orogeny (Litherland *et al.* 1986; Prendergast *et al.* 1998). It is composed of basal ultrabasic rocks (serpentinized dunite, harzburgite, olivine bronzitite and bronzitepicrite), a middle mafic unit (lower norite layer passing upward into a gabbro layer) and an upper felsic unit (granophyre) (Annells *et al.* 1986*a*, *b*; Litherland *et al.* 1986), both units with tholeiitic signature.

The Huanchaca sills and dykes (Lima *et al.* 2011, 2012) crop out mainly in the Bolivian Precambrian Shield and cross-cut an elongated sedimentary tableland that overlies the Paleoproterozoic crust of the Paraguá Block (e.g. Teixeira *et al.* 2010). A U–Pb SHRIMP age in xenotime, extracted from a pelite of the Huanchaca sedimentary succession, constrains the post-depositional diagenetic episode at 1.15 Ga (Santos *et al.* 2005; D'Agrella-Filho *et al.* 2008).

The third node of this LIP consists of mafic dykes of the Rio Perdido Suite (1.11 Ga; Teixeira *et al.* 2019) that cross-cut Early Statherian crust of the Paraguá Block – a close neighbour to the accretionary margin of Amazonia (Teixeira *et al.* 2020; B.V. Ribeiro *et al.* 2020). This LIP comprises WNW–ESE to east–west-trending gabbro and dolerite dykes with 100–200 km in the exposed length and appears to be *c.* 140 km wide.

The possibly fourth LIP node, given the age match, is a metamorphic suite originated at 1.12–1.11 Ga in the state of Rondônia which includes gabbros, troctolites, basalts, dolerites, amphibolites, metagranites and subvolcanic metagranites, in addition to trondhjemites exposed as rounded or oval intrusions, sills and dykes.

Mineral resources. The Rincón del Tigre Complex, a mafic–ultramafic layered intrusion in the eastern lowlands of Bolivia, was investigated during the 1990s after the discovery of a 'Precious Metals Zone', a well-developed but subeconomic strata-bound zone of platinum-group elements, sulfide and gold mineralization (Prendergast 2000).

Copper-dominant, strata-bound disseminated sulfide mineralization was identified within the magnetite gabbro, the upper and thickest lithological unit of the entire layered sequence estimated at around 3000 m, and contains a broad precious metals mineralized zone at its base. The basal zone comprises an upper Cu sulfide-rich subzone 80–185 m thick and contains subeconomic platinum-group metals and gold mineralization. Concentrations of Mn, Cr, Fe, Co and Ni occur in the residual soils overlying the lower ultramafic unit and are the main economic ores in the Bolivian area (Litherland *et al.* 1986; Prendergast 2000 and references therein).

The Don Mario Mineral District is located *c.* 100 km northward from the Rincón del Tigre Complex, as well as the Puquio Norte deposit (Litherland *et al.* 1986; Geraldes *et al.* 2009; Isla-Moreno 2009).

The hydrothermal affinity of the skarn-type Cu–Au mineralization in the Dom Mario deposit is consistent with the following evidence: (1) Cu–Bi–Au–Mo association; (2) Au–Cu–Zn–Pb–Ag–Bi polymetallic association; and (3) nearby occurrence of the Las Senoritas granite dated at 1.00 Ga. The Au-rich sheared zones yielded an Re–Os age in molybdenite of 0.99 Ga (Isla-Moreno 2009). The geology in Puquio Norte consists of (1) banded iron formations (BIFs), (2) sericite-schists and phyllites that host Au–Cu mineralization among other metals associated with hydrothermal fluids that migrated along the Sunsás shear zones and faults and (3) injections of pegmatite (U–Pb zircon age of 1.00 Ga). The carbonate/quartz veins contain free gold grains or inclusions in arsenopyrite. The gangue minerals comprise quartz, carbonate, sericite and chlorite. The sulfide minerals are arsenopyrite, pyrite, chalcopyrite and stibnite. They yielded Pb isotopic constraints akin to mixed mantle and upper crust sources associated with the Sunsás shear zones (Geraldes *et al.* 2009).

The Huanchaca sills and the Rio Perdido Suite, the other two mafic LIP components, do not have any known ore deposits, except that reef-like manganese mineralization has been reported to be locally associated with the sills (e.g. Litherland and Power 1989). However, given that the Rincón del Tigre LIP portion hosts subeconomic PGE mineralized zones, these and the other two mafic nodes may be targets for their economic potential.

Most important economic resources are related to the Rondonian Tin Province (Bettencourt *et al.* 2016 and references therein). This province is composed of three distinct intrusive suites dated at 1.3, 1.1 and 1.0 Ga, respectively, that host primary rare and base-metal mineralization. For instance, one the youngest massifs (Santa Bárbara; 0.99–0.98 Ga) contains rare and base-metal polymetallic deposits (Sn, W, Nb $\pm$ Ta, Be, Zn, Cu, Pb) mainly in greisen, quartz veins and pegmatite injections (e.g. Sparrenberger 2003; Bettencourt *et al.* 2016 and references therein). The origin of this massif, which is post-tectonic to the Sunsás collision, points to a long period of plume-driven magmatism coupled with plate dynamics since 1.11 Ga. This model implies that the thermal inputs from the 1.11 Ga Huanchaca–Rincón del Tigre SLIP triggered the mineralization within the youngest granite suites.

The Santa Bárbara massif includes two subsolvus facies, distinguished in terms of geological relationships and ages, and the previously published U–Pb monazite ages of 0.99 Ga define that of the mineralization (Sparrenberger 2003). The tin granite facies (0.98 Ga) encompasses a medium-grained porphyritic albite–microcline granite and fine-grained equigranular to porphyritic albite–microcline granite; this one is located in the apical part of the cupola. The deposit encloses two styles of mineralization: (1) bed-like cassiterite-bearing topaz–zinnwaldite–quartz–greisen bodies up to 40 m thick and salmon-coloured albitized granites (Taboquinha-greisen); and (2) vein-veinlet/stockwork containing topaz–zinnwaldite–quartz greisen veins, quartz–cassiterite veins, muscovite veins and late kaolinite stockwork/veinlets (Sparrenberger 2003, Bettencourt *et al.* 2005; Figure 8.

The hydrothermal alteration is represented by greisenization, albitization, silicification, muscovitization and argillization during late- to post-magmatic stages (Sparrenberger 2003).

Finally, a further potential result from the thermal influx of the Rincón del Tigre–Huanchaca LIP could be the gold occurrences associated with the basal conglomeratic levels (Sunsás/Aguapeí) and hydrothermal fluids along shear zones (Aguapeí Belt). In this way, Litherland *et al.* (1986) documented that

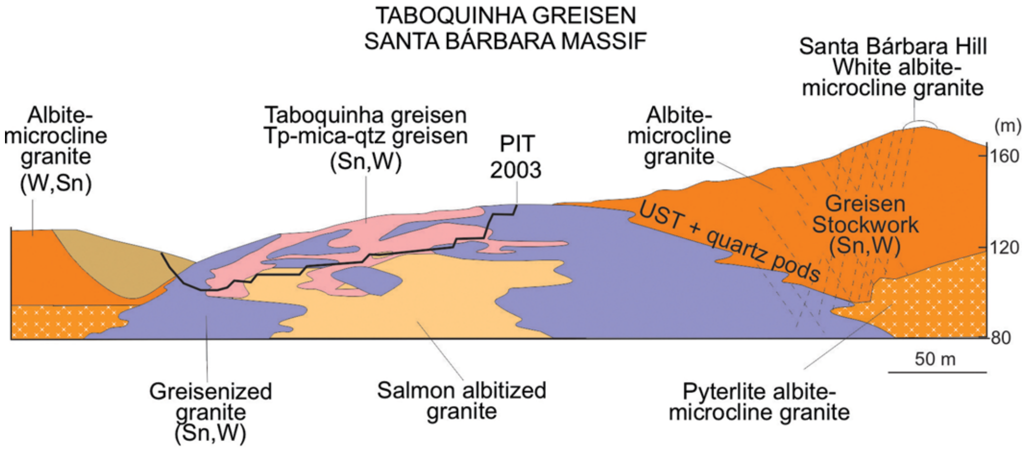

Fig. 8. Style of tin mineralization found in the Santa Bárbara massif (after Sparrenberger 2003).

the conglomerates in the Bolivian counterpart are potential targets for gold mineralization, as placer deposits. On the Brazilian side, gold ores have been exploited from placer, lateritic and hydrothermal quartz (Geraldes *et al.* 1997; Fernandes *et al.* 2006). The Au-rich quartz veins occur mainly disseminated in the conglomerates owing to hydrothermal fluid percolation.

The Pau-a-Pique, Lavrinha, Onça and Ellus gold deposits occur along a branch of the Aguapeí Belt in Brazil (Mato Grosso State), as depicted in Figure 9. Ar–Ar ages in sericite from the hydrothermal veins in the Pau-a-Pique and Ellus deposits yielded ages of 0.91 and 0.93 Ga (Fernandes *et al.* 2006; Table 4. The geochronological and structural data combined with petrographic studies suggest an epigenetic origin for the gold deposits.

The ore mineralogy is composed of quartz and pyrite with gold veins, whereas the associated hydrothermal alteration zones contain quartz, sericite, pyrite (altered to limonite) and magnetite (altered to hematite). Chalcopyrite, galena and sphalerite may be present. Chemical analysis of sulfides indicated high contents of Bi, Se and Te in sulfides and gold, suggesting a primary plutonic involvement for the hydrothermal fluids. The K–Ar dating of hydrothermal sericites from the gold veins yielded apparent ages in sericite from 0.96 to 0.84 Ga, whereas Pb–Pb dating in galena yielded model ages in the range 1.00–0.80 Ga (Onça deposit; Table 4).

Matches with 1.11 Ga magmatism on other crustal blocks. The onset of this Rincón del Tigre–Huanchaca LIP occurred at approximately the same time as the 1.11–1.08 Ga Keweenawan plume of Central Laurentia along the Mid-Continent rift (Heaman *et al.* 2007; Ernst 2014). Choudhary *et al.* (2019) recognized the 1.11 Ga Rincón del Tigre–Huanchaca LIP of Amazonia as belonging to coeval LIP units on other blocks (Bundelkhand Block, India, Kalahari and Congo cratons) in a reconstructed megacontinent (term used in the sense of Wang *et al.* 2020) named Umkondia.

LIP/SLIP events and the geological timescale boundaries

It has recently been proposed that the Precambrian timescale boundaries can be linked to LIPs similarly to many Phanerozoic LIPs where some specific divisions are also markers of dramatic climatic and environmental secular changes (e.g. Ernst and Youbi 2017; Gradstein *et al.* 2020; Kasbohm *et al.* 2020). In fact, Precambrian LIPs can potentially more precisely define the timescale boundaries (Ernst and Youbi 2017; Zhang *et al.* 2018, 2021; Ernst *et al.* 2020, 2021).

When it comes to the Amazonian SLIPs and LIPs, some of them coincide with currently defined timescale periods (Fig. 10). For instance, the 1.79 Ga Avanavero LIP and coeval AFSL can be linked with the Orosirian–Statherian boundary. It could be further suggested that the other LIP/SLIP events of Amazonia at 1.98–1.96, 1.88–1.87 and 1.11 Ga could mark divisions within the Orosirian, Statherian and Stenian periods, respectively, based on the global LIP/SLIP database (Ernst and Youbi 2017; Zhang *et al.* 2021; Ernst *et al.* 2020, 2021).

Figure 10 also shows several other mafic and felsic magmatic activities such as those in the Calymmian and Stenian, interpreted as intermittent intraplate activity throughout the Amazonian Craton (Teixeira *et al.* 2010, 2019). Some of these magmatic episodes are synchronic with sedimentary (e.g. Roraima Supergroup) or volcanic–sedimentary covers (e.g. Vila do Carmo/Roosevelt).

The palaeogeography of the Amazonia and global correlations

Introduction

Geological and geochronological evidence suggests that at two times in the Proterozoic the existing continental masses formed supercontinents: Columbia at 1.6 Ga and Rodinia at 1.0–0.9 Ga (e.g. Li *et al.* 2008; Silver and Behn 2008; Meert 2012; Pisarevsky *et al.* 2014; Wang *et al.* 2020). Recently, Wang *et al.* (2020) used the term Nuna for a megacontinent that resulted from the collision of cratonic blocks that formed Laurentia at *c.* 1.8 Ga owing to the Trans-Hudson orogen, which included Baltica and Siberia. This megacontinent probably enclosed other nearby landmasses, such as Amazonia and West Africa at this time (Johansson 2009; Bispo-Santos *et al.* 2014*a*). The Columbia supercontinent was eventually formed *c.* 200 myr later with the amalgamation of other blocks, such as Australia (Wang *et al.* 2020). Here we follow the terms Nuna (megacontinent) and Columbia (supercontinent) with the meaning as suggested by Wang *et al.* (2020).

Mainly in the last two decades, several geological units from the Amazonian Craton have been studied by palaeomagnetism with important implications for Nuna and Rodinia (see D'Agrella-Filho *et al.* 2016*a*, 2020 for a review). We reassess here the studies of some Brazilian geological units of particular interest to the present manuscript covering the Guiana and Central Brazil shields (Fig. 1): the 1.98–1.96 Ga volcanic rocks in the OSL (Bispo-Santos *et al.* 2014*a*), the 1.88–1.87 Ga volcanic rocks of the USL

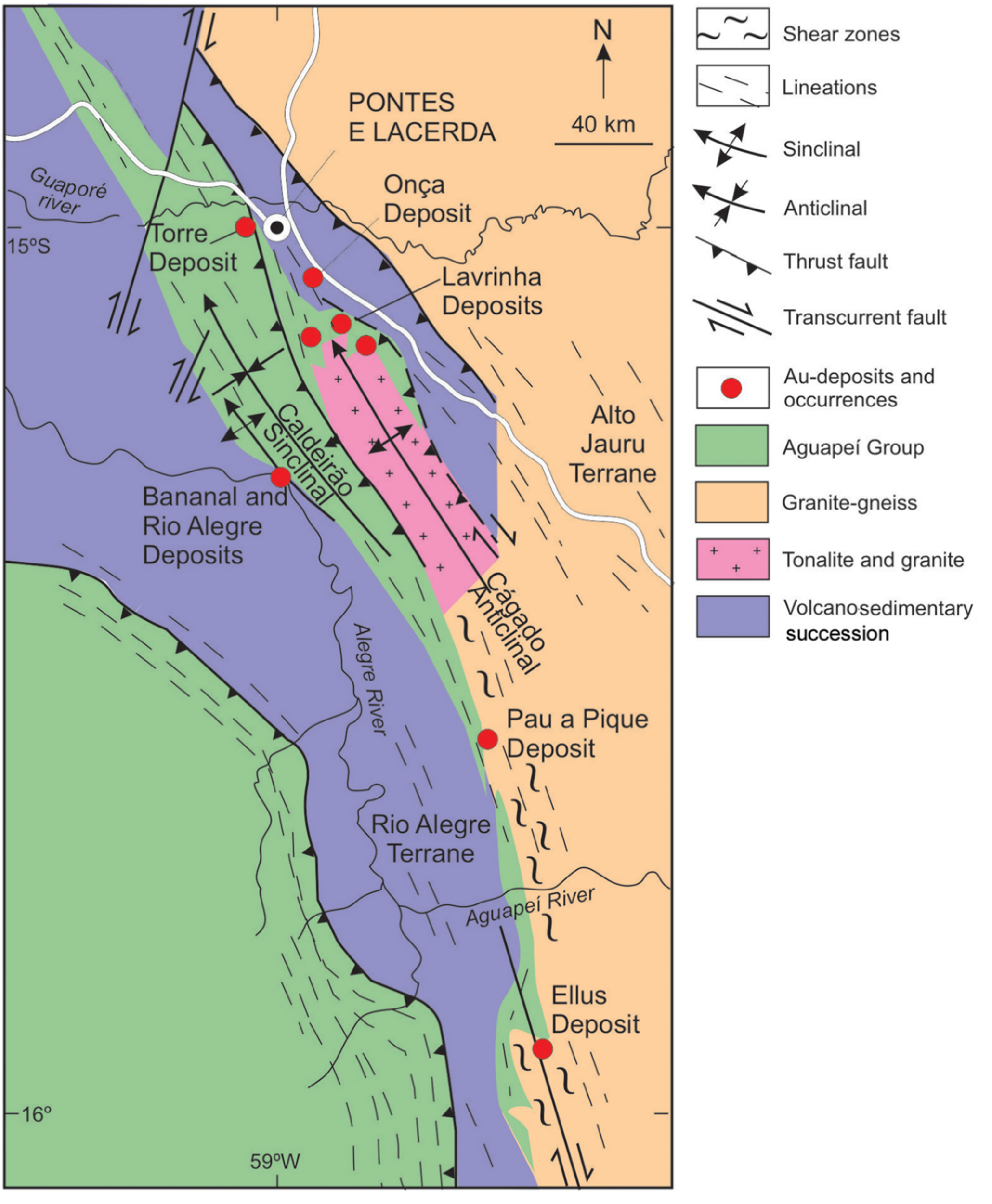

Fig. 9. Geological map of the Aguapeí Belt, showing the location of the gold deposits (Fernandes *et al.* 2006).

(Antonio *et al.* 2017, 2021), the 1.79–1.78 Ga volcanic rocks in the AFSL (Bispo-Santos *et al.* 2008) and the Avanavero LIP (Bispo-Santos *et al.* 2014*b*). Other palaeomagnetic poles from the Amazonian craton relevant to the later Mesoproterozoic times (used hereafter) have been described by Bispo-Santos *et al.* (2012, 2020) and D'Agrella-Filho *et al.* (2008, 2012, 2016*b*).

Based on geological and palaeomagnetic data, it has long ago been suggested that Amazonia docked to West Africa at *c.* 2.00–1.97 Ga in a position where the Guri (in Amazonia) and Sassandra (in West Africa) shear zones were aligned and associated with the same lineament (Onstott and Hargraves 1981; Nomade *et al.* 2003). More recently, Bispo-Santos *et al.* (2014*b*) obtained a palaeomagnetic

Table 4. *Important mineral resources associated directly or indirectly with the Rincón del Tigre–Huanchaca LIP of the Amazonian Craton*

Slip	Local name	Polymetallic association	Host unit/age	Mineralization age	Reference
RTH LIP	RTC (BO)	Orthomagmatic Cu–(Au–PGE) in layered intrusions	Rincón del Tigre Complex [(BdyS) 1110 ± 2 Ma]	1.11 Ga	Litherland *et al.* (1986); Prendergast (2000)
	Santa Clara and YGR (RO)	Nb–Ta–Sn–W–REE-bearing granite	Santa Clara (1.08–1.07 Ga), Santa Bárbara [(MnzS) 993 ± 4.6 Ma] and Oriente Novo – YGR (0.99–0.97 Ga)	1.08–0.97 Ga	Sparrenberger (2003); Leite (2002); Bettencourt *et al.* (2016)
	Dom Mário (BO)	Skarn-type Cu–Au; shear zones; Cu–Bi–Au–Mo association; Au–Cu–Zn–Pb–Ag–Bi polymetallic association	Senoritas Granite (1014 ± 6 Ma; 1004 ± 1 Ma)	MoIRO 994 ± 3 Ma	Isla-Moreno (2009)

Abbreviations: Method – S, U–Pb SHRIMP; RO, Re–Os model age; E, estimated. Mineral (according to Whitney and Evans 2010) – Bdy, baddeleyite; Mnz, monazite; Mol, molybdenite; YGR, younger granites of Rondônia. Country/state – BO, Bolivia; RO, Rondônia.

pole for the I-type volcanics of the OSL. These authors compared the apparent polar wander paths (APWP) for Amazonia and West Africa for the period between 2.10 and 1.95 Ga and suggest that the palaeomagnetic data corroborate the amalgamation of Amazonia and West Africa at *c.* 1.97–1.96 Ga in a similar palaeogeography using the large shear zones referred above. However, based on the same palaeomagnetic data, Antonio *et al.* (2021) tested a slightly different reconstruction for Amazonia and West Africa which aligns the Sassandra shear zone in West Africa and the North Guiana Trough and other shear zones in Guiana Shield (after Chardon *et al.* 2020). According to Antonio *et al.* (2021), this reconstruction is supported by geological and palaeomagnetic data.

Important palaeomagnetic studies were also produced for volcanics of the USL which were interpreted as evidence of a true polar wander event (Antonio *et al.* 2017). New palaeomagnetic data published recently for 1.88 Ga felsic dykes (also from the USL) corroborate this interpretation (Antonio *et al.* 2021).

Below we briefly discuss the implications of palaeomagnetic data for the participation of Amazonia in the establishment of the megacontinent Nuna (Wang *et al.* 2020) at *c.* 1.79–1.78 Ga, its longevity and the formation of Rodinia. The palaeomagnetic pole obtained for the Avanavero LIP plays an important role in this reconstruction (Bispo-Santos *et al.* 2014*b*).

Amazonia in Nuna

The position of Amazonia in Paleoproterozoic times has been the subject of dispute. Some authors suggested that the Amazonia was juxtaposed to Baltica and West Africa, in a configuration named SAMBA (Johansson 2009), based on geological evidence (see also Evans and Mitchell 2011; Baratoux *et al.* 2019). Palaeomagnetic data published for the Avanavero Dolerite (LIP) corroborate the link between Amazonia and Baltica (Bispo-Santos *et al.* 2014*b*). More recently, new palaeomagnetic data from the *c.* 1.54–1.53 Ga anorthosite–mangerite–rapakivi granite complex in Roraima State also support a similar link for Amazonia and Baltica at this time (Bispo-Santos *et al.* 2020). Moreover, these authors suggest a long life for this connection in the palaeogeography, from 1.78 Ga up to 1.53 Ga, at least.

However, the palaeogeographies of Amazonia and Baltica proposed by Bispo-Santos *et al.* (2014*b*) and Bispo-Santos *et al.* (2020) are slightly different from the SAMBA model (Johansson 2009), so much so that Bispo-Santos *et al.* (2020) refer their reconstruction as 'SAMBA-like model'. The problem with the SAMBA model is that no

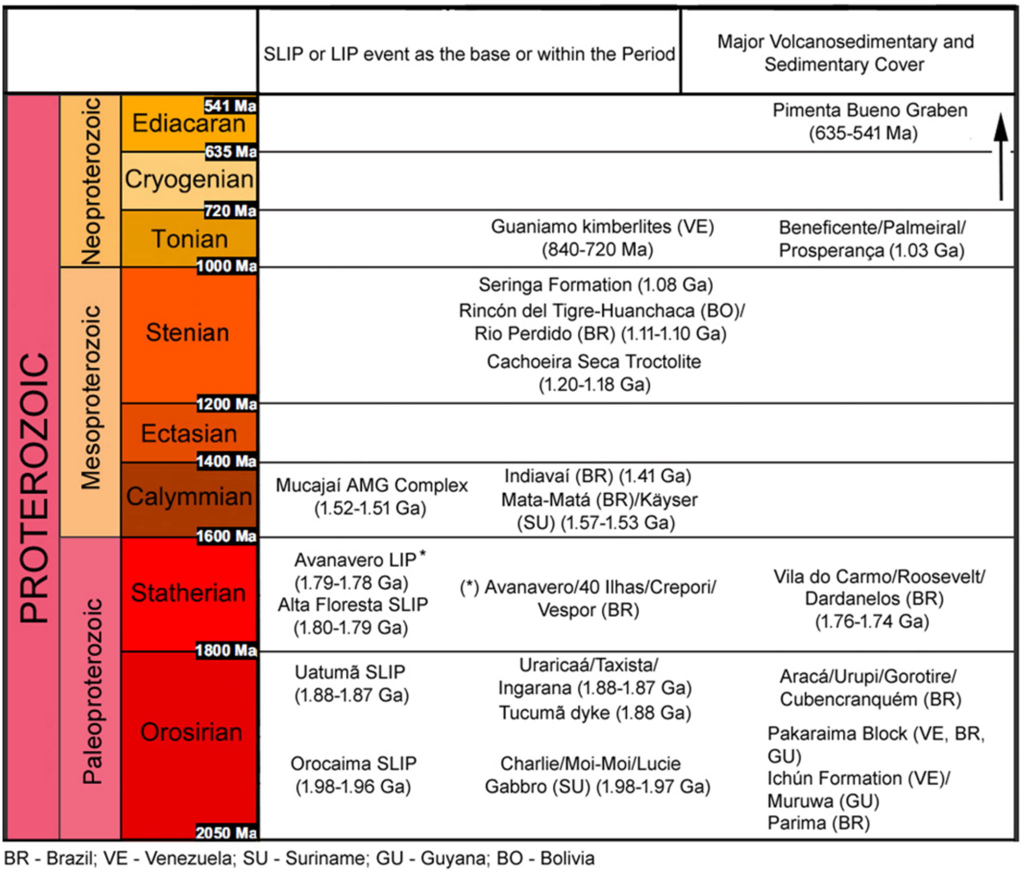

Fig. 10. Chronostratigraphic boundaries of Proterozoic LIP and SLIP scale events and associated basins in the Amazonian Craton.

rotation poles for this reconstruction were originally described by Johansson (2009) that could permit a palaeomagnetic test. Here we conduct this test by calculating Euler rotation poles that bring Baltica and West Africa to Amazonia, trying to get as close as possible the SAMBA model as proposed by Johansson (2009). Figure 11a shows our palaeogeography of the SAMBA connection at *c.* 1.79–1.78 Ga. Amazonia is in its present position while Baltica is rotated −82.80° around a Euler pole at 43.82° N, 195.29° E. For West Africa we used the rotation pole 52.2° N, 336.86° E (−67.03°), which brings this block approximately to the position suggested by Johansson (2009). In their model the west coast of West Africa fits the southeastern margin of Baltica, and the São Luís Block (SLB in Fig. 11a) is located between the Ivory Coast (Africa) and the embayment outboard of Suriname on the Amazonian coast. The main geotectonic/geochronological provinces of Baltica, Amazonia and West Africa are also shown in Figure 11a. The dashed lines establish the approximate limits between coeval provinces in Baltica and Amazonia. The position of Laurentia is not the same as that proposed by Johansson (2009) since the Laurentian palaeomagnetic data did not corroborate his reconstruction. Therefore, we used a Euler rotation pole (62.36° N, 258.1° E, −96.73°) that depicts the same reconstruction as proposed by Evans and Pisarevsky (2008) for Laurentia linked to Baltica.

Selected palaeomagnetic poles (Table 5) with ages between 1.79 and 1.75 Ga for Laurentia, Baltica and Amazonia are also shown in Figure 11a. Poles from Laurentia and Baltica were rotated using the same Euler poles as used in the SAMBA reconstruction (Fig. 11a). Four poles are presently available for Baltica, whose mean is represented by pole B5 (mean age of 1.78 Ga) in Figure 11a (Table 5). Amazonia is represented by the Avanavero pole (pole A1 in Fig. 11a) whose mean age is 1.79 Ga. Their confidence circles intercept each other, and if we consider the uncertainty in the pole ages, one can say that they corroborate the SAMBA model of Johansson (2009).

The I-type Colíder volcanics from the Alta Floresta LIP (1.79 Ga) were also the subject of a palaeomagnetic study (Bispo-Santos *et al.* 2008). Although this suite and the Avanavero sills are coeval, their palaeomagnetic poles are distinct. The possibility that the Colíder pole represents a younger remagnetization is endorsed by the following facts: (1) the Avanavero pole was obtained for anorogenic rocks from the Guiana Shield, which are only partially affected in its southern part by the 1.2 Ga K'Mudku Episode (Cordani *et al.* 2010), and a positive baked contact test obtained for these rocks attests to the primary nature of the Avanavero sills' directions (Bispo-Santos *et al.* 2014*b*); and (2) Bispo-Santos *et al.* (2008) argue in favour of a primary nature for the Colíder pole referred to as felsic volcanic rocks, but no field tests were conducted in their study. The Colíder volcanics occur in the southern part of Amazonian Craton not far from the Mesoproterozoic NW–SE-trending magmatic arcs related to the final collision of Paraguá Block at *c.* 1.33 Ga (Bettencourt *et al.* 2010). Therefore, the Colíder pole could have experienced remagnetizations owing to such a collisional episode (see also D'Agrella-Filho *et al.* 2016*a*, 2020). The ongoing palaeomagnetic study of the 1.78 Ga Vespor mafic rocks attributed to the Avanavero LIP may bring new insights into the palaeogeography of the Amazonia.

For West Africa, no 1.79–1.75 Ga poles are presently available to test its position in the reconstruction of Figure 11a. However, we stress that, although the palaeomagnetic data corroborate a collision of Amazonia and West Africa culminating at *c.* 1.97 Ga (see above), the exact position of the link between these two cratons cannot be established owing to the uncertainties in the palaeomagnetic poles and their ages, and the Amazonia link to West Africa as in the SAMBA model is equally possible.

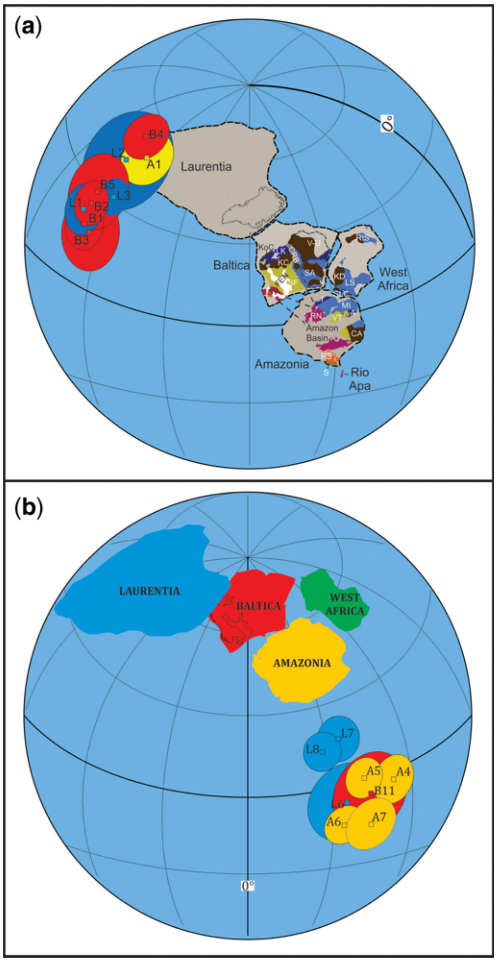

Fig. 11. (**a**) Palaeogeography at 1.79–1.78 Ga showing the link of Laurentia, Baltica, Amazonia and West Africa according to the SAMBA model of Johansson (2009). Selected 1.79–1.75 Ga poles for Laurentia, Baltica and Amazonia (Table 5) are also shown. Amazonia in its present position. Euler rotation poles used for Laurentia, Baltica and West Africa and respective poles are described in Table 5. The main geotectonic/geochronological provinces of Baltica, Amazonia and West Africa are also shown (according to Bogdanova *et al.* 2008; Johansson 2009; Macambira *et al.* 2020): Baltica – V-U, Vulgo–Uralia; SA, Sarmatia; FEN, Fennoscandia; KoC, Kola Craton; KC, Karelia Craton; LK, Lapland–Kola Belt; CRB, Central Russian Belt; SF, Svecofennian Orogeny; SV, Sveconorwegian Orogeny. Amazonian Craton (after Cordani and Teixeira 2007) – CA, Central Amazonia Province; I, Imataca Block; A, Rio Apa Block; MI, Maroni–Itacaiúnas Province; VT, Ventuari–Tapajós Province; RN, Rio Negro–Juruena Province; RS, Rondonian–San Ignacio Province; S, Sunsás–Aguapeí Province. West Africa – RtS, Reguitibat Shield; KD, Kenema Man Domain; LS, Leo Shield; SLB, São Luís Block. The dashed lines establish the approximate limits between coeval provinces in Baltica and Amazonia. (**b**) Reconstruction proposed by Pehrsson *et al.* (2016) at 1.44 Ga. for Laurentia, Baltica, Amazonia and West Africa. Respective palaeomagnetic poles in the 1.46–1.40 Ga time interval are also shown. Palaeomagnetic poles and Euler rotation poles used are described in Table 5. Palaeomagnetic poles are represented in the same colour as the respective continental blocks. Circles represent the 95% confidence cones (A_{95}).

Table 5. *Selected palaeomagnetic poles for Baltica, Laurentia and Amazonia between 1.79 and 1.40 Ga*

Landmasses/geological unit	Code	Age (Ga)	Plat. (°N)	Plong. (°E)	A_{95} (deg)	RPlat. (°N)	RPlong. (°E)	RPlat. (°N)	RPlong. (°E)	RPlat. (°N)	RPlong. (°E)	Reference
Baltica – rotation pole						43.82° N, 195.29° E (−82.80°)*		48.97° N, 215.77° E (−80.63)**		47.5° N, 1.5° E (49°)***		
Ropruchey sill	B1	1.78–1.76	41	230	8	19	201	37	209			1
Schoksha Fm. #	B2	1.79–1.77	42	221	7	25	199	44	207			2
Hoting gabbro #	B3	1.80–1.77	43	233	12	18	204	36	213			3
Småland dykes #	B4	1.78–1.77	46	183	8	53	198	71	210			4
Mean – B1, B2, B3 and B4 poles	B5	1.78	44	216	12	29	200	48	208			
Turinge gabbro-diabase #	B6	1.70	52	220	5	29	209	47	220			5
Häme DB dyke #	B7	1.64	24	210	15	26	176	44	179			6
SE-quartz porphyry dyke	B8	1.69–1.62	30	175	9	57	170	73	154			7, 8
Sipoo porphyry	B9	1.63	26	181	9	52	166	67	154			9
Mean – Åland intrusion #, Satakunta dykes # and Dala sandstone poles	B10	1.55	28	188	8	46	172	63	167			10
Mean – Tuna dyke, Salmi Fm., Lake Ladoka dykes #, Bunkris–Glysjön–Öje dyke poles	B11	1.46	17	181	14	48	153	60	140	−5	44	10
Laurentia – rotation pole						62.36° N, 258.10° E (−96.73°)*		52.79° N, 267.46° E (−99.97°)**		In its present position***		
Dubawnt Group	L1	1.79	7	277	8	22	198	32	209			12
Jeanlake granite	L2	1.76	24	264	17	43	200	51	220			13
Cleaver dyke	L3	1.74	19	277	6	32	206	39	222			14
Melville Bugt dyke	L4	1.63	5	274	9	22	193	33	205			15
Western Channel Dyke	L5	1.59	9	245	7	42	168	56	180			16, 17
Mean – St Francois mountains, Tabacco Root dykes, Michikamau intrusion, Spokane Fm., Harp Lake complementary poles	L6	1.46	−6	217	13	35	128	49	127	6	37	10
Mean – Mean rock mountain, Purcell lava, Laramie anorthosite, Electra Lake gabbro, Belt Supergroup	L7	1.43	−17	215	8	24	126	38	127	17	35	10
McNamara Formation	L8	1.40	−14	208	7	27	118	40	118	14	28	10
Amazonia – in its present position						in its present position*		in its present position**		53.9° N, 291.1° E (122.2°)***		
Avanavero Sill	A1	1.79	48	208	10							18
Parguaza Granite (G1 component)	A2	1.52–1.59	54	174	10							19
Mucajaí Complex	A3	1.53–1.54	38	180	13							10
Salto do Céu sill	A4	1.44	56	99	8					1	42	20
Rio Branco sedimentary rock	A5	>1.44	46	90	7					−3	53	20
Nova Guarita dyke	A6	1.42	48	66	7					−14	34	21
Indiavaí Intrusive	A7	1.42	57	70	9					−16	43	22
West Africa – rotation pole						52.20° N, 336.86° E (−67.03°)*		45.51° N, 327.86° E (−58.18°)**		58.3° N, 304.9° E (85.8°)***		

Plat., pole latitude; Plong., pole longitude; A_{95}, radius of 95% confidence cone; Rlat, rotated pole latitude; Rlong, rotated pole longitude. *Euler rotation pole used to construct Figures 11a and 12b. **Euler rotation pole used to construct Figure 12a (according to Bispo-Santos *et al.* 2020). ***Euler rotation pole used to construct Figure 11b (according to Pehrsson *et al.* 2016). # Key palaeomagnetic pole (Baltica). References: 1, Fedotova *et al.* (1999); 2, Pisarevsky and Sokolov (2001); 3, Elming *et al.* (2009); 4, Pisarevsky and Bylund (2010); 5, Elming *et al.* 2019; 6, Salminen *et al.* (2017); 7, Neuvonen (1986); 8, Salminen *et al.* (2016); 9, Mertanen and Pesonen (1995); 10, Bispo-Santos *et al.* (2020); 11, Pisarevsky and Bylund (2010); 12, Park *et al.* (1973); 13, Gala *et al.* (1995);14, Irving *et al.* (2004); 15, Halls *et al.* (2011); 16, Irving *et al.* (1972); 17, Hamilton and Buchan (2010); 18, Bispo-Santos *et al.* (2014*a*); 19, Valdespino and Costanzo-Alvarez (1997); 20, D'Agrella-Filho *et al.* (2016*b*); 21, Bispo-Santos *et al.* (2012); 22, D'Agrella-Filho *et al.* (2012).

Longevity of Nuna and assembly of Columbia

Bispo-Santos *et al.* (2020) advocate a long life for their SAMBA-like connection, based on the comparison of palaeomagnetic poles from Baltica, Laurentia and Amazonia in the interval 1.79–1.40 Ga (Fig. 12a). These authors also suggest that either Amazonia/West Africa broke up from SAMBA at some time between 1.54 and 1.44 Ga or this landmass rotated counterclockwise relative to Baltica, preserving the integrity of Nuna. The Laurentia/Baltica link may have had a yet longer life, probably kept united up to 1.27 Ga (e.g. Salminen *et al.* 2017). Siberia is also considered as part of the core of a long-lived Nuna, where the present southern and eastern margins of Siberia juxtapose directly adjacent to, respectively, the arctic margin of Laurentia and the Uralian margin of Baltica (e.g. Evans and Mitchell 2011; Ernst *et al.* 2016; Evans *et al.* 2016; Salminen *et al.* 2017), although a looser fit is also proposed (Pisarevsky *et al.* 2014).

Here we test again the longevity of the Amazonia–Baltica link, but now using the reconstruction of Figure 11a (SAMBA connection). As in Bispo-Santos *et al.* (2020) we used the APWP between 1.79 and 1.4 Ga for Baltica as a reference (Fig. 12b, Table 5). Several poles from Baltica in this time interval are classified as key poles (see Table 5). The ages associated with these poles calibrate the APWP traced for Baltica in Figure 12b. Selected palaeomagnetic poles from Amazonia and Laurentia for the same time interval (Table 5) were also plotted in this polar path, after rotating them using the same Euler poles as used in our reconstruction of SAMBA (Fig. 11a).

A relatively good agreement of Amazonia and Laurentia poles can be observed along this path except for the 1.44–1.42 Ga Amazonian poles, which suggests that this landmass may have already broken up from the core of Columbia (already assembled at *c.* 1.6 Ga), considering the model of Wang *et al.* (2020). An alternative interpretation for the 1.44–1.40 Ga Amazonia, Baltica and Laurentia poles is the reconstruction proposed by Pehrsson *et al.* (2016) at this time (Fig. 11b). In this reconstruction, Amazonia/West Africa appears rotated counterclockwise relative to Baltica, compared with its position in the SAMBA model of Figure 11a, suggesting that rotation of this landmass eventually may have occurred inside Columbia at some time between 1.53 and 1.42 Ga. The confidence circles (A_{95}) of the 1.53–1.52 Ga poles for the Parguaza and Mucajaí intrusions (A2 and A3 in Fig. 12b, respectively) intercept each other and their poles fall around the 1.55 Ga part of the APWP traced for Baltica. This age is slightly older than the ages obtained for these rocks, but the Baltica APWP between 1.64 and 1.46 Ga suggests a low polar drift rate for the core of Nuna. Also, the positions of the Parguaza and Mucajaí poles fall in a

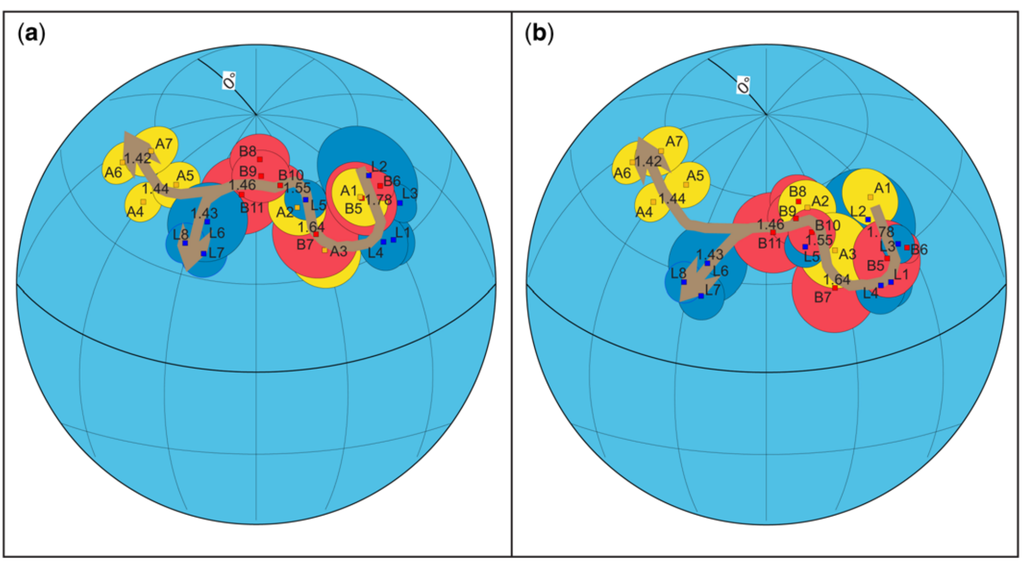

Fig. 12. (**a**) Comparison of the Amazonia (in yellow) and Laurentian (in blue) palaeomagnetic poles with the apparent polar wander path between 1.79 and 1.40 Ga traced for Baltica (poles in red) (Salminen *et al.* 2017), according to the reconstruction proposed by Bispo-Santos *et al.* (2020) for Laurentia, Baltica and Amazonia. (**b**) The same as in (a), but considering the SAMBA model reconstruction shown in Figure 11a. Palaeomagnetic poles and Euler rotation poles for both APWPs are described in Table 5. Circles represent the 95% confidence cones (A_{95}).

yet older part of the Baltica APWP, if we consider the reconstruction proposed by Bispo-Santos *et al.* (2020) (compare Fig. 12a, b), suggesting that the SAMBA model (Fig. 11a) could represent a better palaeogeography for the Baltica–Amazonia–West Africa link at 1.55–1.53 Ga ago in the configuration of Columbia. The link of West Africa in the SAMBA palaeogeography is supported by the age match with the 1.53 Ma Essakane swarm (Baratoux *et al.* 2019). A long-lived Nuna is also consistent with the Paleo- to Mesoproterozoic geological evidence (e.g. Vigneresse 2005; D'Agrella-Filho *et al.* 2020).

Amazonia in Rodinia

There is relative consensus that Amazonia participated in the Rodinia Supercontinent through the collision of this landmass with Laurentia along the 1.2–0.9 Ga Sunsás and Grenville orogens (e.g. Sadowsky and Bettencourt 1996; Tohver *et al.* 2002, 2004; D'Agrella-Filho *et al.* 2008; Li *et al.* 2008; Evans 2013; Johansson 2014; Cawood and Pisarevsky 2017). However, the dynamics that operated during this collision remain a matter of discussion, with three models proposed in the literature: (1) an oblique collision of Amazonia with the southwestern Laurentia at 1.2 Ga, along the Lhano orogen, in the Texas area, followed by a transcurrent movement of Amazonia relative to Laurentia, up to its final position in the Labrador area, when it collided with Baltica at *c.* 1.0 Ga (e.g. Tohver *et al.* 2002, 2004); (2) rupture of Amazonia–West Africa and Baltica from the nucleus of Nuna (in the SAMBA configuration), which rotated clockwise and collided again with Laurentia (e.g. Evans 2013); and (3) a frontal collision of the Amazonia–West Africa with Laurentia (e.g. Li *et al.* 2008; Cawood and Pisarevsky 2017).

Only two reliable poles are presently available from the Amazonian Craton: for 1.2 Ga (Tohver *et al.* 2002) and 1.15 Ga (D'Agrella-Filho *et al.* 2008). Comparison of these poles with coeval poles from Laurentia supports the model described by D'Agrella-Filho *et al.* (2008). Ibañez-Mejia *et al.* (2011) adopted a similar model to explain the Colombian–Oaxaquian peri-Amazonian fringing arc system (Putumayo Orogeny) outboard of Amazonia that would have evolved during the Amazonia transcurrent movement up to its final collision with Baltica at *c.* 1.0–0.9 Ga. Also, the origin of the 1.11–1.09 Ga mafic events (i.e. the Keweenawan plume) associated with the Mid-Continental rift in Laurentia and the 1.11 Ga Rincón del Tigre–Huanchaca LIP has been explained using this same model (Stein *et al.* 2014). The authors suggested, however, that this magmatism resulted from the Amazonia–Laurentia break-up, after the transcurrent motion up to 1.1 Ga.

Finally, we are aware that, because of the palaeolongitude ambiguity owing to the symmetry of the geomagnetic axial dipole field, and the polarity ambiguity for Precambrian poles, models 2 and 3 may not be discarded (see Evans 2013; Cawood and Pisarevsky 2017). Only with the determination of new reference poles in the 1.3–1.0 Ga time interval for the Amazonian Craton may one discard one or two of these models.

Final remarks

We reassessed the impressive background of precise U–Pb geochronology, isotopic–geochemical constraints and geological setting of the main Proterozoic SLIPs and LIPs in the Amazonian Craton and their potential links with important ore deposits. This preliminary approach outlined here between LIP/SLIP events and ore deposit type models should be refined in the future as far more regional detailed geological and metallogenic constraints are acquired.

We revisited five large igneous events of LIP/SLIP scale and considered them as potential triggers for metallogenic provinces through time and space, where the Uatumã and AFSLs are of most importance for metallogenetic potential. The Orocaima (1.98–1.96 Ga), Uatumã (1.88–1.87 Ga) and Alta Floresta (1.80–1.79 Ga) SLIP events, represented by the intracontinental volcanic–plutonic igneous belts, formed in post-orogenic to anorogenic settings. They show coherent association in time with convergent orogenic episodes that progressively built the Amazonia throughout the Paleoproterozoic, post-dating the Transamazonian/Eburnean orogeny. From a geodynamic perspective, these three SLIPs may be related to thermal perturbation in the upper mantle with associated mafic underplating from a plume. The palaeomagnetic evidence suggests that the 1.98–1.96 Ga Orocaima event occurred soon after collision of Amazonia and West Africa (Bispo-Santos *et al.* 2014*b*; Antonio *et al.* 2021, this work).

The Uatumã and AFSLs host the most important mineral resources within the Amazonian Craton, taking account the Pitinga, Tapajós, Alta Floresta and Carajás mineral provinces where a dozen gold and polymetallic deposits remain the focus of exploration. These SLIPs were the source of the fluid and heat that caused the hydrothermal system that led to the development of the mineral deposits. These deposits are directly related to the volcanic–plutonic activity and intraplate environment. It is noteworthy that in Carajás Mineral Province a younger epigenetic phase associated with Cu–Zn and Cu–Co deposits is related to the remobilization of pre-existing mineralization during the recognized 1.88 Ga anorogenic granitic magmatism intruding the Carajás–Rio Maria ancient crust. The relationship between the

USL and 1.88 Ga granitic magmatism also extends to the Pitinga Mineral Province where Sn-, Nb-, Ta-, U-, REE-, Zr- and F-rich bodies are exploited.

The Avanavero (1.79–1.78 Ga) in the Guiana Shield represent additional voluminous magmatism of intraplate character. This LIP formed over the already cooled and stabilized continental crust. From a broader perspective, the palaeomagnetic results for the 1.79 Ga Avanavero Dolerite corroborate the SAMBA model of Johansson (2009), suggesting that Amazonia and West Africa took part in the Columbia supercontinent. Alternatively, this LIP together with contemporary large-scale magmatic episodes probably followed the process of amalgamation of several blocks forming Nuna at 1.78 Ga (after Wang *et al.* 2020).

The youngest LIP – 1.11 Ga Rincón del Tigre–Huanchaca – is coeval with the Sunsás orogeny whose aftermath consolidated the Amazonia as a Craton. There is consensus that the Sunsás–Grenville collision between the Amazonia and Laurentia represents the process of amalgamation of the Rodinia supercontinent (e.g. D'Agrella-Filho *et al.* 2008; Li *et al.* 2008; Johansson 2014), although the collision dynamics remains a matter of debate. Resolution depends on obtaining additional key palaeomagnetic poles in the 1.3–1.0 Ga time interval for the Amazonian Craton.

From a metallogenetic perspective, two granitic suites collectively known as the Younger Granites of Rondônia (1.07–1.08 Ga; 0.99–0.97 Ga) could be tentatively related to the thermal inputs of the 1.11 Ga LIP. Separated by *c.* 90 myr these suites host rare metal polymetallic deposits mainly in greisen, quartz veins and pegmatite injections. They fit the post-tectonic context of the Sunsás collision, suggesting a long time period of plume-driven magmatism coupled with plate dynamics since 1.11 Ga. A further potential economic link for this LIP could be the gold occurrences produced by hydrothermal fluids along the network of shear zones outboard the Sunsás Belt in Bolivia and Brazil.

Finally, the Proterozoic LIP/SLIP events of Amazonia are consistent with the current defined boundaries between the Orosirian, Statherian and Stenian periods of the Geologic Time Scale.

Acknowledgements W. Teixeira is grateful to the CNPq/Brazil for the Research Productivity Scholarship. This paper represents a contribution to the CNPq working group Evolution of Cratonic Terranes managed by W. Teixeira.

Declaration of interest The authors declare that they have no known competing financial interests or personal relationships that could have appeared to influence the work reported in this paper.

Author contributions **NJR**: conceptualization (lead), data curation (lead), investigation (lead), methodology (lead), validation (lead), visualization (lead), writing – original draft (lead); **WT**: conceptualization (lead), data curation (lead), investigation (lead), methodology (lead), validation (lead), visualization (lead), writing – original draft (lead); **MSD-F**: investigation (lead), methodology (lead), validation (lead), visualization (lead), writing – original draft (lead); **JSB**: methodology (equal), visualization (equal), writing – original draft (equal); **REE**: conceptualization (equal), validation (equal), writing – original draft (equal); **LEG**: conceptualization (equal), methodology (equal), visualization (equal), writing – original draft (equal).

Funding M. S. D'Agrella-Filho thanks FAPESP and CNPq for the financial support for the palaeomagnetism work.

Data availability All data generated or analysed during this study are included in this published article (and its supplementary information files).

References

Aguja-Bocanegra, M.A. 2013. *Mineralizações Epitermal Low-Sulfidations e do tipo Pórfiro Superpostas associadas os Magmatismo Félsico de 1.88 Ga na Parte Norte da Província Mineral do Tapajós (PA)*. MSc thesis, Universidade de São Paulo, Instituto de Geociências, São Paulo.

Åhäll, K.-I. and Larson, S.Å. 2000. Growth-related 1.85–1.55 Ga magmatism in the Baltic Shield: a review addressing the tectonic characteristics of Svecofennian, TIB 1–related, and Gothian events. *GFF, Journal of the Geological Society of Sweden*, **122**, 193–206.

Alexandre, P. 2010 Mineralogy and geochemistry of the sodium metasomatism-related uranium occurrence of Aricheng South, Guyana. *Mineralium Deposita*, **45**, 351–367, https://doi.org/10.1007/s00126-010-0278-7

Almeida, M.E. 2006. *Evolução Geológica da porção centro-sul do Escudo das Guianas com base no estudo geoquímico, geocronológico e isotópico dos granitóides Paleoproterozóicos do sudeste de Roraima, Brasil*. PhD thesis, Centro de Geociências da Universidade Federal do Pará, Belém.

Almeida, M.E. 2016. Geologia e Recursos Minerais da Folha Sumaúma – SB.20–Z-D, Estado do Amazonas, escala 1:250 000. Projeto Sumaúma-Roosevelt-Mutum. *In*: Almeida, M.E., Costa, U.A.P. and da Oliveira, A.C.S. (eds) Serviço Geológico do Brasil – CPRM, Manaus, http://rigeo.cprm.gov.br/jspui/handle/doc/18292

Almeida, M.E., Macambira, M.J.B. and de Valente, S.C. 2008. New geological and single-zircon Pb evaporation data from the Central Guyana Domain, southeastern Roraima, Brazil: tectonic implications for the central region of the Guyana Shield. *Journal of South*

American Earth Sciencies, **26**, 318–328, https://doi.org/10.1016/j.jsames.2008.08.003

Alves, C.L., Sabóia, A.M., Martins, E.G. and Stropper, J.L. 2010. *Geologia e Recursos Minerais das Folhas São José do Xingu – SC.22-Y-A e Rio Comandante Fontoura – SC.22-Y-B. Escala 1:250.000*. CPRM, Projeto Noroeste-Nordeste do Mato Grosso, Goiânia, http://rigeo.cprm.gov.br/jspui/handle/doc/11359

Alves, C.L., Rizzotto, G.J., Rios, F.S., Duarte, T.B. and Gonçalves, G.F. 2019. Estratigrafia. *In*: Alves, C.L., Rizzotto, G.J., Rios, F.S., Duarte, T.B. and Gonçalves, G.F. (eds) *Áreas de Relevante Interesse Mineral (ARIM) – Evolução Crustal e Metalogenia da Província Mineral Juruena-Teles Pires*. Mato Grosso, Brasil, CPRM, Goiânia, http://rigeo.cprm.gov.br/jspui/handle/doc/21324

Annells, R.N., Fletcher, C.J.N., Styles, M.T., Burton, C.C.J., Evans, R.B. and Harding, R.R. 1986*a*. *The Rincón del Tigre Igneous Complex: a Major Layered Ultramafic–Mafic Intrusion of Proterozoic age in the Prepotash Shield of Eastern Bolivia. Part I. Geology and Mineral Potential (with 1:100 000 Scale Geological map)*. British Geological Survey, Overseas Geology and Mineral Resources.

Annells, R.N., Fletcher, C.J.N., Styles, M.T., Appleton, J.D., Burton, C.C.J., Evans, R.B. and Harding, R.R. 1986*b*. Mineral potential of the Rincón del Tigre Igneous Complex: a major Upper Proterozoic layered intrusion in the shield of eastern Bolivia. *In*: Gallagher, M.J., Ixer, R., Neary, C.R. and Prichard, H.M. (eds) *Metallogeny of Basic and Ultrabasic Rocks*. Institution of Mining and Metallurgy, London, 487–498.

Antonio, P.Y.J., D'Agrella-Filho, M.S. *et al*. 2017. Turmoil before the boring billion: paleomagnetism of the 1880–1860 Ma Uatumã event in the Amazonian craton. *Gondwana Research*, **49**, 106–129, https://doi.org/10.1016/j.gr.2017.05.006

Antonio, P.Y.J., D'Agrella-Filho, M.S. *et al*. 2021. New constraints for paleogeographic reconstructions at ca. 1.88 Ga from geochronology and paleomagnetism of the Carajás dyke swarm (eastern Amazonia). *Precambrian Research*, **353**, https://doi.org/10.1016/j.precamres.2020.106039

Assis, R.R. 2015. *Depósitos auríferos associados ao magmatismo félsico da Província de Alta Floresta (MT), Cráton Amazônico: litogeoquímica, idade das mineralizações e fonte dos fluidos*. PhD thesis, Universidade Estadual de Campinas, Campinas, Brasil.

Assis, R.R., Xavier, R.P. and Creaser, R.A. 2017. Linking the timing of disseminated granite hosted gold-rich deposits to paleoproterozoic felsic magmatism at Alta Floresta Gold Province, Amazon Craton, Brazil: insights from pyrite and molybdenite Re–Os geochronology. *Economic Geology*, **112**, 1937–1957, https://doi.org/10.5382/econgeo.2017.4535

Assunção, R.F.S. and Klein, E.L. 2014. The Moreira Gomes deposit of the Cuiú-Cuiú goldfield: fluid inclusions and stable isotope constraints and implications for the genesis of granite-hosted gold mineralization in the Tapajós Gold Province, Brazil. *Journal of South American Earth Sciences*, **49**, 85–105, https://doi.org/10.1016/j.jsames.2013.11.004

Baratoux, L., Söderlund, U. *et al*. 2019. New U–Pb baddeleyite ages of mafic dyke swarms of the West African and Amazonian cratons: implication for their configuration in supercontinents through time. *In*: Srivastava, R.K., Ernst, R.E. and Peng, P. (eds) *Dyke Swarms of the World: A Modern Perspective*. Springer Geology, https://doi.org/10.1007/978-981-13-1666-1_7

Barreto, C.J.S., Lafon, J.M., Rosa-Costa, L.T. and Lima, E.F. 2014. Paleoproterozoic (∼1.89 Ga) felsic volcanism of the Iricoumé Group, Guyana Shield, South America: geochemical and Sm–Nd isotopic constraints on sources and tectonic environment. *International Geology Review*, **56**, 1332–1356, https://doi.org/10.1080/00206814.2014.930800

Bastos Neto, A.C., Pereira, V., Pires, A.C., Barbanson, L. and Chauvet, A. 2012. F-rich xenotime from the Nb–Ta–Sn Madeira world-class deposit associated with the albite-enriched granite at Pitinga (Amazonian, Brazil). *Canadian Mineralogist*, **50**, 1453–1466, https://doi.org/10.3749/canmin.50.6.1453

Bastos Neto, A.C., Ferron, J.T.M.M., Chauvet, A., Chemale, Jr F., Lima, E.F., Barbanson, L. and Costa, C.F.M. 2014. U–Pb dating of the Madeira Suite and structural control of thealbite-enriched granite at Pitinga (Amazonia, Brazil): evolution of the A-type magmatism and implications for the genesis of the Madeira Sn–Ta–Nb (REE, cryolite) world-class deposit. *Precambrian Research*, **243**, 181–196, https://doi.org/10.1016/j.precamres.2013.12.021

Bettencourt, J.S., Leite Júnior, W.B., Goraieb, C.L., Sparrenberger, I., Bello, R.M.S. and Payolla, B.L. 2005. Sn-polymetallic greisen-type deposits associated with latest age Rapakivi granites, Brazil: fluid inclusion and stable isotope characteristics. *Lithos*, **80**, 363–386, https://doi.org/10.1016/j.lithos.2004.03.060

Bettencourt, J.S., Leite, W., Jr, Ruiz, B., Matos, A.S., Payolla, R.S. and Tosdal, R.M. 2010. The Rondonian–San Ignacio Province in the SW Amazonian Craton: an overview. *Journal of South American Earth Sciences*, **29**, 28–46, https://doi.org/10.1016/j.jsames.2009.08.006

Bettencourt, J.S., Juliani, C. *et al*. 2016. Metallogenetic systems associated with granitoid magmatism in the Amazonian Craton: an overview of the present level of understanding and exploration significance. *Journal of South American Earth Sciences*, **68**, 22–49, https://doi.org/10.1016/j.jsames.2015.11.014

Betiollo, L.M., Reis, N.J., Almeida, M.E., Bahia, R.C., Splendor, F., Costa, U.P. and Luzardo, R. 2009. Magmatismo Máfico Calimiano (Sill Mata-Matá), rio Aripuanã, Amazonas – Implicações Geológicas, presented at *Simpósio de Geologia da Amazônia*, **XI**, Manaus.

Biondi, J.C. 2020. Formation of the Tocantinzinho 1989 Ma gold-only deposit (Pará State, northern Brazil), based on sulfur, oxygen, hydrogen, and carbon isotope data. *Journal of South American Earth Sciences*, **97**, https://doi.org/10.1016/j.jsames.2019.102366

Biondi, J.C., Borgo, A., Chauvet, A., Monié, P., Bruguier, O. and Ocampo, R. 2018. Structural, mineralogical, geochemical and Geochronological constraints on ore genesis of the gold-only Tocantinzinho deposit (Pará State, Brazil). *Ore Geology Review*, **102**, 154–194, https://doi.org/10.1016/j.oregeorev.2018.08.007

Bispo-Santos, F., D'Agrella-Filho, M.S. *et al*. 2008. Columbia revisited: paleomagnetic results from the 1790 Ma Colíder volcanics (SW Amazonian Craton, Brazil). *Precambrian Research*, **164**, 40–49, https://doi.org/10.1016/j.precamres.2008.03.004

Bispo-Santos, F., D'Agrella-Filho, M.S. *et al*. 2012. Tectonic implications of the 1419 Ma Nova Guarita mafic intrusives paleomagnetic pole (Amazonian Craton) on the longevity of Nuna. *Precambrian Research*, **196–197**, 1–22, https://doi.org/10.1016/j.precamres.2011.10.022

Bispo-Santos, F., D'Agrella-Filho, M.S., Janikian, L., Reis, N.J., Reis, M.A.A.A. and Trindade, R.I.F. 2014*a*. Towards Columbia: paleomagnetism of 1980–1960 Ma Surumu volcanic rocks, Northern Amazonian Craton. *Precambrian Research*, **244**, 123–138, https://doi.org/10.1016/j.precamres.2013.08.005

Bispo-Santos, F., D'Agrella-Filho, M.S., Trindade, R.I.F., Janikian, L. and Reis, N.J. 2014*b*. Was there SAMBA in Columbia? Paleomagnetic evidence from 1790 Ma Avanavero mafic sills (Northern Amazonian craton). *Precambrian Research*, **244**, 139–155, https://doi.org/10.1016/j.precamres.2013.11.002

Bispo-Santos, F., D'Agrella-Filho, M.S., Pesonen, L.J., Salminen, J.M., Reis, N.J. and Silva, J.M. 2020. The long life of SAMBA connection in Columbia: a paleomagnetic study of the 1535 Ma Mucajaí Complex, Northern Amazonian Craton, Brazil. *Gondwana Research*, **80**, 285–302, https://doi.org/10.1016/j.gr.2019.09.016

Bleeker, W. and Ernst, R.E. 2006. Short-lived mantle generated magmatic events and their dyke swarms: the key to unlocking Earth's paleogeographic record back to 2.5 Ga. Paper presented at the Fifth International Dyke Conference, July–August 2005, Balkema, Rotterdam.

Bogdanova, S.V., Bingen, B., Gorbatschev, R., Kheraskova, T.N., Koslov, V.I., Puchkov, V.N. and Volozh, Y.A. 2008. The East European Craton (Baltica) before and during the assembly of Rodinia. *Precambrian Research*, **160**, 23–45, https://doi.org/10.1016/j.precamres.2007.04.024

Borges, R.M.K., Dall'Agnol, R. and Costi, H.T. 2003. Geologia, Petrografia e Química Mineral das micas dos greisens estaníferos associados ao Pluton Água Boa, Pitinga (AM). *Revista Brasileira de Geociências*, **33**, 51–62, https://doi.org/10.25249/0375-7536.20033315162

Borges, R.M.K., Villas, R.N.N., Fuzikawa, K., Dall'Agnol, R. and Pimenta, M.A. 2009. Phase separation, fluid mixing, and origin of the greisens and potassic episyenite associated with the Água Boa pluton, Pitinga tin province, Amazonian Craton, Brazil. *Journal of South American Earth Sciences*, **27**, 161–183, https://doi.org/10.1016/j.jsames.2008.11.006

Borgo, A., Biondi, J.C. *et al*. 2017. Geochronological, geochemical and petrographic constraints on the Paleoproterozoic Tocantinzinho gold deposit (Tapajos Gold Province, Amazonian Craton, Brazil). Implications for timing, regional evolution and deformation style of its host rocks. *Journal of South American Earth Sciences*, **75**, 92–115, https://doi.org/10.1016/j.jsames.2017.02.003

Briceño, H.O., Tapia, J. and Estanga, J. 1989. Formación Ichún. Volcanismo Acido del Grupo Roraima, presented at *Congreso de Geología Venezolano*, **7**, Caracas, 52–81.

Bryan, S. and Ernst, R.E. 2008. Revised definition of large igneous provinces (LIPs). *Earth Science Review*, **86**, 175–202, https://doi.org/10.1016/j.earscirev.2007.08.008

Bryan, S.E. and Ferrari, L. 2013. Large igneous provinces and silicic large igneous provinces: progress in our understanding over the last 25 years. *Geological Society of America Bulletin*, **125**, 1053–1078, https://doi.org/10.1130/B30820.1

Butt, C.R.M. and Zeegers, H. 1989. Classification of geochemical exploration models for tropically weathered terrains. *Journal of Geochemical Exploration*, **32**, 65–74, https://doi.org/10.1016/0375-6742(89)90048-4

Cawood, P.A. and Pisarevsky, S.A. 2017. Laurentia–Baltica–Amazonia relations during Rodinia assembly. *Precambrian Research*, **292**, 386–397, https://doi.org/10.1016/j.precamres.2017.01.031

Chardon, D., Bamba, O. and Traoré, K. 2020. Eburnean deformation pattern of Burkina Faso and the tectonic significance of shear zones in the West African craton. *Bulletin de la Société Géologique de France*, 191.

Choudhary, B.R., Ernst, R.E. *et al*. 2019. Geochemical characterization of a reconstructed 1110 Ma Large Igneous Province. *Precambrian Research*, **332**, 105382, https://doi.org/10.1016/j.precamres.2019.105382

Cinelu, S. and Cuney, M. 2006. Sodic metasomatism and U–Zr mineralization: a model based on the Kurupung batholith (Guyana). *Geochimica et Cosmochimica Acta*, **70**, A103, https://doi.org/10.1016/j.gca.2006.06.120

Cordani, U.G. and Teixeira, W. 2007. Proterozoic accretionary belts in the Amazonian Craton. *Geological Society of America Memoir*, **200**, 297–319, https://doi.org/10.1130/2007.1200

Cordani, U.G., Fraga, L.M., Reis, N.J., Tassinari, C.C.G. and Brito-Neves, B.B. 2010. On the origin and tectonic significance of the intra-plate events of Grenvillian-type in South America: a discussion. *Journal of South American Earth Sciences*, **29**, 143–159, https://doi.org/10.1016/j.jsames.2009.07.002

Corrêa-Lima, R.G. and Klein, E.L. 2020. Hydrothermal alteration, mineralization and fluid inclusions in the Pista and Fofão prospects: implications for the genetic model of the Coringa polymetallic deposit, SE Tapajós Mineral Province, Amazonian Craton, Brazil. *Journal of the Geological Survey of Brazil*, **3**, 33–59, https://doi.org/10.29396/jgsb.2020.v3.n1.3

Costi, H.T., Dall'Agnol, R. and Moura, C.A.V. 2000. Geology and Pb–Pb geochronology of Paleoproterozoic volcanic and granitic rocks of Pitinga Province, Amazonian Craton, northern Brazil. *International Geology Review*, **42**, 832–849, https://doi.org/10.1080/00206810009465114

Costi, H.T., Dall'Agnol, R., Pichavant, M. and Rämo, O.T. 2009. The peralkaline tin-mineralized Madeira cryolite albite-rich granite of Pitinga, Amazonian Craton, Brazil: petrography, mineralogy and crystallization processes. *Canadian Mineralogist*, **47**, 1301–1327, https://doi.org/10.3749/canmin.47.6.1301

CPRM, Geological Survey of Brazil. 1999. Programa Levantamentos Geológicos Básicos do Brasil. Roraima Central, Folhas NA.20-X-B e NA.20-X-D (integrais), NA.20-X-A, NA.20-X-C, NA.21-V-A e NA.21-V-C (parciais). Escala 1:500 000. Estado de Roraima. *In*: Fraga, L.M. (ed.). Projeto Roraima Central, Manaus, http://rigeo.cprm.gov.br/jspui/handle/doc/8510

CPRM, Geological Survey of Brazil. 2010. Programa Geologia do Brasil. Programa Cartografia da Amazônia. Geologia e Recursos Minerais da Folha Vila de Tepequém, NA.20-X-A-III. Escala 1:100 000. Estado de Roraima. *In*: Fraga, L.M. and Dreher, A.M. (eds). Projeto Roraima Central, Manaus, http://rigeo.cprm.gov.br/jspui/handle/doc/10920

D'Agrella-Filho, M.S., Tohver, E., Santos, J.O.S., Elming, S.-Å., Trindade, R.I.F., Pacca, I.G. and Geraldes, M.C. 2008. Direct dating of paleomagnetic results from Precambrian sediments in the Amazon craton: evidence for Grenvillian emplacement of exotic crust in SE Appalachians of North America. *Earth and Planetary Science Letters*, **267**, 188–199, https://doi.org/10.1016/j.epsl.2007.11.030

D'Agrella-Filho, M.S., Trindade, R.I.F. *et al*. 2012. The 1420 Ma Indiavaí Mafic Intrusion (SW Amazonian Craton): paleomagnetic results and implications for the Columbia supercontinent. *Gondwana Research*, **22**, 956–973, https://doi.org/10.1016/j.gr.2012.02.022

D'Agrella-Filho, M.S., Bispo-Santos, F., Trindade, R.I.F. and Antonio, P.Y.J. 2016*a*. Paleomagnetism of the Amazonian Craton and its role in paleocontinents. *Brazilian Journal of Geology*, **46**, 275–299, https://doi.org/10.1590/2317-4889201620160055

D'Agrella-Filho, M.S., Trindade, R.I.F., Queiroz, M.V.B., Meira, V.T., Janikian, L., Ruiz, A.S. and Bispo-Santos, F. 2016*b*. Reassessment of Aguapeí (Salto do Céu) Paleomagnetic pole of the Amazonian Craton and implications for Proterozoic supercontinents. *Precambrian Research*, **272**, 1–17, https://doi.org/10.1016/j.precamres.2015.10.021

D'Agrella-Filho, M.S., Antonio, P.Y.J., Trindade, R.I.F., Teixeira, W. and Bispo-Santos, F. 2020. Precambrian drift history and paleogeography of Amazonia. *In*: Pesonen, L.P., Salminen, J., Evans, D.A.D., Elming, S.-Å. and Veikkolainen, T. (eds) *Ancient Supercontinents and the Paleogeography of the Earth*. Elsevier, Chapter 6.

Davey, S.C. 2019. *Testing the paleogeography of late Archean supercraton Superia using pre-breakup 2.51–1.98 Ga dyke and sill provinces – with a focus on the relationship between the Karelia–Kola and Superior cratonic fragments*. PhD thesis, Carleton University.

Dezula, S.E.M., Barros, M.A.S., Pierosan, R., Santos, J.O.S. and Assis, R.R. 2018. Granito Aragão – Suíte intrusiva Nhandú – um granito oxidado, tipo A2, de 1967 a 1964 Ma na Província Aurífera Alta Floresta – Cráton Amazônico. *Revista do Instituto de Geociências – USP, Série Científica*, **18**, 20.

Dreher, A.M., Almeida, M.E., Ferreira, A.L., Brito, M.F., Popini, M.V. and Monteiro, M.A. 1999. Veios e brechas hidrotermais da Província Aurífera Tapajós: Aspectos Texturais e Implicações para a Exploração do Au Primário, presented at *Simpósio de Geologia da Amazônia*, **6**, Manaus, 114–117.

Duarte, T.B. and Lopes, L.B.L. 2015. Metalogenia das províncias minerais do Brasil: Província Aurífera Juruena–Teles Pires–Aripuanã; Geologia e Recursos da Ilha Porto Escondido – SC.21-V-C-III, estado do Mato Grosso, Goiânia, CPRM, http://rigeo.cprm.gov.br/jspui/handle/doc/16714

Echeverri-Misas, C.M. 2010. *Geologia e Gênese do Depósito de Au–(Cu) do Palito, Província Aurífera do Tapajós*. Dissertação de Mestrado, IG/USP.

Echeverri-Misas, C.M. 2015. *Geologia e alteração hidrotermal nas rochas vulcânicas e plutônicas paleoproterozoicas na porção Sul da Província Mineral do Tapajós (PA)*. Universidade de São Paulo, Tesis, http://www.teses.usp.br/teses/disponiveis/44/44141/tde-27082015-101343/

Elming, S.-Å., Moakhar, M.O., Layer, P. and Donadini, F. 2009. Uplift deduced from remanent magnetization of a proterozoic basic dyke and the baked country rock in the Hoting area, Central Sweden: a palaeomagnetic and $^{40}Ar/^{39}Ar$ study. *Geophysical Journal International*, **179**, 59–78, https://doi.org/10.1111/j.1365-246X.2009.04265.x

Elming, S.-Å., Layer, P. and Söderlund, U. 2019. Cooling history and age of magnetization of a deep intrusion: a new 1.7 Ga key pole and Svecofennian–post Svecofennian APWP for Baltica. *Precambrian Research*, **329**, 182–194, https://doi.org/10.1016/j.precamres.2018.05.022

Ernst, R.E. 2014. *Large Igneous Provinces*. Cambridge University Press.

Ernst, R.E. and Bleeker, W. 2010. Large Igneous Provinces (LIPs), giant dyke swarms, and mantle plumes: significance for breakup events within Canada (and selected adjacent regions) from 2.5 Ga to present. *Canadian Journal of Earth Sciences*, **47**, 695–739, https://doi.org/10.1139/E10-025.

Ernst, R.E. and Jowitt, S.M. 2013. Large igneous provinces (LIPs) and metallogeny. *Society of Economic Geologists, Special Publications*, **17**, 17–51.

Ernst, R.E. and Youbi, N. 2017. How Large Igneous Provinces affect global climate, sometimes cause mass extinctions, and represent natural markers in the geological record. *Palaeogeography, Palaeoclimatology, Palaeoecology*, **478**, 30–52, https://doi.org/10.1016/j.palaeo.2017.03.014

Ernst, R.E., Bleeker, W., Söderlund, U. and Kerr, C.A. 2013. Large igneous provinces and supercontinents: toward completing the plate tectonic revolution. *Lithos*, **174**, 1–14, https://doi.org/10.1016/j.lithos.2013.02.017

Ernst, R.E., Hamilton, M.A. *et al*. 2016. Long-lived connection between southern Siberia and northern Laurentia in the Proterozoic. *Nature Geoscience*, **9**, 464–469, https://doi.org/10.1038/ngeo2700

Ernst, R.E., Bond, D.P.G. and Zhang, S.H. 2020. Influence of large igneous provinces. *In*: Gradstein, F.M., Ogg, J.G., Schmitz, M.D. and Ogg, G.M. (eds) *Geologic Time Scale 2020*. 345–356, https://doi.org/10.1016/B978-0-12-824360-2.00012-7

Ernst, R.E., Bond, D.P.G. *et al*. 2021. Large igneous province record through time and implications for secular environmental changes and Geological Time-Scale boundaries. *In*: Ernst, R.E., Dickson, A.J. and Bekker, A. (eds) *Large Igneous Provinces: A Driver of Global Environmental and Biotic Changes*. AGU, Geophysical Monographs.

Evans, D.A.D. 2013. Reconstructin pre-Pangean supercontinents. *Geological Society of America Bulletin*, **125**, 1735–1751, https://doi.org/10.1130/B30950.1

Evans, D.A.D. and Mitchell, R.N. 2011. Assembly and breakup of the core of Paleoproterozoic–Mesoproterozoic supercontinent Nuna. *Geology*, **39**, 443–446, https://doi.org/10.1130/G31654.1

Evans, D.A.D. and Pisarevsky, S.A. 2008. Plate tectonics on early Earth? Weighing the paleomagnetic evidence. *In*: Condie, K.C. and Pease, V. (eds) *When Did Plate Tectonics Begin on Planet Earth?* Geological Society of America, Special Papers, **440**, 249–263.

Evans, D.A.D., Veselovsky, R.V., Petrov, P.Y., Shatsillo, A.V. and Pavlov, V.E. 2016. Paleomagnetism of Mesoproterozoic margins of the Anabar Shield: a hypothesized billion-year partnership of Siberia and northern Laurentia. *Precambrian Research*, **281**, 639–655, https://doi.org/10.1016/j.precamres.2016.06.017

Fedotova, M.A., Khramov, N.A., Pisakin, B.N. and Priyatkin, A.A. 1999. Early Proterozoic palaeomagnetism: new results from the intrusives and related rocks of the Karelian, Belomorian and Kola provinces, eastern Fennoscandian Shield. *Geophysical Journal Interiors*, **137**, 691–712, https://doi.org/10.1046/j.1365-246x.1999.00817.x

Feio, G.R.L., Dall'Agnol, R. and Borges, R.M.K. 2007. Greisens associados ao topázio-granito do pluton Água Boa, Província Estanífera de Pitinga: Petrografia e Balanço de massa. *Revista Brasileira de Geociências*, **37**, 2–17.

Fernandes, C.J., Kuyumjian, R.M., Pulz, G.M., Geraldes, M.C. and Pinho, F.E.C. 2006. Geologia Estrutural e idade $^{40}Ar/^{39}Ar$ do Depósito de Ouro Pau-Apique, Faixa Móvel Aguapeí, Sudoeste do Estado do Mato Grosso. *Revista Brasileira de Geociências*, **36**(l – suppl), 3–15, https://doi.org/10.25249/0375-7536.200636S10315

Fernandes, C.M.D., Juliani, C., Moura, C.A.V. and Lagler, B. 2008. Paleoproterozoic bimodal volcanism of the São Félix do Xingu region, South Pará State, Amazonian Craton, Brazil, presented at *33rd International Geological Congress*, Oslo.

Fernandes, C.M.D., Juliani, C., Monteiro, L.V.S., Lagler, B. and Echeverri-Misas, C.M. 2011. High-K calc-alkaline to A-type fissure-controlled volcano-plutonism of the São Felix do Xingu region, Amazonian craton, Brazil: exclusively crustal sources or only mixed Nd model ages? *Journal of South American Earth Sciences*, **32**, 351–368, https://doi.org/10.1016/j.jsames.2011.03.004

Ferron, J.M.T.M., Bastos Neto, A.C., de Lima, F., Nardi, L.V.S., Costi, H.T., Pierosan, R. and Prado, M. 2010. Petrology, geochemistry, and geochronology of Paleoproterozoic volcanic and granitic rocks (1.89–1.88 Ga) of the Pitinga Province, Amazonian Craton, Brazil. *Journal of South American Earth Sciences*, **29**, 483–497, https://doi.org/10.1016/j.jsames.2009.05.001

Fraga, L.M.B., Haddad, R.C. and Reis, N.J. 1997. Aspectos Geoquímicos das Rochas Granitóides da Suíte Intrusiva Pedra Pintada, Norte do Estado de Roraima. *Revista Brasileira de Geociências*, **27**, 3–12, https://doi.org/10.25249/0375-7536.1997312

Fraga, L.M., Reis, N.J., Dall'Agnol, R. and Armstrong, R. 2008. Cauarane–Coeroene Belt – the tectonic southern limit of the preserved Rhyacian crustal domain in the Guyana Shield, Northern Amazonian Craton, presented at *International Geological Congress*, 6–14 August, Oslo.

Fraga, L.M., Cordani, U., Kroonenberg, S.B., de Roever, E.W.F., Nadeau, S. and Maurer, V.C. 2017*a*. U–Pb SHRIMP: new data on the high-grade supracrustal rocks of the Cauarane–Coeroeni Belt – insights on the tectonic Eo-Orosirian evolution of the Guiana Shield, presented at *Simpósio de Geologia da Amazônia*, **15**, Belém.

Fraga, L.M., Cordani, U., Reis, N.J., Nadeau, S. and Maurer, V.C. 2017*b*. U–Pb SHRIMP and LA-ICPMS new data for different A-type granites of the Orocaima Igneous Belt, Central Guiana Shield, Northern Amazonian Craton, presented at *Simpósio de Geologia da Amazônia*, **15**, Belém.

Fraga, L.M., Vasquez, M.L., Almeida, M.E., Dreher, A.M. and Reis, N.J. 2017*c*. A Influência da Orogenia Eo-Orosiriana na formação da SLIP Uatumã, parte central do Cráton Amazônico, presented at *Simpósio de Geologia da Amazônia*, **15**, Belém.

Fraga, L.M., Lafon, J-M. and Tassinari, C.C.G. 2020. Geologia e Evolução Tectônica das porções central e nordeste do Escudo das Guianas e sua estruturação em cinturões eo-orosirianos. *In*: Bartorelli, A., Teixeira, W. and de Neves, B.B.B. (eds) *Geocronologia e Evolução Tectônica do Continente Sul-Americano: A Contribuição de Umberto Giuseppe Cordani*. Solaris Edições Culturais, São Paulo, 92–110.

Gala, M.G., Symons, D.T.A. and Palmer, H.C. 1995. Paleomagnetism of the Jan Lake Granite, Trans-Hudson Orogen. Summary of Investigations 1995, Saskatchewan Geological Survey. *Saskatchewan Energy and Mines Miscellaneous Reports*, **95**(4), 145–152.

Galé, M.G. 2018. *Gênese das mineralizações associadas ao magmatismo ácido na região do Garimpo do Papagaio, noroeste da Província Aurífera de Alta Floresta (MT)*. PhD thesis, Universidade de São Paulo, Instituto de Geociências, São Paulo.

Geraldes, M.C., Tassinari, C.C.G. and Ebert, H.D. 1997. Middle Proterozoic vein-hosted gold deposit in the Pontes e Lacerda region, southwestern Amazonian craton, Brazil. *International Geology Review*, **39**, 438–448, https://doi.org/10.1080/00206819709465282

Geraldes, M.C., Van Schmus, W.R., Condie, K.C., Bell, S., Teixeira, W. and Babinski, M. 2001. Proterozoic geologic evolution of the SW part of the Amazonian craton in Mato Grosso state, Brazil. *Precambrian Research*, **11**, 91–108, https://doi.org/10.1016/S0301-9268(01)00158-9

Geraldes, M.C., Herkenhoff, A.V., Vargas-Matos, G.L., Matos, R. and Teixeira, W. 2009. Estudos petrográficos e isotópicos do Depósito Aurífero de Puquio Norte (sudeste da Bolivia), sudoeste do Cráton Amazonico. *In*: Rizzotto, G., do Quadros, M.L.E.S. and Vasquez, M.L. (eds) *Contribuições à Geologia da Amazonia*. Porto Velho, **6**, 85–98.

Gibbs, A.K. and Barron, C.N. 1993. *The Geology of the Guiana Shield*. Oxford University Press.

Giovanardi, T., Girardi, V.A.V., Teixeira, W. and Mazzucchelli, M. 2019. Mafic dyke swarms at 1882, 535 and 200 Ma in the Carajás region, Amazonian Craton: SrNd isotopy, trace element geochemistry and inferences on their origin and geological settings. *Journal* *of South America Earth Science*, **92**, 197–208, https://doi.org/10.1016/j.jsames.2019.02.017

Goulart, L.E.A., Lopes, P.R.S., Vasquez, M.L. and Oliveira, A.C.S. 2019. Caracterização da primeira ocorrência de anortosito com titanomagnetita vanadífera no Escudo das Guianas, Roraima, Brasil. *Serviço Geológico do Brasil, Informe Técnico*, **15**, https://doi.org/10.29396/itcprm.2019.15

Gradstein, F.M., Ogg, J.G., Schmitz, M.D. and Ogg, G.M. (eds) 2020. *Geologic Time Scale 2020*. Elsevier, https://doi.org/10.1016/C2020-1-02369-3

Grainger, C.J., Groves, D.I., Tallarico, F.H.B. and Fletcher, I.R. 2008. Metallogenesis of the Carajás Mineral Province, southern Amazon Craton, Brazil: varying styles of Archean through Paleoproterozoic to Neoproterozoic baseando precious-metal mineralization. *Ore Geology Reviews*, **33**, 451–489, https://doi.org/10.1016/j.oregeorev.2006.10.010

Guimarães, S.B. and Klein, E.L. 2020. Geochemical and isotopic constraints on the host rocks of the magmatic–hydrothermal Coringa gold–silver (Cu–Pb–Zn) deposit of the Tapajos mineral province, Amazonian Craton, Brazil. *Journal of South American Earth Sciences*, **103**, https://doi.org/10.1016/j.jsames.2020.102726

Guimarães, S.B., Klein, E.L., Harris, C. and Costa, I.S.L. 2021. Metallogenesis of the Orosirian epithermal Coringa gold–silver (Cu–Pb–Zn) deposit, Southeastern Tapajós Mineral Province, Amazonian Craton, Brazil. *Ore Geology Reviews*, **128**, https://doi.org/10.1016/j.oregeorev.2020.103908

Halls, H.C., Hamilton, M.A. and Denyszyn, S.W. 2011. The Melville Bugt dyke swarm of Greenland: a connection to the 1.5–1.6 Ga Fennoscandian Rapakivi Granite Province? *In*: Srivastava, R.K. (ed.) *Dyke Swarms: Keys for Geodynamic Interpretation*. Springer, Berlin, 509–535.

Hamilton, M.A. and Buchan, K.L. 2010. U–Pb geochronology of the Western Channel Diabase, northwestern Laurentia: implications for a large 1.59 Ga magmatic province, Laurentia's APWP and paleocontinental reconstructions of Laurentia, Baltica and Gawler craton of southern Austrália. *Precambrian Research*, **183**, 463–473, https://doi.org/10.1016/j.precamres.2010.06.009

Heaman, L.M., Easton, R.M., Hart, T.R., Hollings, P., MacDonald, C.A. and Smyk, M. 2007. Further refinement of the timing of Mesoproterozoic magmatism, Lake Nipigon region, Ontario. *Canadian Journal of Earth Sciences*, **44**, 1055–1086, https://doi.org/10.1139/E06-117

Heinonen, A.P., Fraga, L.M., Rämö, O.T., Dall'Agnol, R., Mänttäri, I. and Andersen, T. 2012. Petrogenesis of the igneous Mucajaí AMG Complex, northern Amazonian craton, U–Pb geochronological, and Nd–Hf–O isotopic constraints. *Lithos*, **151**, 17–34, https://doi.org/10.1016/j.lithos.2011.07.016

Ibañez-Mejia, M., Ruiz, J., Valencia, V.A., Cardona, A., Gehrels, G.E. and Mora, A.R. 2011. The Putumayo Orogen of Amazonia and its implications for Rodinia reconstructions: new U–Pb geochronological insights into the Proterozoic tectonic evolution of northwestern South America. *Precambrian Research*, **191**, 58–77, https://doi.org/10.1016/j.precamres.2011.09.005

Irving, E., Donaldson, J.A. and Park, J.K. 1972. Palaeomagnetism of the Western Channel diabase and associated rocks. Northwest Territories. *Canadian Journal of Earth Sciences*, **9**, 960–971, https://doi.org/10.1139/e72-080

Irving, E., Baker, J., Hamilton, M. and Wynne, P.J. 2004. Early Proterozoic geomagnetic field in western Laurentia: implications for paleolatitudes, local rotations and stratigraphy. *Precambrian Research*, **129**, 251–270, https://doi.org/10.1016/j.precamres.2003.10.002

Isla-Moreno, L. 2009. Distrito Don Mario, un deposito de Au–Cu hidrotermal asociado a zonas de cizalla, presented at *Congreso Geológico de Bolivia*, **18**, Potosi, Bolívia.

Johansson, A. 2009. Baltica, Amazonia and the SAMBA connection – 1000 million years of neighbourhood during the Proterozoic? *Precambrian Research*, **175**, 221–234, https://doi.org/10.1016/j.precamres.2009.09.011

Johansson, A. 2014. From Rodinia to Gondwana with the 'SAMBA' model – a distant view from Baltica towards Amazonia and beyond. *Precambrian Research*, **244**, 226–235, https://doi.org/10.1016/j.precamres.2013.10.012

Jowitt, S.M. and Ernst, R.E. 2013. Geochemical assessment of the metallogenic potential of Proterozoic LIPs of Canada. *Lithos*, **174**, 291–307, https://doi.org/10.1016/j.lithos.2012.03.026

Juliani, C. and Fernandes, C.M.D. 2010. Well-preserved Late Paleoproterozoic volcanic centers in the São Félix do Xingu region, Amazonian Craton, Brazil. *Journal of Volcanology and Geothermal Research*, **191**, 167–179, https://doi.org/10.1016/j.jvolgeores.2010.01.016

Juliani, C., Rye, R.O. *et al*. 2005. Paleoproterozoic high-sulfidation mineralization in the Tapajós Gold Province, Amazonian Craton, Brazil: geology, mineralogy, alunite argon age and stable-isotope constraints. *Chemical Geology*, **215**, 95–125, https://doi.org/10.1016/j.chemgeo.2004.06.035

Juliani, C., Carneiro, C.C., Carreiro-Araújo, S.A., Fernandes, C.M.D., Monteiro, L.V.S. and Crosta, A.P. 2013. Estruturação dos arcos magmáticos paleoproterozoicos na porção sul do Craton Amazônico: implicações geotectônicas e metalogenéticas, presented at *Simpósio de Geologia da Amazônia*, **13**, Belém.

Juliani, C., Vasquez, M.L. *et al*. 2014. Metalogênese da Província Tapajós. 229–268.

Kasbohm, J., Schoene, B. and Burgess, S. 2020. Radiometric constraints on the timing, tempo, and effects of large igneous province emplacement. *In*: Ernst, R.E., Dickson, A.J. and Bekker, A. (eds) *Large Igneous Provinces: A Driver of Global Environmental and Biotic Changes*. AGU, Geophysical Monographs, 255 (in press).

Klein, E.L. and Carvalho, J.M.A. 2008. Recursos minerais. *In*: Vasquez, M.L. and Rosa-Costa, L.T. (eds) *Geologia e Recursos Minerais do Estado do Pará: Sistema de Informações Geográficas e SIG: texto explicativo dos mapas Geológico e Tectônico e de Recursos Minerais do Estado do Pará. Escala 1:1.000.000*. CPRM e Serviço Geológico do Brasil, Belém, 217–262, http://rigeo.cprm.gov.br/jspui/handle/doc/10443

Klein, E.L., Almeida, M.E. and Rosa-Costa, L.T. 2012. The 1.89–1.87 Ga Uatumã Silicic Large Igneous Province, northern South America. November 2012 LIP of the Month, http://www.largeigneousprovinces.org/12nov

Klein, E.L., Rodrigues, J.B., Queiroz, J.D.S., Oliveira, R.G., Guimarães, S.B. and Chaves, C.L. 2016. Deposition and tectonic setting of the Palaeoproterozoic Castelo de Sonhos metasedimentary formation, Tapajós Gold Province, Amazonian Craton, Brazil: age and isotopic constraints. *International Geology Review*, **59**, 864–883, https://doi.org/10.1080/00206814.2016.1237311

Kroonenberg, S.B. and de Roever, E.W.F. 2010. Geological evolution of the Amazonian Craton. *In*: Hoorn, C. and Wesselingh, F.P. (eds) *Tectonic Processes as Driving Mechanisms for Palaeogeographical and Palaeoenvironmental Evolution in Amazonia*, 1st edn. Blackwell, 9–28.

Kroonenberg, S.B., de Roever, E.W.F. *et al*. 2016. Paleoproterozoic evolution of the Guiana Shield in Suriname: a revised model. *Netherlands Journal of Geosciences, Geologie en Mijnbouw*, **95**, 491–522, https://doi.org/10.1017/njg.2016.10

Lamarão, C.N., Dall'Agnol, R., Lafon, J.M. and Lima, E.F. 2002. Geology, Geochemistry, and Pb–Pb zircon Geochronology of the Paleoproterozoic magmatism of Vila Riozinho, Tapajós Gold Province, Amazonian Craton, Brazil. *Precambrian Research*, **119**, 189–223, https://doi.org/10.1016/S0301-9268(02)00123-7

Lamarão, C.N., Dall'Agnol, R. and Pimentel, M.M. 2005. Nd isotopic composition of Paleoproterozoic volcanic and granitoid rocks of Vila Riozinho: implications of the crustal evolution of the Tapajós gold province, Amazon craton. *Journal of South American Earth Sciences*, **18**, 277–292, https://doi.org/10.1016/j.jsames.2004.11.005

Lamarão, C.N., de Souza, K.S., Dall'Agnol, R. and Galarza, M.A. 2008. Granitos pórfiros da região de vila Riozinho, província aurífera do Tapajós: petrografia e geocronologia. *Revista Brasileira de Geociências*, **38**, 533–543, https://doi.org/10.25249/0375-7536.2008383533543

Landivar, G., Roca, J., Carvajal, R. and Barroso, E. 1996. Mapa Geológico Serranias SanJosé – San Diablo. Servicio Nacional de Geología y Minería, SERGEOMIN. 1 sheet (1: 250 000 scale).

Leal, R.E., Lafon, J.M., Rosa-Costa, L.T. da and Dantas, E.L. 2018. Orosirian magmatic episodes in the Erepecuru-Trombetas Domain (southeastern Guyana shield): implications for the crustal evolution of the Amazonian Craton. *Journal of South American Earth Sciences*, **85**, 278–297, https://doi.org/10.1016/j.jsames.2018.04.011

Leite, W.B. Jr. 2002. *A Suíte Intrusiva Santa Clara (RO) e a mineralização primária polimetálica (Sn, W, Nb, Ta, Zn, Cu e Pb) associada*. PhD thesis, Instituto de Geociências, Universidade de São Paulo.

Lenharo, S.L.R. 1998. *Evolução magmática e modelo metalogenético dos granitos mineralizados da região de Pitinga, Amazonas, Brasil*. PhD thesis, Universidade de São Paulo, Escola Politécnica, Departamento de Engenharia de Minas, São Paulo.

Lenharo, S.L.R., Pollard, P.J. and Born, H. 2003. Petrology and textural evolution of granites associated with tin and rare-metals mineralization at the Pitinga mine, Amazonas, Brazil. *Lithos*, **66**, 37–61, https://doi.org/10.1016/S0024-4937(02)00201-3

Li, Z.X., Bogdanova, S.V. *et al*. 2008. Assembly, configuration, and break-up history of Rodinia: a synthesis. *Precambrian Research*, **160**, 179–210, https://doi.org/10.1016/j.precamres.2007.04.021

Lima, G.A., Sousa, M.Z.A., Ruiz, A.S. and Sécolo, D.B. 2011. Enxame de Diques e Sills Máficos da Suíte Intrusiva Huanchaca: evidências da ruptura do Supercontinente Rodínia no SW do Craton Amazônico, presented at *Simpósio Nacional de Estudos Tectônicos – SNET*, **8**, Campinas.

Lima, G.A., Sousa, M.Z.A., Ruiz, A.S., D'agrella Filho, M.S. and Vasconcelos, P. 2012. Sills máficos da Suíte Intrusiva Huanchaca – SW do Cráton Amazônico: registro de magmatismo fissural relacionado à ruptura do Supercontinente Rodínia. *Revista Brasileira de Geociências*, **42**, 111–129, https://doi.org/10.25249/0375-7536.2012421111129

Lima, I.F., Pierosan, R., Barros, M.A.S., Rubert, R.R., Sommer, C.A. and Okuno, D.I.A. 2021. The 1.88 Ga Uatumã Magmatism in the Serra dos Magalhães region: petrology and implications to the ectension of the southeastern edge of the Amazonian Craton. *Brazilian Journal of Geology*, **51**, 1–21, https://doi.org/10.1590/2317-4889202120200046

Lindenmayer, Z.G., Fleck, A. *et al*. 2005. Caracterização geológica do alvo Estrela (Cu–Au), Serra dos Carajas. *In*: Marini, O.J., Queiroz, E.T. and Ramos, B.W. (eds) *Caracterização de Depósitos Minerais em Distritos Mineiros da Amazônia*. DNPM/ADIMB, Brasília, 137.

Lira, R.R.C. and Lopes, P.R.S. 2020. Carta Geológica-Geofísica Folha Boa Vista – NA.20-X-D-II. Manaus: CPRM, 2020. 1 mapa Color., Escala 1:100.000. Projeto Centro-Sudeste de Roraima. Ação Levantamento Geológico e de Potencial Novas Fronteiras. Programa de Geologia, Mineração e Transformação Mineral, http://rigeo.cprm.gov.br/jspui/handle/doc/20483

Litherland, M. and Power, P.E.J. 1989. The geologic and geomorphologic evolution of Serrania Huanchaca, eastern Bolivia: the legendary 'Lost World'. *Journal of South American Earth Sciences*, **2**, 1–17, https://doi.org/10.1016/0895-9811(89)90023-0

Litherland, M., Annels, R.N. *et al*. 1986. The geology and mineral resources of the Bolivian Precambrian shield. Overseas Memoir. *British Geological Survey Paper*, **9**.

Lopes, A.A.C. and Moura, M.A. 2019. The Tocantinzinho paleoproterozoic porphyry-style gold deposit, Tapajós Mineral Province (Brazil): geology, petrology and fluid inclusion evidence for ore-forming processes. *Minerals*, **9**, https://doi.org/10.3390/min9010029

Lubnina, N.V., Stepanova, A.V., Ernst, R.E., Nilsson, M. and Söderlund, U. 2016. New U–Pb baddeleyite age, and AMS and paleomagnetic data for dolerites in the Lake Onega region belonging to the 1.98–1.95 Ga regional Pechenga–Onega Large Igneous Province. *GFF, Journal of the Geological Society of Sweden*, **138**, 54–78.

Macambira, M.J.B., Barros, C.E.M., Silva, D.C.C. and Santos, M.C.C. 2001. Idades de cristais detríticos de zircão da Serra dos Carajás, Pará: evidências sobre a formação da crosta, presented at *Simpósio de Geologia da Amazônia*, **7**, Belém.

Macambira, M.J.B., Teixeira, W. and Vaquez, M.L. 2020. O Cráton Amazônico e suas províncias geocronológicas: o legado de Umberto Cordani. *In*: Bartorelli, A., Teixeira, W. and Brito Neves, B.B. (eds) *Geocronologia e Evolução Tectônica do Continente Sul-Americano: a Contribuição de Umberto Giuseppe Cordani*, 1st edn. Solares Edições Culturais, São Paulo, 47–62.

Machado, N., Lindenmayer, Z., Krogh, T.E. and Lindenmayer, D. 1991. U–Pb geochronology of Archean magmatism and basement reactivation in the Carajás area, Amazon Shield, Brazil. *Precambrian Research*, **49**, 329–354, https://doi.org/10.1016/0301-9268(91)90040-H

Meert, J.G. 2012. What's the name? The Columbia (Paleopangea/Nuna) supercontinent. *Gondwana Research*, **21**, 987–993, https://doi.org/10.1016/j.gr.2011.12.002

Mertanen, S. and Pesonen, L.J. 1995. Palaeomagnetic and rock magnetic investigations of the Sipoo Sub-jotnian quartz porphyry and diabase dykes, southern Fennoscandia. *Physics of the Earth and Planetary Interiors*, **88**, 145–175, https://doi.org/10.1016/0031-9201(94)02992-K

Miguel, Jr E. 2011. *Controle Estrutural das mineralizações auríferas e idades U–Pb das rochas encaixantes ao longo do Lineamento Peru-Trairão: Província Aurífera de Alta Floresta, Mato Grosso*. Msc thesis, Universidade Estadual de Campinas, Campinas, Brasil.

Mitchell, W.I. 1979. *La geología y potencial de minerales del área de Santo Corazón– Rincón del Tigre (Cuadrantes SE 21-5, con parte de SE 21-9 y SE 21-6 con partede SE 21-10)*. British Geological Survey – Servicio Geológico de Bolivia (1 map), Santa Cruz de la Sierra.

Moreto, C.P.N., Monteiro, L.V.S. *et al*. 2015. Timing of multiple hydrothermal events in the iron oxide–copper–gold deposits of the Southern Copper Belt Carajás Province, Brazil. *Mineralium Deposita*, **50**, 517–546, https://doi.org/10.1007/s00126-014-0549-9

Mudd, G.M. 2010. Global trends and environmental issues in nickel mining: sulfides v. laterites. *Ore Geology Reviews*, **38**, 9–26, https://doi.org/10.1016/j.oregeorev.2010.05.003

Mudd, G.M. 2012. Key trends in the resource sustainability of platinum group elements. *Ore Geology Reviews*, **46**, 106–117, https://doi.org/10.1016/j.oregeorev.2012.02.005

Nadeau, S. and Heesterman, L. 2010. *Guyana Geology and Mines Commission, Geological Map of Guyana – scale 1:1 million*. Guyana Geology and Mines Commission, https://www.ggmc.gov.gy/services/all/geological-services

Nadeau, S., Chen, W. *et al*. 2013. Guyana: the Lost Hadean Crust of South America? *Brazilian Journal of Geology*, **43**, 601–606, https://doi.org/10.5327/Z2317-48892013000400002

Neuvonen, K.J. 1986. On the direction of remanent magnetization of the quartz pophyry dykes in SE Finland. *Bulletin of the Geological Society of Finland*, **58**, 195–201, https://doi.org/10.17741/bgsf/58.1.013

Nironen, M., Elliott, B.A. and Rämo, O.T. 2000. 1.88–1.87 Ga post-kinematic intrusions of the Central Finland Granitoid Complex: a shift from C-type to A-type magmatism during lithospheric convergence. *Lithos*, **53**, 37–58, https://doi.org/10.1016/S0024-4937(00)00007-4

Nomade, S., Chen, Y. *et al*. 2003. The Guiana and West African Shield Palaeoproterozoic grouping: new palaeomagnetic data for French Guiana and Ivory Coast. *Geophysical Journal International*, **154**, 677–694, https://doi.org/10.1046/j.1365-246X.2003.01972.x

Oliveira, A.C.da S. and Almeida, M.E. 2019. Faixa Deformacional Roosevelt-Guariba, presented at *Simpósio Nacional de Estudos Tectônicos – SNET*, 16 May, Bento Gonçalves.

Oliveira, H.T., Borges, R.M.K., Klein, E.L., Lamarão, C.N., Marques, G.T. and Lima, R.G.C. 2019. Alteração hidrotermal e fluidos mineralizantes no alvo Jerimum de Baixo, Campo Mineralizado do Cuiú-Cuiú, Província Aurífera do Tapajós: um estudo baseado em petrografia, inclusões fluidas e química mineral. *Revista do Instituto de Geociências*, **19**.

Onstott, T.C. and Hargraves, R.B. 1981. Proterozoic transcurrent tectonics: palaeomagnetic evidence from Venezuela and Africa. *Nature*, **289**, 131–136, https://doi.org/10.1038/289131a0

Park, J.K., Inving, E. and Donaldson, J.A. 1973. Paleomagnetism of the Precambrian Dubawnt Group. *Geological Society of American Bulletin*, **103**, 522–537, https://doi.org/10.1130/0016-7606(1991)103<0522:CGBAAT>2.3.CO;2

Pehrsson, S.J., Eglington, B.M., Evans, D.A.D., Huston, D. and Reddy, S.M. 2016. Metallogeny and its link to orogenic style during the Nuna supercontinent cycle. *Geological Society, London, Special Publications*, **424**, 83–94, https://doi.org/10.1144/SP424.5

Peng, P. 2015. Precambrian mafic dyke swarms in the North China Craton and their geological implications. *Science China Earth Sciences*, **58**, 649–675, https://doi.org/10.1007/s11430-014-5026-x

Peng, P., Bleeker, W., Ernst, R.E., Söderlund, U. and McNicoll, V. 2011. U–Pb baddeleyite ages, distribution and geochemistry of 925 Ma mafic dykes and 900 Ma sills in the North China craton: evidence for a Neoproterozoic mantle plume. *Lithos*, **127**, 210–221, https://doi.org/10.1016/j.lithos.2011.08.018

Pinheiro, R.S.C. 2019. *Evolução paragenética e regime de fluidos no sistema Cu–Co Tarzan, Província Carajás*. MSc thesis, Universidade Estadual de Campinas, São Paulo, Brasil.

Pinho, M.A.S.R., Chemale, Jr F., Van Schmus, W.R. and Pinho, F.E.C. 2003. U–Pb and Sm–Nd evidence for 1.76–1.77 Ga magmatism in the Moriru region, Mato Grosso, Brazil: implications for province boundaries in the SW Amazonian Craton. *Precambrian Research*, **126**, 1–25, https://doi.org/10.1016/S0301-9268(03)00126-8

Pinho, S.C.C., Fernandes, C.M.D., Teixeira, N.P., Paiva Junior, A.L., Cruz, V.L., Lamarão, C.N. and Moura, C.A.V. 2006. O magmatismo paleoproterozóico da região de São Félix do Xingu, Província Estanífera do Sul do Pará: Petrografia e Geocronologia. *Revista Brasileira de Geociências*, **36**, 724–732, https://doi.org/10.25249/0375-7536.2006364724732

Pisarevsky, S.A. and Bylund, G. 2010. Paleomagnetism of 1780–1770 Ma mafic and composite intrusions of Småland (Sweden): implications for the Mesoproterozoic

Supercontinent. *American Journal of Science*, **310**, 1168–1186, https://doi.org/10.2475/09.2010.15

Pisarevsky, S.A. and Sokolov, S.J. 2001. The magnetostratigraphy and a 1780 Ma palaeomagnetic pole from the red sandstones of Vazhinka River section, Karelia, Russia. *Geophysical Journal International*, **146**, 531–538, https://doi.org/10.1046/j.0956-540x.2001.01479.x

Pisarevsky, S.A., Elming, S.Å., Pesonen, L.J. and Li, Z.X. 2014. Mesoproterozoic paleogeography: supercontinent and beyond. *Precambrian Research*, **244**, 207–225, https://doi.org/10.1016/j.precamres.2013.05.014

Pollard, P.J., Taylor, R.G., Peters, L., Matos, F., Freitas, C., Saboia, L. and Huhn, S. 2018. $^{40}Ar/^{39}Ar$ dating of Archean iron oxide Cu–Au and Paleoproterozoic granite-related Cu–Au deposits in the Carajas Mineral Province, Brazil: implications for genetic models. *Mineralium Deposita*, **54**, 329–346, https://doi.org/10.1007/s00126-018-0809-1

Prendergast, M.D. 2000. Layering and precious metals mineralization in the Rincón del Tigre Complex, Eastern Bolivia. *Economic Geology*, **95**, 113–130, https://doi.org/10.2113/gsecongeo.95.1.113

Prendergast, M., Bennett, M. and Henicke, O. 1998. *Platinum Exploration in the Rincon del Tigre Complex, Eastern Bolivia, ROYAUME-UNI*. Institution of Mining and Metallurgy, B39–B47.

Queiroz, J.D. da S. and Klein, E.L. 2018. The Paleoproterozoic metaconglomerate-hosted Castelo de Sonhos gold deposit, Tapajós Gold Province, Amazonian Craton: a modified paleoplacer origin. *Journal of the Geological Survey of Brazil*, **1**, 81–99, https://doi.org/10.29396/jgsb.2018.v1.n2.3

Reis, N.J. and de Carvalho, A.S. 1996. Coberturas sedimentares do Mesoproterozóico do Estado de Roraima. Avaliação e Discussão de seu Modo de Ocorrência. *Revista Brasileira de Geociências*, **26**, 217–226, https://doi.org/10.25249/0375-7536.19964217226

Reis, N.J. and Ramos, M.N. 2017. *Programa Geologia do Brasil. Programa Cartografia da Amazônia. Geologia e Recursos Minerais da Folha Ilha de Maracá, NA.20-X-A*. Escala 1:250 000. Estado de Roraima. Projeto Ilha de Maracá. Manaus, Explanatory Note, http://rigeo.cprm.gov.br/jspui/handle/doc/21205

Reis, N.J. and Yánez, G. 2001. O Supergrupo Roraima ao longo da Faixa Fronteiriça entre Brasil e Venezuela (Santa Elena de Uairén – Monte Roraima). *In*: Reis, N.J. and Monteiro, M.A.S. (eds) *Contribuições à Geologia da Amazônia*. Manaus, **2**, 115–147.

Reis, N.J., Teixeira, W., Hamilton, M.A., Bispo-Santos, F., Almeida, M.E. and D'Agrella-Filho, M.S. 2013*a*. Avanavero mafic magmatism, a Late Paleoproterozoic LIP in the Guiana Shield, Amazonian Craton: U–Pb ID–TIMS baddeleyite, geochemical and paleomagnetic evidence. *Lithos*, **174**, 175–195, https://doi.org/10.1016/j.lithos.2012.10.014

Reis, N.J., Bahia, R.C. *et al*. 2013*b*. O Supergrupo Sumaúma no Contexto Geológico da Folha SB.20-Z-D (Sumaúma), Sudeste do Amazonas: modo de ocorrência, discussão de idades em zircões detríticos e correlações no SW do Cráton do Amazonas. *In*: Wankler, F.L., Holanda, E.C. and Vasquez, M.L. (eds) *Contribuições à Geologia da Amazônia*. Belém, **8**, 197–220.

Reis, N.J., Fraga, L.M.B. and Almeida, M.E. 2014. Programa Geologia do Brasil, Levantamento da Geodiversidade. Geodiversidade do Estado de Roraima. *In*: Holanda, J.L.R., Marmos, J.L. and Maia, M.A.M. (eds) *Arcabouço Geológico*. CPRM – Serviço Geológico do Brasil, 17–32, http://rigeo.cprm.gov.br/jspui/handle/doc/14711

Reis, N.J., Nadeau, S. *et al*. 2017*a*. Stratigraphy of the Roraima Supergroup along the Brazil–Guyana border in the Guiana shield, Northern Amazonian Craton – results of the Brazil–Guyana Geology and Geodiversity Mapping Project. *Brazilian Journal of Geology*, **47**, 43–57, https://doi.org/10.1590/2317-4889201720160139

Reis, N.J., de Oliveira, A.C., de Oliveira, A.A. and Bahia, R.B.C. 2017*b*. *Programa Geologia do Brasil. Programa Cartografia da Amazônia. Geologia e Recursos Minerais da Folha Mutum, SB.20-Z-B, Escala 1:250 000*. Estado do Amazonas. Superintendência Regional de Manaus, http://rigeo.cprm.gov.br/jspui/handle/doc/17804

Reis, N.J., Cordani, U., Goulart, L.E.A., Almeida, M.E., Oliveira, V., Maurer, V.C. and Wahnfried, I. 2021. Zircon U–Pb SHRIMP ages of the Demêni–Mocidade Domain, Roraima, southern Guiana Shield, Brazil: extension of the Uatumã Silicic Large Igneous Province. *Journal of the Geological Survey of Brazil*, **4**, 61–76, https://doi.org/10.29396/jgsb.2021.v4.n1.4

Renaud, J.A. 2014. *The Aricheng Basement-hosted Albitite-type Uranium Deposit, Roraima Basin, Co-operative Republic of Guyana, South America*. PhD thesis, University of Western Ontario.

Ribeiro, B.V., Cawood, P.A. *et al*. 2020. A long-lived active margin revealed by zircon U–Pb–Hf data from the Rio Apa Terrane (Brazil): new insights into the Paleoproterozoic evolution of the Amazonian Craton. *Precambrian Research*, **350**, https://doi.org/10.1016/j.precamres.2020.105919

Ribeiro, P.S.E. and Duarte, T.B. 2010. *Geologia e Recursos Minerais das folhas Rio Guariba e Rio Aripuana. Projeto Noroeste-Nordeste de Mato Grosso; Programa Geologia do Brasil – PGB*. CPRM, Goiania, http://rigeo.cprm.gov.br/jspui/handle/doc/11355

Rios, F.S. 2019. *O Depósito de Au (Cu–Ag) Serrinha de Guarantã, Cráton Amazônico, Brasil: um depósito aurífero não-convencional associado ao sistema pórfiro – epitermal paleoproterozoico Juruena Teles Pires*. MSc thesis, Instituto de Geociências, Universidade de Brasília – UnB, Brasília.

Rios, F.S., Alves, C.L., Rizzotto, G.J. and Duarte, T.B. 2019. Recursos Minerais. *In*: Alves, C.L., Rizzotto, G.J., Rios, F.S. and Gonçalves, G.F. (eds) *Áreas de relevante interesse mineral – Projeto Evolução Crustal e Metalogenia da Província Mineral Juruena-Teles Pires, Estado do Mato Grosso*. SGB/CPRM, Goiânia, http://rigeo.cprm.gov.br/jspui/handle/doc/21324

Rizzotto, G.J., Quadros, M.L.E.S., Bahia, R.B.C., Dall'Igna, L.G. and Cordeiro, A.V. 2004. Folha SC.20-Porto Velho. *In*: Schobbenhaus, C., Gonçalves, J.H. *et al*. (eds) *Carta Geológica do Brasil ao Milionésimo, SIG, Programa Geologia do Brasil*. CPRM, Brasília, http://rigeo.cprm.gov.br/jspui/handle/doc/4981

Rizzotto, G.J., Alves, C.L., Rios, F.S. and Barros, M.A.S. 2019. The Western Amazonia Igneous Belt. *Journal* *of South American Earth Sciences*, **96**, https://doi.org/10.1016/j.jsames.2019.102326

Rocha, M.L.B.P., Chemale Junior, F. *et al*. 2020. U–Th–Pb Shrimp dating of hydrothermal monazite from the Trairão Gold Deposit – Alta Floresta Gold Province (Amazon Craton). *Brazilian Journal Geology*, **50**.

Sadowsky, G.R. and Bettencourt, J.S. 1996. Neoproterozoic tectonic correlations between east Laurentia and the western border of the Amazon Craton. *Precambrian Research*, **76**, 213–227, https://doi.org/10.1016/0301-9268(95)00026-7

Salminen, J.M., Klein, R., Mertanen, S., Pesonen, L.J., Fröjdö, S., Mänttäri, I. and Eklund, O. 2016. Palaeomagnetism and U–Pb geochronology of ca. 1570 Ma intrusives from Åland archipelago, SW Finland implications for Nuna. *Geological Society, London, Special Publications*, **424**, 95–118, http://doi.org/10.1144/SP424.3

Salminen, J.M., Klein, R., Veikkolainen, T., Mertanen, S. and Mänttäri, I. 2017. Mesoproterozoic geomagnetic reversal asymmetry in light of new paleomagnetic and geochronological data for the Häme dyke swarm, Finland: implications for the Nunasupercontinent. *Precambrian Research*, **288**, 1–22, https://doi.org/10.1016/j.precamres.2016.11.003

Samal, A.K., Srivastava, R.K., Ernst, R.E. and Söderlund, U. 2019. Mapping and naming of distinct Neoarchean–Mesoproterozoic mafic dyke swarms of the Indian Shield using Google™ Earth images and ArcGIS™ and their possible association to Large Igneous Provinces: current status and future prospects. *In*: Srivastava, R.K., Ernst, R.E. and Peng, P. (eds) *Dyke Swarms of the World – A Modern Perspective*. Springer, 335–390.

Santiago, E.S.B., Villas, R.N. and Ocampo, R.C. 2013. The Tocantinzinho gold deposit, Tapajós province, state of Pará: host granite, hydrothermal alteration and mineral chemistry. *Brazilian Journal of Geology*, **43**, 185–208, https://doi.org/10.5327/Z2317-48892013000100015

Santos, J.O.S. 2003. Geotectônica dos Escudos das Guianas e Brasil Central. *In*: Bizzi, L.A., Schobbenhaus, C., Vidotti, R.M. and Gonçalves, J.H. (eds) *Geologia, Tectônica e Recursos Minerais do Brasil: texto, mapas e SIG*. CPRM – Serviço Geológico do Brasil. Cap. 4, 169–226.

Santos, J.O.S., Hartmann, L.A., Gaudette, H.E., Groves, D.I., McNaughton, N.J. and Flecher, I.R. 2000. New understanding of the Amazon Craton provinces, based on on integration of field mapping and U–Pb and Sm–Nd geochronology. *Gondwana Research*, **3**, 453–488, https://doi.org/10.1016/S1342-937X(05)70755-3

Santos, J.O.S., Hartmann, L.A., McNaughton, N.J. and Fletcher, I.R. 2001. Timing of mafic magmatism in the Tapajós Province (Brazil) and implications for the evolution of the Amazon Craton – evidence from baddeleyite and zircon U–Pb SHRIMP geochronology. *Journal of South American Earth Sciences*, **15**, 409–429, https://doi.org/10.1016/S0895-9811(02)00061-5

Santos, J.O.S., Hartmann, L.A., McNaughton, N.J. and Fletcher, I.R. 2002. Timing of mafic magmatism in the Tapajós Province (Brazil) and implications for the evolution of the Amazon Craton: evidence from baddeleyite and zircon U–Pb SHRIMP geochronology. *Journal of South America Earth Sciences*, **15**, 409–429, https://doi.org/10.1016/S0895-9811(02)00061-5

Santos, J.O.S., Reis, N.J., Chemale, F., Hartmann, L.A., da Pinheiro, S.S. and McNaughton, N.J. 2003*a*. Paleoproterozoic Evolution of Northwestern Roraima State – Absence of Archean Crust, based on U–Pb and Sm-Nd isotopic evidence, presented at *South American Symposium on Isotope Geology*, Short Papers, 278–281.

Santos, J.O.S., Potter, P.E., Reis, N.J., Hartmann, L.A., Fletcher, I.R. and McNaughton, N.J. 2003*b*. Age, source and regional stratigraphy of the Roraima Supergroup and Roraima-like sequences in Northern South América, based on U–Pb geochronology. *Geological Society of America Bulletin*, **115**, 331–348, https://doi.org/10.1130/0016-7606

Santos, J.O.S., Van Breemen, O.B., Groves, D.I., Hartmann, L.A., Almeida, M.E., McNaughton, N.J. and Fletcher, I.R. 2004. Timing and evolution of multiple Paleoproterozoic magmatic arcs in the Tapajós Domain, Amazon Craton: constraints from SHRIMP and TIMS zircon, baddeleyite and titanite U–Pb geochronology. *Precambrian Research*, **131**, 73–109, https://doi.org/10.1016/j.precamres.2004.01.002

Santos, J.O.S., McNaughton, N.J., Hartmann, L.A., Fletcher, I.R. and Matos, R.S. 2005. The age of deposition of the Aguapeí Group, Western Amazon Craton, based on U–Pb study of diagenetic xenotime and detrital zircon, presented at *Congreso Latino-americano de Geologia*, **12**, Quito, Ecuador.

Santos, J.O.S., Hartmann, L.A., de Faria, M.S.G., Riker, S.R.L., de Souza, M.M., Almeida, M.E. and McNaughton, N.J. 2006. A Compartimentação do Cráton Amazonas em Províncias: Avanços ocorridos no período 2000–2006, presented at *Simpósio de Geologia da Amazônia*, **9**, Belém.

Scandolara, J.E., Correa, R.T. *et al*. 2017. Paleo-Mesoproterozoic arc-accretion along the southwestern margin of the Amazonian craton: the Juruena accretionary orogen and possible implications for Columbia supercontinente. *Journal of South American Earth Sciences*, **73**, 223–247, https://doi.org/10.1016/j.jsames.2016.12.005

Schwarz, M. and Frantz, J. 2013. Cu–Zn Pojuca Corpo Quatro Deposit: IOCG or VMS? *Pesquisas em Geociências*, **40**, 5–19, https://doi.org/10.22456/1807-9806.42425

Serrato, A.A.A. 2014. *Geocronologia e evolução do sistema hidrotermal do depósito aurífero de Juruena, Província Aurífera de Alta Floresta (MT), Brasil*. Msc thesis, Universidade Estadual de Campinas, Campinas, Brasil.

Shumlyanskyy, L., Ernst, R., Söderlund, U., Billström, K., Mitrokhin, O. and Tsymbal, S. 2016*a*. New U–Pb ages for mafic dykes in the Northwestern region of the Ukrainian shield: coeval tholeiitic and jotunitic magmatism. *GFF, Journal of the Geological Society of Sweden*, **138**, 79–85.

Shumlyanskyy, L., Mitrokhin, O. *et al*. 2016*b*. The ca. 1.8 Ga mantle plume related magmatism of the central part of the Ukrainian shield. *GFF, Journal of the Geological Society of Sweden*, **138**, 86–101.

Shumlyanskyy, L., Ernst, R.E., Billstrom, K., Wing, B.A. and Bekker, A. 2016*c*. Age and sulfur isotope composition of the Prutivka intrusion (the 1.78 Ga Prutivka–Novogol Large Igneous Province in Sarmatia). *Mineralogical Journal: Geochemistry (Ukraine)*, **38**, 91–101.

Shumlyanskyy, L., Hawkesworth, C. *et al*. 2017. The origin of the Palaeoproterozoic AMCG complexes in the Ukrainian Shield: new U–Pb ages and Hf isotopes in zircon. *Precambrian Research*, **292**, 216–239, https://doi.org/10.1016/j.precamres.2017.02.009

Sidder, G.B. and Mendoza, S.V. 1991. Geology of the Venezuelan Guyana Shield and its Relation to the Entire Guyana Shield. USGS Open-File Report **91-0141**.

Silva, M.G. and Abram, M.B. 2008. *Projeto Metalogenia da Província Aurífera Juruena–Teles Pires, Mato Grosso*. *In*: Silva, M.G. and Abram, M.B. (eds) Geological Service of Brazil – CPRM, http://rigeo.cprm.gov.br/jspui/handle/doc/1745

Silva, C.A.S., Jr and Klein, E.L. 2016. Geology and characteristics of the mineralizing fluid in the Jerimum de Cima and Babi gold prospects, Cuiú-Cuiú goldfield, Tapajós Gold Province, Amazonian Craton, a fluid inclusion and stable isotope study. *Boletim do Museu Paraense Emílio Goeldi, Belém*, **10**, 199–230.

Silva, C.A.S., Jr, Klein, E.L. *et al*. 2015. Zircon geochronology and Pb isotope systematics in sulfides: implications for the genesis of gold mineralization in the Cuiú-Cuiú Goldfield, Tapajós Gold Province, Amazonian Craton, Brazil. *In*: Gorayaeb, P.S.S. and Lima, A.M.M. (eds) *Contribuições à Geologia da Amazônia*. Belém, **9**, 453–465.

Silver, P.G. and Behn, D. 2008. Intermittent plate tectonics. *Science (New York)*, **319**, 85–88, https://doi.org/10.1126/science.1148397

Simões, M.S., Meloni, R.E. and Santos, J.O.S. 2020. Stratigraphy, depositional environments and zircon U–Pb (LA–ICP–MS) ages of the Statherian volcano-sedimentary Beneficente Group: implications for tectonics and gold mineralization in SW of the Amazon Craton. *Precambrian Research*, **345**, 1–23, https://doi.org/10.1016/j.precamres.2020.105756

Sparrenberger, I. 2003. *Evolução da mineralização primária estanífera associada ao maciço granítico Santa Bárbara, Rondônia*. PhD thesis, Instituto de Geociências, Universidade de São Paulo, São Paulo, SP, Brazil.

Stein, C.A., Stein, S., Merino, M., Keller, G.R., Flesch, L.M. and Jurdy, D.M. 2014. Was the Midcontinent Rift part of a successful seaflor-spreading episode? *Geophysical Research Letters*, **41**, 1465–1470, https://doi.org/10.1002/2013GL059176

Tallarico, F.H.B. 2003. *O Cinturão Cupro-Aurífero de Carajás, Brasil*. PhD thesis, Universidade Estadual de Campinas.

Tallarico, F.H.B., McNaughton, N.J. *et al*. 2004. Geological and SHRIMP II U–Pb constraints on the age and origin of the Breves Cu–Au–(W–Bi–Sn) deposit, Carajás, Brazil. *Mineralium Deposita*, **39**, 68–86, https://doi.org/10.1007/s00126-003-0383-y

Tassinari, C.G.C. and Macambira, M.J.B. 2004. A Evolução Tectônica do Cráton Amazônico. *In*: SBG (ed.) *Geologia do Continente Sul-Americano – Evolução da Obra de Fernando Flávio de Almeida*. Ed. Beca. Capítulo XXVIII, São Paulo, 471–486.

Tavares, F.M., Trouw, R.A.J., Silva, C.M.G., Justo, A.P. and Oliveira, J.K.M. 2018. The multistage tectonic evolution of the northeastern Carajás Province, Amazonian Craton, Brazil: revealing complex structural patterns. *Journal of South American Earth Sciences*, **88**, 238–252, https://doi.org/10.1016/j.jsames.2018.08.024

Teixeira, N.P., Bettencourt, J.S., Moura, C.A.V., Dall'Agnol, R. and Macambira, E.M.B. 2002. Archean crustal sources for paleoproterozoic tin-mineralized granites in the Carajás Province, SSE Pará, Brazil: Pb–Pb geochronology and Nd isotope geochemistry. *Precambrian Research*, **119**, 257–275, https://doi.org/10.1016/S0301-9268(02)00125-0

Teixeira, W., Geraldes, M.C., Matos, R., Ruiz, A.S., Saes, G. and Vargas-Mattos, G. 2010. A review of the tectonic evolution of the Sunsás belt, SW Amazonian Craton. *Journal of South American Earth Sciences*, **29**, 47–60, https://doi.org/10.1016/j.jsames.2009.09.007

Teixeira, W., Hamilton, M.A., Lima, G.A., Matos, R. and Ernst, R.E. 2015. Precise ID–TIMS U–Pb baddeleyite ages (1110–1112 Ma) for the Rincón del Tigre–Huanchaca large igneous province (LIP) of the Amazonian Craton: implications for the Rodinia supercontinent. *Precambrian Research*, **265**, 273–285, https://doi.org/10.1016/j.precamres.2014.07.006

Teixeira, W., Reis, N.J., Bettencourt, J.S., Klein, E.F. and Oliveira, D. 2019. Intraplate Proterozoic magmatism in the Amazonian Craton reviewed: geochronology, crustal tectonics and global barcode matches. *In*: Srivastava, R.K., Ernst, R.R. *et al*. (eds) *Dyke Swarms of the World-A Modern Perspective*. Springer Geology, 111–154, https://doi.org/10.1007/978-981-13-1666-1_4

Teixeira, W., Cordani, U.G., Faleiros, F.M., Sato, K., Maurer, V.C., Ruiz, A.S. and Azevedo, E.J.P. 2020. The Rio Apa Terrane reviewed: U Pb zircon geochronology and provenance studies provide paleotectonic links with a growing Proterozoic Amazonia. *Earth-Science Reviews*, **202**, 103089, https://doi.org/10.1016/j.earscirev.2020.103089

Tedeschi, M.T., Hagemann, S.G., Kemp, A.I.S., Kirkland, C.L. and Ireland, T.R. 2020. Geochronological constrains on the timing of magmatism, deformation and mineralization at the Karouni orogenic gold deposit: Guyana, South America. *Precambrian Research*, **337**, 1–25, https://doi.org/10.1016/j.precamres.2019.04.015

Tohver, E., van der Pluijm, B., Van der Voo, R., Rizzotto, G. and Scandolara, J.E. 2002. Paleogeography of the Amazon craton at 1.2 Ga: early Grenvillian collision with the Llano segment of Laurentia. *Earth and Planetary Science Letters*, **199**, 185–200, https://doi.org/10.1016/S0012-821X(02)00561-7

Tohver, E., Bettencourt, J.S., Tosdal, R., Mezger, K., Leite, W.B. and Payolla, B.L. 2004. Terrane transfer during the Grenville orogeny: tracing the Amazonian ancestry of southern Appalachian basement through Pb and Nd isotopes. *Earth and Planetary Science Letters*, **228**, 161–176, https://doi.org/10.1016/j.epsl.2004.09.029

Tokashiki, C.C., Juliani, C., Monteiro, L.V.S., Echeverri-Misas, C.M., Aguja, A.A. and Arrais, L.B. 2013. Eventos vulcânicos de 1.97 Ga com mineralizações de ouro epitermal Low- e intermediate sulfidation, na porção sul da província aurífera do Tapajós (PA), presented at *Simpósio de Geologia da Amazônia*, **13**, Belém, 625–628.

Trendall, A.F., Basei, M.A.S., De Laeter, J.R. and Nelson, D.R. 1998. SHRIMP zircon U–Pb constraints on the age of the Carajás Formation, Grão Pará Group, Amazon Craton. *Journal of South American Earth Sciences*, **11**, 265–277, https://doi.org/10.1016/S0895-9811(98)00015-7

Trunfull, E.F., Hagemanna, S.G., Xavier, R.P. and Moreto, C.P.N. 2020. Critical assessment of geochronological data from the Carajás Mineral Province, Brazil: implications for metallogeny and tectonic evolution. *Ore Geology Reviews*, **121**, 103556, https://doi.org/10.1016/j.oregeorev.2020.103556

Valdespino, O.E.M. and Costanzo-Alvarez, V. 1997. Paleomagnetic and rock magnetic evidence for inverse zoning in the Parguaza batholith (southwestern Venezuela) and its implications about tectonics of the Guyana shield. *Precambrian Research*, **85**, 1–25, https://doi.org/10.1016/S0301-9268(97)00020-X

Valério, C.S., Souza, V.S. and Macambira, M.J.B. 2009. The 1.90–1.88 Ga magmatism in the southernmost Guyana Shield, Amazonas, Brazil: geology, geochemistry, zircon geochronology, and tectonic implications. *Journal of South American Earth Sciences*, **28**, 304–320, https://doi.org/10.1016/j.jsames.2009.04.001

Vasquez, M.L. and Dreher, A.M. 2011. Uma avaliação da estratigrafia dos eventos magmáticos de 1900–1860 Ma do Cráton Amazônico, presented at *Simpósio de Geologia da Amazônia*, **12**, Boa Vista.

Vasquez, M.L., Rosa-Costa, L.T., Silva, C.M.G. and Klein, E.L. 2008. Compartimentação tectônica. *In*: Vasquez, M.L. and Rosa-Costa, L.T. (eds) *Geologia e Recursos Minerais do Estado do Pará: texto explicativo do mapa geológico e de recursos minerais do estado do Pará, Escala 1:1.000.000*. CPRM, Belém, 39–112, http://rigeo.cprm.gov.br/jspui/handle/doc/10443

Vasquez, M.L., Cordani, U.G., Sato, K., Barbosa, J.P.O., Faraco, M.T.L. and Maurer, V.C. 2019. U–Pb SHRIMP dating of basement rocks of the Iriri–Xingu domain, Central Amazonian province, Amazonian craton, *Brazil Brazilian Journal of Geology*, **49**, https://doi.org/10.1590/2317-4889201920190067

Veloso, A.S.R. and Santos, M.D. 2013. Geologia, petrografia e geocronologia das rochas do depósito aurífero Ouro Roxo, Província Tapajós, Jacareacanga (PA), Brasil. *Brazilian Journal of Geology*, **43**, 22–36, https://doi.org/10.5327/Z2317-48892013000100004

Vigneresse, J.L. 2005. The specific case of the Mid-Proterozoic rapakivi granites and associated suite within the context of the Columbia Supercontinent. *Precambrian Research*, **137**, 1–34, https://doi.org/10.1016/j.precamres.2005.01.001

Villas, R.N.N., Santiago, E.S.B. and Castilho, M.P. 2013. Contexto geológico, estudos isotópicos (C, O e Pb) e associação metálica do depósito aurífero Tocantinzinho, domínio Tapajós, Província Tapajós-Parima. *Geol USP, Série Científica, São Paulo*, **13**, 11–138, https://doi.org/10.5327/Z1519-874X2013000100008

Voicu, G., Bardoux, M. and Stevenson, R. 2001. Lithostratigraphy, geochronology and gold metallogeny in the northern Guiana Shield South America: a review. *Ore Geology Review*, **18**, 211–236, https://doi.org/10.1016/S0169-1368(01)00030-0

Wang, C., Mitchell, R.N., Murphy, J.B., Peng, P. and Spencer, C.J. 2020. The role of mega-continents in the supercontinent cycle. *Geology*, **49**, https://doi.org/10.1130/G47988.1

Whitney, D.L. and Evans, B.W. 2010. Abbreviations for names of rock-forming minerals. *American Mineralogist*, **95**, 185–187, https://doi.org/10.2138/am.2010.3371

Zhang, S.-H., Ernst, R.E., Pei, J.-L., Zhao, Y., Zhou, M.-F. and Hu, G.-H. 2018. A temporal and causal link between ca. 1380 Ma large igneous provinces and black shales: implications for the Mesoproterozoic time-scale and paleoenvironment. *Geology*, **46**, 963–966, https://doi.org/10.1130/G45210.1

Zhang, S.-H., Ernst, R.E., Pei, J.-L., Zhao, Y. and Hu, G.-H. 2021. Large igneous provinces (LIPs) and anoxia events in 'The Boring Billion'. *In*: Ernst, R.E., Dickson, A.J. and Bekker, A. (eds) *Large Igneous Provinces: A Driver of Global Environmental and Biotic Changes*, 1st edn. AGU, Geophysical Monographs, 255, https://doi.org/10.1002/9781119507444.ch20